Calhoun: The NPS Institutional Archive

DSpace Repository

Theses and Dissertations | 1. Thesis and Dissertation Collection, all items

2002-09

Meteorological and model traits knowledge bases for North Indian Ocean tropical cyclones

Spollen, Rachael A.

Monterey, California. Naval Postgraduate School

http://hdl.handle.net/10945/4480

This publication is a work of the U.S. Government as defined in Title 17, United States Code, Section 101. Copyright protection is not available for this work in the United States.

Downloaded from NPS Archive: Calhoun

http://www.nps.edu/library

Calhoun is the Naval Postgraduate School's public access digital repository for research materials and institutional publications created by the NPS community. Calhoun is named for Professor of Mathematics Guy K. Calhoun, NPS's first appointed -- and published -- scholarly author.

Dudley Knox Library / Naval Postgraduate School
411 Dyer Road / 1 University Circle
Monterey, California USA 93943

NAVAL POSTGRADUATE SCHOOL
Monterey, California

THESIS

METEOROLOGICAL AND MODEL TRAITS KNOWLEDGE BASES FOR NORTH INDIAN OCEAN TROPICAL CYCLONES

by

Rachael A. Spollen

September 2002

Thesis Advisor:	Russell L. Elsberry
Second Readers:	Patrick A. Harr
	Mark A. Boothe

Approved for public release; distribution is unlimited

THIS PAGE INTENTIONALLY LEFT BLANK

REPORT DOCUMENTATION PAGE			Form Approved OMB No. 0704-0188
Public reporting burden for this collection of information is estimated to average 1 hour per response, including the time for reviewing instruction, searching existing data sources, gathering and maintaining the data needed, and completing and reviewing the collection of information. Send comments regarding this burden estimate or any other aspect of this collection of information, including suggestions for reducing this burden, to Washington headquarters Services, Directorate for Information Operations and Reports, 1215 Jefferson Davis Highway, Suite 1204, Arlington, VA 22202-4302, and to the Office of Management and Budget, Paperwork Reduction Project (0704-0188) Washington DC 20503.			
1. AGENCY USE ONLY *(Leave blank)*	**2. REPORT DATE** September 2002	**3. REPORT TYPE AND DATES COVERED** Master's Thesis	
4. TITLE AND SUBTITLE: Title (Mix case letters) Meteorological and Model Traits Knowledge Bases for North Indian Ocean Tropical Cyclones			**5. FUNDING NUMBERS**
6. AUTHOR(S) LT Rachael A. Spollen			
7. PERFORMING ORGANIZATION NAME(S) AND ADDRESS(ES) Naval Postgraduate School Monterey, CA 93943-5000			**8. PERFORMING ORGANIZATION REPORT NUMBER**
9. SPONSORING / MONITORING AGENCY NAME(S) AND ADDRESS(ES) N/A			**10. SPONSORING / MONITORING AGENCY REPORT NUMBER**
11. SUPPLEMENTARY NOTES The views expressed in this thesis are those of the author and do not reflect the official policy or position of the Department of Defense or the U.S. Government.			
12a. DISTRIBUTION / AVAILABILITY STATEMENT Distribution Statement (mix case letters)			**12b. DISTRIBUTION CODE**

13. ABSTRACT ***(maximum 200 words)***

These tropical cyclone Meteorology and Model Traits Knowledge Bases for the North Indian Ocean (NIO) complete the global coverage required for application of the Systematic Approach to tropical cyclone track forecasting introduced by Carr and Elsberry (1994). The database for the NIO Meteorological Knowledge Base includes 64 storms during 1991-2001. All of the 656 cases could be classified in three common synoptic patterns that have been found to apply in other basins, with no unique patterns. About 75% of the cases are in the standard pattern.

This preliminary Model Traits Knowledge Base includes only eight tropical cyclones during 2000-2001. The model forecast track errors are relatively small, and only 33%, 62%, and 70% of the Navy global, regional, and UK Meteorological Office models, respectively, exceed 150 n mi at 72 h. Only 12 cases of large (> 225 n mi at 72 h) track forecast errors occur. Half of these large-error cases are associated with erroneous model predictions in the midlatitudes. One third of the large errors originate from improper model treatments of the tropical circulations, and the remaining two cases originate from erroneous initial cyclone positions. Since these are the same error sources as in other basins, the Systematic Approach has global application.

14. SUBJECT TERMS Tropical cyclone track forecasting, Systematic Approach application, Dynamical model track errors			**15. NUMBER OF PAGES** 140
			16. PRICE CODE
17. SECURITY CLASSIFICATION OF REPORT Unclassified	**18. SECURITY CLASSIFICATION OF THIS PAGE** Unclassified	**19. SECURITY CLASSIFICATION OF ABSTRACT** Unclassified	**20. LIMITATION OF ABSTRACT** UL

THIS PAGE INTENTIONALLY LEFT BLANK

METEOROLOGICAL AND MODEL TRAITS KNOWLEDGE BASES FOR NORTH INDIAN OCEAN TROPICAL CYCLONES

Rachael A. Spollen
Lieutenant, United States Navy
B.S. Jacksonville University, 1995

Submitted in partial fulfillment of the
requirements for the degree of

MASTER OF SCIENCE IN METEOROLOGY AND PHYSICAL OCEANOGRAPHY

from the

NAVAL POSTGRADUATE SCHOOL
September 2002

Author:

Rachael A. Spollen

Approved By:

Russell L. Elsberry, Thesis Advisor

Patrick A. Harr, Second Reader

Mark A. Boothe, Second Reader

Carlyle H. Wash, Chairman
Department of Meteorology

THIS PAGE INTENTIONALLY LEFT BLANK

ABSTRACT

These tropical cyclone Meteorology and Model Traits Knowledge Bases for the North Indian Ocean (NIO) complete the global coverage required for application of the Systematic Approach to tropical cyclone track forecasting introduced by Carr and Elsberry (1994). The database for the NIO Meteorological Knowledge Base includes 64 storms during 1991-2001. All of the 656 cases could be classified in three common synoptic patterns that have been found to apply in other basins, with no unique patterns. About 75% of the cases are in the standard pattern.

This preliminary Model Traits Knowledge Base includes only eight tropical cyclones during 2000-2001. The model forecast track errors are relatively small, and only 33%, 62%, and 70% of the Navy global, regional, and UK Meteorological Office models, respectively, exceed 150 n mi at 72 h. Only 12 cases of large (> 225 n mi at 72 h) track forecast errors occur. Half of these large-error cases are associated with erroneous model predictions in the midlatitudes. One third of the large errors originate from improper model treatments of the tropical circulations, and the remaining two cases originate from erroneous initial cyclone positions. Since these are the same error sources as in other basins, the Systematic Approach has global application.

THIS PAGE INTENTIONALLY LEFT BLANK

TABLE OF CONTENTS

I. INTRODUCTION 1
A. MOTIVATION 1
B. BACKGROUND ON THE SYSTEMATIC APPROACH 3
C. PURPOSE OF THIS THESIS 5
II. GLOBAL METEOROLOGICAL KNOWLEDGE BASE – ENVIRONMENT STRUCTURE 7
A. ENVIRONMENT STRUCTURE 7
1. Standard Pattern 8
2. Poleward Pattern 11
3. Midlatitude Pattern 12
4. Western North Pacific Monsoon Gyre Pattern 12
5. Eastern/Central North Pacific Low Pattern 14
6. Atlantic Upper-Level Low Pattern 14
7. Southern Hemisphere High-Amplitude Pattern 14
B. NORTH INDIAN OCEAN TC MOTION METEOROLOGY KNOWLEDGE BASE 15
C. ENVIRONMENT STRUCTURE IN THE NIO 16
D. SYNOPTIC PATTERNS AND REGIONS IN THE NIO 17
1. NIO Standard Pattern 19
a. S/TE pattern/region 19
b. S/TE pattern/region case study 21
c. S/PF pattern/region 23
d. S/PF pattern/region case study 23
e. S/EF pattern/region 25
f. S/EF pattern/region case study 25
g. S/EW pattern/region 25
h. S/EW pattern/region case study 27
2. NIO Poleward Pattern 27
a. P/PF pattern/region 30
b. Malay Peninsula anticyclone P/PF case study 30
c. Northern anticyclone P/PF case study 32
d. P/EW pattern/region 32
3. NIO Midlatitude Pattern 32
a. M/PF pattern/region 35
b. M/PF case study 36
c. M/MW and M/EF pattern/regions 36
d. M/MW case study 38
E. TC STRUCTURE 38

III. GLOBAL METEOROLOGICAL KNOWLEDGE BASE – TRANSITIONAL MECHANISMS 41
A. ENVIRONMENTAL EFFECTS 41
1. Advection 41
2. Midlatitude System Evolutions 42
a. Midlatitude Cyclogenesis/ Cyclolysis (MCG/MCL) 42
1. Conceptual Model 42
2. NIO MCG/MCL Case Studies 43
b. Midlatitude Anticyclogenesis/ Anticyclolysis (MAG/MAL) 47
1. Conceptual Model 47
2. MAG/MAL Case Studies 48
B. TC-ENVIRONMENT TRANSFORMATIONS 51
1. Beta –Effect Related Transformations 51
a. Beta-Effect Propagation (BEP) 51
b. Ridge Modification by a TC (RMT) 53
2. Cyclone Interactions 57
a. Direct Cyclone Interaction (DCI) 59
b. Semi-Direct Cyclone Interaction (SCI) 60
c. Indirect Cyclone Interaction (ICI) 61
d. SCI and ICI case study 63
3. Midlatitude –Related – Response to Vertical Shear (RVS) 66
C. NIO TRANSITIONAL MECHANISMS 67
D. CASE STUDIES 72
1. S/TE-S/PF-P/PF-M/PF 72
2. S/EW-S/TE-S/PF-M/PF-M/MW 77
3. S/TE-S/PF-S/EF 80
E. CONCLUSIONS 84
IV. NORTH INDIAN OCEAN MODEL TRAITS KNOWLEDGE BASE 85
A. OBJECTIVE 85
B. METHODOLOGY 85
C. TRACK ERRORS OVERVIEW 86
D. CASE STUDY ANALYSIS 89
1. Erroneous Midlatitude System Evolutions 91
a. GFDN E-MCG Case Study 93
b. GFDN E-MAL Case Study 98
c. UKMO E-MAG Case Study 100
2. Erroneous Equatorial Wind Burst 102
3. Erroneous Ridge Modification by a TC 106
4. Initial Position Error 110
a. UKMO IPE Case Study 110
b. NOGAPS IPE Case Study 111
E. CONCLUSIONS 112

V. CONCLUSIONS 115
A. SUMMARY 115
B. FUTURE RESEARCH 117

LIST OF REFERENCES 119

INITIAL DISTRIBUTION LIST 121

THIS PAGE INTENTIONALLY LEFT BLANK

LIST OF FIGURES

1.1 Systematic Approach Conceptual Framework 4

2.1 TC motion Meteorology Knowledge Base Framework 7
2.2 Common Global Synoptic Pattern/Regions 9
2.3 Frequency of Synoptic Patterns by Oceanic Basin 10
2.4 Unique Global Synoptic Pattern/Regions 13
2.5. TC Motion Meteorology Knowledge Base for the NIO 16
2.6 Graphic of all NIO tracks for all Synoptic Pattern/Regions 18
2.7 Standard Pattern/Region Schematic 19
2.8 NIO Pattern/ Region Climatology 20
2.9 NIO S Pattern Tracks 20
2.10 Track and NOGAPS 500 mb wind field for TC 04A 1998 22
2.11 Track and 500 mb wind field for TC 06B 1998 24
2.12 Track and 500 mb wind field for TC 04B 2001 26
2.13 Track and 500 mb wind field for TC 01A 1993 28
2.14 Poleward Pattern/Region and NIO P Pattern Tracks 29
2.15 Track and 500 mb wind field for TC 04B 1999 31
2.16 Track and 500 mb wind fields for TC 02A 1999 33
2.17 Midlatitude Pattern/Region and M Pattern Tracks 35
2.18 Track and 500 mb wind fields for TC 01A 1998 37
2.19 Track and 500 mb wind fields for TC 30W 1992 39

3.1 MCG-MCL Conceptual Model 42
3.2 Track and 500 mb wind fields for TC 07 B 1998 44
3.3 Track and 500 mb wind fields for TC 02B 2000 46
3.4 MAG-MAL Conceptual Model 48
3.5 Track and 500 mb wind fields for TC 07B 1992 49
3.6 Track, MSLP, and 500 mb wind fields for TC 02A 1998 52
3.7 RMT Conceptual Model 53
3.8 Track and 500 mb wind fields for TC 10 B 1992 54
3.9 Track and 500 mb wind fields for TC 02B 1997 58
3.10 DCI Conceptual Model 60
3.11 SCI Conceptual Model 60
3.12 ICI Conceptual Model 62
3.13 Track and 500 mb wind fields for TC 05A 1996 64
3.14 RVS Conceptual Model 66
3.15 Track and 500 mb wind fields for TC 32W 2001 68
3.16 NIO Environment Structure Transitions 1991-2001 71
3.17 Track and 500 mb wind fields for TC 02 B
S/TE-S/PF-P/PF-M/PF Case Study 73
3.18 Track and 500 mb wind fields for TC 01A 1993
S/EW-S/TE-S/PF-M/PF-M/MW Case Study 78

3.19 Track and 500 mb wind fields for TC 05A 1999
S/TE-S/PF-S/EF Case Study 81

4.1 72-h track forecast error vs. frequency for NOGAPS, UKMO,
and GFDN models..... 86
4.2 NIO non-homogeneous FTE averages during 2000-2001 87
4.3 NIO homogeneous FTE averages during 2000-2001..... 88
4.4 GFDN and NOGAPS model forecast tracks of TC 01A 2001 initiated
at 06 UTC 22 May2001..... 93
4.5 TC 01A 2001 forecast and analysis fields initiated at 06 UTC 22 May 2001 95
4.6 GFDN forecast track and 500 mb wind analysis for TC 01A 2001 valid at
06 UTC 23 May 2001..... 98
4.7 TC 01A 2001 forecast and analysis fields initiated at 06 UTC 23 May 2001 99
4.8 UKMO forecast track of TC01A 2001 initiated at 12 UTC 25 May 2001 100
4.9 TC01A forecast and analysis fields initiated at12 UTC 25 May 2001 ..... .101
4.10 EWB Conceptual Model 103
4.11 NOGAPS forecast track of TC02A 2001 initiated at
12 UTC 24 September 2001..... 104
4.12 TC02A 2001 700 mb forecast and analysis fields initiated at
12 UTC 24 September 2001..... 105
4.13 Erroneous Ridge Modification by a TC (E-RMT) conceptual model..... 106
4.14 NOGAPS forecast track and 500 mb analysis of TC01A 2001
intiated at 12 UTC 23 May 2001..... 107
4.15 TC01A 2001 500 mb forecast and analysis fields initiated at
12 UTC 23 May..... 108
4.16 UKMO forecast track of TC04B 2000 initiated at 00 UTC 25 May..... 111
4.17NOGAPS forecast track of TC04B 2001 initiated at
00 UTC 9 November..... 112

LIST OF TABLES

Table 1 Occurrences of synoptic pattern/regions by month..... 21

Table 1 NOGAPS, UKMO, and GFDN 72-H forecasts exceeding 225 n mi in 2000-2001 90

Table 2 Meanings and frequencies of the causes of large NOGAPS, UKMO, and GFDN forecast track errors in the NIO during 2000-2001 91

THIS PAGE INTENTIONALLY LEFT BLANK

ACKNOWLEDGMENTS

I would like to sincerely thank my advisor, Dr. Russell Elsberry and Mark Boothe for their expertise in the development of this Thesis. I have gained a valuable skill and have learned so much as a result of their guidance.

I would also like to thank my husband, Kevin, for his unwavering support throughout the entire process of completing my graduate education here at NPS.

THIS PAGE INTENTIONALLY LEFT BLANK

I. INTRODUCTION

A. MOTIVATION

Tropical cyclone track forecasting has evolved significantly since the inception of numerical weather prediction. New prediction methods continue to decrease the errors associated with track forecasts. More accurate warnings can be used to reduce the cost in emergency preparation along highly populated coastal regions. The expenditures based on decisions to divert deployed Naval assets around the high winds and seas associated with a tropical system depend on model accuracy and forecaster knowledge. The command to sortie Naval units in port is even more costly with regards to man-hours, fuel expenditures, and rations. Waiting on a decision to sortie puts several units at risk of damage and loss. Improved accuracy of longer-range track forecasts means decisions are made with higher confidence and farther in advance.

Computing speed has been growing at an exponential rate since the 1950's, and model accuracy increases at a rate proportional to computing power. A new plateau in numerical track prediction has been achieved since October 1994 when several centers introduced better specifications of the tropical cyclone in the initial conditions (Elsberry 1995). The skill of a model will eventually reach a predictability limit, such that it cannot predict environmental conditions with any further accuracy since it cannot account for turbulent effects.

As the model-generated errors are reduced, the major source of error becomes the uncertainty in the initial conditions, especially as tropical cyclones form and move over data-sparse oceans. To account for the initial condition uncertainty of an individual model, the method of ensemble forecasting was developed. These tropical cyclone ensemble forecast sets may be tracks predicted by global and regional models at various forecast centers (so-called poor man's ensemble), or a single model to which perturbations have been applied to initial model conditions. In general, the mean of the track ensemble will be more accurate than any of the individual members.

Value can be added to a tropical cyclone track ensemble prediction system with skillful forecaster input, which requires a solid TC Motion Meteorology Knowledge Base of the basin in which the storm occurs and a knowledge of the track error mechanisms

characteristic to various global and regional models. The specific objective is to isolate and eliminate from the ensemble any erroneous tracks before calculating the mean of the remaining tracks to produce the optimum forecast.

The Joint Typhoon Warning Center (JTWC), Pearl Harbor, HI has set a goal for tropical cyclone track forecasting accuracy of 50 n mi, 100 n mi, and 150 n mi at 24 h, 48 h, and 72 h, respectively (Cantrell and Jeffries 2002). This is necessary to ensure Naval Commands are provided with the most accurate track predictions, which will allow vessels at sea to be routed for optimum safety and fuel efficiency, while assets ashore are sortied only when necessary.

One of the tools the JTWC forecasters use is the Systematic and Integrated Approach to Tropical Cyclone (TC) Track Forecasting (hereafter the Systematic Approach), which was first introduced by Carr and Elsberry (1994) for the western North Pacific region. Its primary aim is that the forecaster will generate a track forecast with improved accuracy, provided they have available: (i) a TC Motion Meteorology Knowledge Base of sound conceptual models that classify various TC-environment situations; (ii) a Dynamical Model Forecast Traits Knowledge Base of recurring TC track forecast errors attributed to various combinations of TC structure and environment structure, and the anticipated changes; and (iii) an implementing methodology or strategy for applying these two knowledge bases to particular TC forecast situations. The Systematic Approach Forecasting Aid (SAFA), which is an ensemble-like or consensus prediction system based on the Systematic Approach, is already in place at JTWC, and has proven to be a significant forecasting aid for western North Pacific TCs (Cantrell and Jeffries 2002). A key contribution to the operational application of SAFA is a training module that has been provided to educate the JTWC forecasters of the synoptic characteristics and model track error mechanisms for the western North Pacific. The TC Motion Meteorology Knowledge Base for the western North Pacific evolved from Carr et al. (1994) and Carr and Elsberry (1997), while the Dynamical Model Forecast Traits Knowledge Base is described by Carr and Elsberry (1999, 2000a, and 2000b). A TC Motion Meteorology Knowledge Base for Atlantic TCs has been prepared by Boothe et al. (2000), and a preliminary Dynamical Model Forecast Traits Knowledge Base for the

Atlantic has been provided by Brown (2000). A TC Motion Meteorology Knowledge Base for the central and eastern North Pacific is given in Boothe (1997). The TC Motion Meteorology Knowledge Base for the Southern Hemisphere was prepared by Bannister et al. (1997, 1998) and Reader et al. (1999), and the Dynamical Model Forecast Traits Knowledge Base for that region was developed by Reader et al. (2000). A more complete description of the Systematic Approach will be provided in Chapter II.

The North Indian Ocean (NIO) is the last of the global TC basins to be considered for the application of the Systematic Approach. Although it is the smallest and least active of the tropical cyclone basins, it is one of the most operationally important to Naval units. Both Pacific and Atlantic Fleet assets must transit the NIO enroute to the Arabian Gulf while the threat of a TC is present for 11 months of a year. When the strong winds and heavy storm surge of a TC devastate the low-lying regions of the northern Bay of Bengal, humanitarian efforts by U.S. Navy and Marine Corps personnel are typically ordered.

B. BACKGROUND ON THE SYSTEMATIC APPROACH

The Systematic Approach concept mentioned previously was established by Carr and Elsberry (1994) in an effort to improve utilization of the forecasting guidance available to JTWC forecasters. The current Systematic Approach conceptual framework (SAFA training module) is illustrated in Fig. 1.1, and is made up of three phases. In the first phase, an evaluation of the current synoptic situation is based on the analysis of the dynamical model analyses, TC working best track, observations and imagery. These are the resources and analysis products commonly available to the forecaster. The TC Motion Meteorology Knowledge Base is then incorporated into the analysis when the forecaster evaluates the causes for the TC track and interprets the available imagery to determine TC size, intensity, and past motion. The resources and knowledge bases are then combined to determine the current synoptic situation. In Phase II, the resources include dynamical model track and field forecasts and objective aid track forecasts. The Dynamical Model Forecast Traits and Objective Aid Forecast Traits Knowledge Bases provide the forecaster with the tools to accurately interpret the model and objective aid forecasts. If conclusive evidence of an error exists based on the evaluations from Phase I

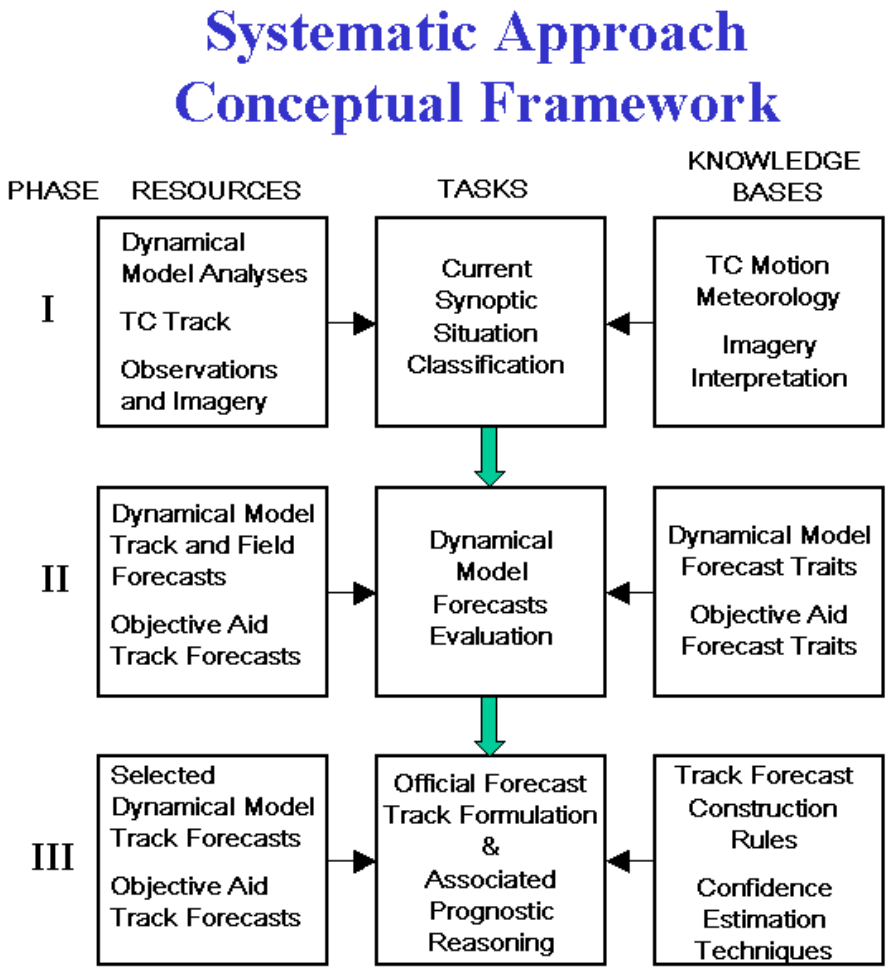

Figure 1.1. Flow chart of the three phases of the Systematic Approach in which forecasters use resources (left) and Knowledge Bases (right) to accomplish tasks (middle) (adapted from original version in Carr and Elsberry 1994)

and Phase II, the forecaster then rejects that forecast and forms a selective consensus model forecast from the remaining model tracks. In Phase III, the forecaster interprets the accepted model forecasts to formulate an official track forecast and provide associated prognostic reasoning.

The keystones to the Systematic Approach are the TC Motion Meteorology and Dynamical Model Forecast Traits Knowledge Bases and are described in detail below.

C. PURPOSE OF THIS THESIS

The purpose of this thesis is to derive similar TC Motion Meteorology and Dynamical Model Forecast Traits Knowledge Bases for TCs in the NIO basin, and to provide guidance to JTWC for use in a SAFA-like extension to the NIO. The approach and database for producing the TC Motion Meteorology Knowledge Base for the NIO will be presented in Chapters II and III. The Dynamical Model Forecast Traits Knowledge Base for the NIO will be described in Chapter IV. A summary, conclusions, and recommendations will be given in Chapter V.

THIS PAGE INTENTIONALLY LEFT BLANK

II. GLOBAL TC MOTION METEOROLOGY KNOWLEDGE BASE – ENVIRONMENT STRUCTURE

The TC Motion Meteorology Knowledge Base Framework in Fig. 2.1 contains three sets of conceptual models that may be used to characterize the motion of a tropical cyclone: Environment Structure; TC Structure; and Transitional Mechanisms.

A. ENVIRONMENT STRUCTURE

Environment structure is used in the Systematic Approach to describe the general synoptic environmental features related to tropical cyclone motion, such as the subtropical ridge, monsoon trough, and midlatitude flow. The environment structure is then divided into synoptic patterns and synoptic regions. A synoptic pattern describes the orientation of the dominant cyclones and anticyclones relative to the tropical cyclone. The synoptic region describes the position of the TC in relation to the predominant flow regime within the pattern. A pattern and region combination then defines the environment structure that is the first-order effect on tropical cyclone motion. The prior studies (see list in Chapter I) have demonstrated that each pattern/region combination has a characteristic track orientation, and each transition from one pattern/region combination

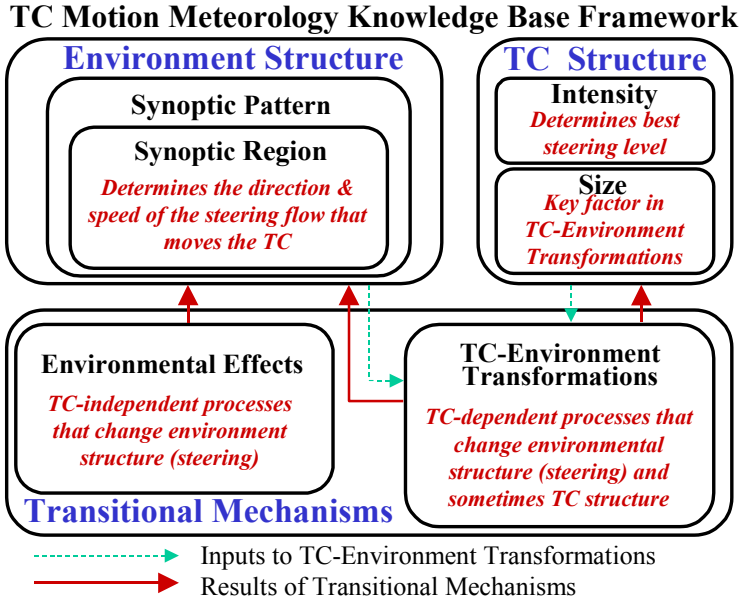
TC Motion Meteorology Knowledge Base Framework
Environment Structure
Synoptic Pattern
Synoptic Region
Determines the direction & speed of the steering flow that moves the TC
TC Structure
Intensity
Determines best steering level
Size
Key factor in TC-Environment Transformations
Environmental Effects
TC-independent processes that change environment structure (steering)
TC-Environment Transformations
TC-dependent processes that change environmental structure (steering) and sometimes TC structure
Transitional Mechanisms
Inputs to TC-Environment Transformations
Results of Transitional Mechanisms

Figure 2.1. The TC Motion Meteorology Knowledge Base Framework including the three sets of conceptual models that characterize the motion of a tropical cyclone (from Carr and Elsberry 1994).

to another implies a corresponding track change. Carr and Elsberry (1999), Boothe (1997), Boothe et al. (2000), and Reader et al. (1999) have identified three common patterns (Standard, Poleward, and Midlatitude – in Fig. 2.2 to be described below) that exist in the western North Pacific, central and eastern North Pacific, Atlantic, and Southern Hemisphere Oceans, respectively. However, each basin has a fourth pattern that is special to that basin. These special patterns will be described below after discussion of the three common patterns.

1. Standard Pattern

The Standard (S) pattern in Fig. 2.2 is the most common synoptic pattern that occurs 60%, 84%, 48%, 64% and 35% of the time in the western North Pacific, eastern/central North Pacific, Atlantic, South Indian and South Pacific Oceans, respectively (Fig. 2.3). The S pattern is characterized by two extensions of a predominantly zonal subtropical anticyclone with equatorial buffer cells (cyclonic or anticyclonic) to the south (north) in the Northern (Southern) Hemisphere. When an equatorial or monsoon trough is at least 8-10 deg. latitude from the equator, equatorial westerlies occur between the monsoon trough and the buffer cells. Between the monsoon trough and subtropical anticyclone are the tradewind easterlies.

The S pattern contains four synoptic regions where the TC motion is determined by the predominant flow around the subtropical anticyclone and the equatorial or monsoon trough. For example, the Tropical Easterlies (TE) region is south (north) of the subtropical anticyclone in the Northern (Southern) Hemisphere. Most TC tracks within this TE region are straight-runners moving westward, generally parallel to the subtropical ridge axis.

In the Poleward Flow (PF) and Equatorward Flow (EF) synoptic regions of the S Pattern (Fig. 2.2), the TC is being steered by the flow on the southwestern and southeastern (Northern Hemisphere) flanks of the subtropical anticyclone, respectively. The TC is moving toward (away from) a col between the subtropical anticyclone cells in the PF (EF) regions. The col may have been created as the anticyclone was weakened by advection of positive vorticity by the TC, by a midlatitude cyclone on the poleward side,

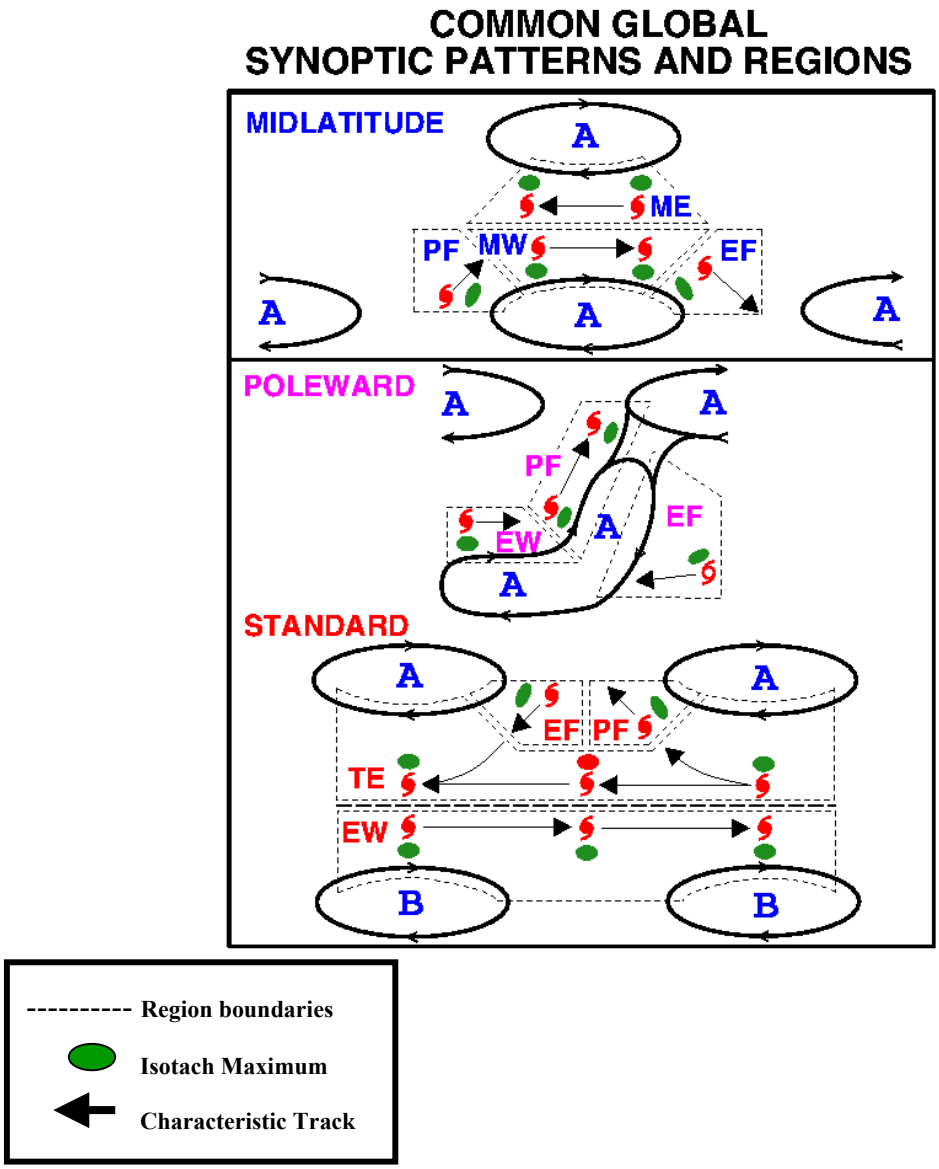

Figure 2.2. Common synoptic pattern and region conceptual models in the Systematic Approach TC Motion Meteorology Knowledge Base for the entire North Pacific, Atlantic, and Southern Hemisphere TCs relative to adjacent anticyclones (A) and buffer (B) circulations. Key to region abbreviations: EW = equatorial westerlies; TE = tropical easterlies; PF = poleward flow; EF = equatorward flow; MW = midlatitude westerlies; ME = midlatitude easterlies.

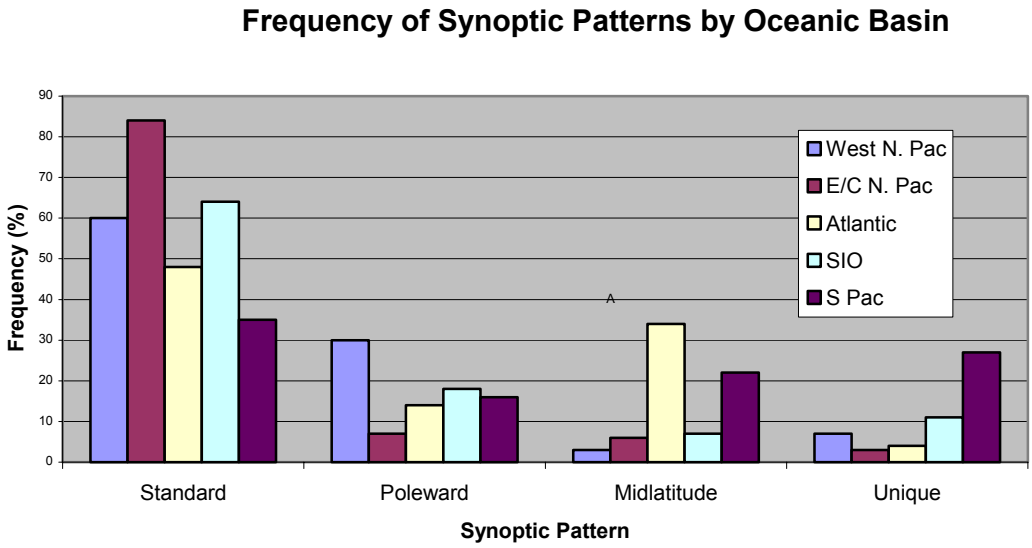

Figure 2.3. Frequency of occurrence for the common (Standard, Poleward, and Midlatitude) and the unique patterns in different tropical cyclone basins.

or by a combination of both. Given these steering flows, the TC tracks tend to be toward the northwest in a PF region and toward the southwest in an EF region. At times, the TC track may have a "stair-step" characteristic in which westward motion in the TE region is followed by poleward motion in the PF region, and then a return to a more westward track after a transition to the EF region. Such a PF to EF transition will occur as the steering flow exerted by the eastern (western) subtropical anticyclone cell weakens (strengthens). Thus, the TC translation speed will decrease, and the TC may remain nearly stationary until the western subtropical anticyclone gains steering control, which will then advect the TC toward the west-southwest.

As shown in Fig. 2.2, equatorial westerlies occur with cross-equatorial flow in response to the displacement of the monsoon trough away from the equator. A TC in the Equatorial Westerlies (EW) region is then steered by the flow between the equatorial buffer cells and the monsoon trough. Tropical cyclones in this EW region tend to move eastward for only a short time in the Northern Hemisphere before they cross the monsoon trough axis and are advected toward the west by the tropical easterly flow. This is an example of an EW-to-TE region transition within the S pattern that exhibits a track change from eastward to westward motion.

2. Poleward Pattern

The second-most common synoptic pattern is the Poleward (P) pattern (Fig. 2.3). This pattern is characterized by a meridionally-oriented trough/anticyclone, which typically forms as a result of Rossby wave dispersion from a large TC, but may also form with a "digging" midlatitude trough to the northwest (Northern Hemisphere). This P pattern is more common with the large TCs in the western North Pacific, whereas the smaller storms in the central and eastern North Pacific do not typically build a strong "peripheral anticyclone" via Rossby wave dispersion. When the peripheral anticyclone in this Rossby wake connects with the subtropical anticyclone, a TC moving westward in the TE region may have a sharp turn to a northwestward or north-northeastward track on the western side of the peripheral anticyclone. A TC in this region of the Poleward pattern is therefore in the Poleward Flow (PF) region.

A TC in the Equatorial Westerlies (EW) region of the P pattern is often at a lower latitude and is steered by the westerly flow between the monsoon trough and the equatorial buffer cells. The typical transition from the EW region in the P pattern is into the PF region as the monsoon trough changes from an east-west orientation to a meridional orientation. Tropical Cyclone then becomes steered by the flow between the poleward-oriented (or reverse-oriented) monsoon trough and the peripheral anticyclone. As in the EW region of the S pattern, a TC typically remains in this (EW) region of the P pattern for only a short time before a transition occurs to another pattern/region. Thus, the track changes from eastward to north-northeastward, as long as the P pattern persists.

When a second TC is present to the southeast of a Rossby wave train associated with a TC, the track of the second TC will be steered primarily by the northerly flow on the eastern side of the peripheral anticyclone. This region is thus termed the Equatorward Flow (EF) region. A TC in the EF region typically will experience a transition from a westward track (Northern Hemisphere) toward a more equatorward track as it comes under the steering influence of the southeastern flank of the peripheral anticyclone. However, this is a transient situation, and the tracks in the EF region of the P pattern tend to be short.

3. Midlatitude Pattern

The least frequent (Fig. 2.3) of the common patterns in every global region (Fig. 2.2) is the Midlatitude (M) pattern. A TC is considered to have entered the M pattern once it has tracked poleward of the subtropical anticyclone axis. A TC typically is decreasing in intensity in this pattern because: (i) it is at higher latitudes, the sea-surface temperature drops, vertical shear of horizontal wind increases, and conditional instability decreases; and (ii) extratropical transition begins. In other words, the TC is nearing the end of its life cycle by the time it enters the midlatitude flow associated with this pattern.

Four synoptic regions are associated with the M pattern. A typical track scenario is first in the PF region with a transition to the Midlatitude Westerlies (MW) region, and then perhaps to the EF region through simple advection of the TC around the poleward half of the subtropical anticyclone. The Midlatitude Easterlies (ME) region is formed when a midlatitude anticyclone is formed poleward of the subtropical anticyclone. A TC in the ME region is steered toward the west.

Each of the western North Pacific, central and eastern North Pacific, Atlantic, and Southern Hemisphere basins also has a synoptic pattern unique to that area as detailed in Fig. 2.4.

4. Western North Pacific Monsoon Gyre

The monsoon Gyre (G) pattern (Fig. 2.4a) is based on the existence of a large (up to 2500 km diameter) monsoon gyre that forms over the western North Pacific an average of three times per year (Boothe 1997). A TC will typically form on the eastern periphery of the monsoon gyre and be advected northward in the PF region. A bifurcation point is reached in which the steering will either advect the TC northeastward out of the G pattern and into the midlatitudes in association with the eastern subtropical anticyclone cell, or toward the northwest, where it will enter the TE region. The G/TE pattern/region is very similar to the S/TE pattern/region with the exception that it is still affected by the westward flow between the gyre and the displaced subtropical ridge. Tropical cyclones in this pattern occurred in 7% of the 4017 cases examined in the western North Pacific during 1989-1996 (Carr et al. 1997).

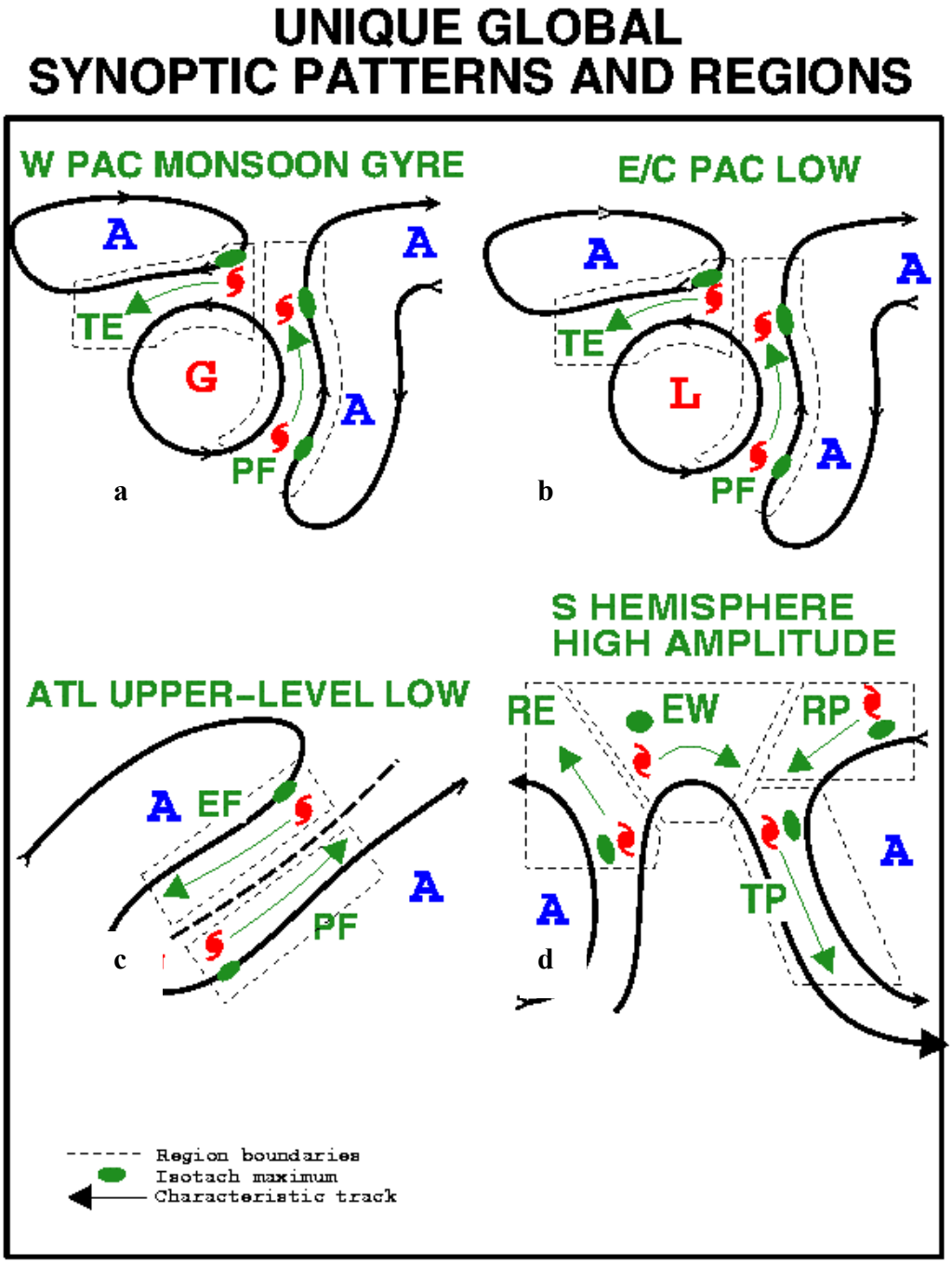

Figure 2.4. Schematic as in Fig. 2.2 of unique synoptic patterns and regions by oceanic basin: (a) Western North Pacific Monsoon Gyre; (b) Eastern and Central North Pacific Low pattern; (c) Atlantic Upper-Level Low; and (d) Southern Hemisphere High Amplitude pattern.

5. Eastern/Central North Pacific Low Pattern

Due to the southward transport of cold water by the California Current and coastal upwelling along the western boundaries of North America, an environment structure similar to the western North Pacific monsoon Gyre pattern is not found in the central and eastern North Pacific. However, upper-level lows from the midlatitudes often become cutoff and drift southwestward into lower latitudes. Thus, an upper-level synoptic pattern is created that has a steering environment somewhat similar to that of the lower-tropospheric monsoon gyre in the western North Pacific. This synoptic pattern is called the eastern/central North Pacific Low (L) pattern (Fig. 2.4b). Depending upon the location of the TC and the structure of the cutoff low, the upper-level flow will either shear apart a TC or advect it poleward. As a TC approaches the Low from the east in the TE region, it will be advected poleward around the eastern periphery of the low in the PF region. Because the TC is steered over cooler water in this region, the TC tends to dissipate before reaching a bifurcation point. Tropical cyclones in this pattern occurred in only 3% of the 1858 cases in the central/eastern North Pacific during 1990-1996 (Boothe 1997).

6. Atlantic Upper-Level Low Pattern

The upper-level Low (L) synoptic pattern in the Atlantic (Fig. 2.4c) is characterized by an upper-level midlatitude trough or low that has become the dominant steering flow for the affected TC. The trough typically has a northeast-to-southwest tilt with correspondingly tilted anticyclones to the east and the west. In the Equatorward Flow (EF) region, a TC will be steered by the southwestward flow between the anticyclone to the northwest and the trough to the southeast. A TC in the Poleward Flow (PF) region will be steered by the northeastward flow between the trough to the northwest and the anticyclone to the southeast. This pattern occurred in 4.4% of the 1568 cases analyzed in the Atlantic during 1990-1998 (Boothe et al. 2000).

7. Southern Hemisphere High-Amplitude Pattern

The subtropical anticyclone between the east African coast and the central South Pacific is highly transient and does not maintain the steady zonal orientation that is often found in the Northern Hemisphere. The subtropical anticyclone is comparatively weak

because it is often disrupted by high-amplitude trough/ridge systems that are tilted northwest-to-southeast (Bannister et al. 1997).

Four synoptic regions are defined for this High-amplitude (H) synoptic pattern (Fig. 2.4d). The Equatorial Westerlies (EW) region occurs when a TC is in the region of eastward steering between the apex of the high-amplitude trough and the equator. Tropical Cyclone may then be advected into the Trough Poleward (TP) region between the trough and the eastern subtropical anticyclone. In this special case, the TC is continued in the H pattern/ PF region even after it is advected through the subtropical ridge axis, rather than being defined to having experienced a transition to the M pattern (Reader et al. 1999). A TC in the Ridge Poleward (RP) region on the northwestern periphery of the eastern subtropical anticyclone may also be advected into the TP region. A TC in the Ridge Equatorward (RE) region is being steered by the equatorward flow between the high amplitude trough and the western subtropical anticyclone. In Fig. 2.4d, only a single anticyclone to the west or to the east may be present. This H pattern occurred in 11% of the South Indian Ocean and 27% of the South Pacific Ocean cases out of 2731 Southern Hemisphere cases studied between 1990-1999 (Reader et al. 1999).

B. NORTH INDIAN OCEAN TC MOTION METEOROLOGY KNOWLEDGE BASE

The synoptic pattern/region was determined through examination of NOGAPS analysis fields at four primary atmospheric levels from 1991-2001 to derive a TC Motion Meteorology Knowledge Base for the NIO. The 200 mb level was used to look for vertical shear and evidence of anticyclonic outflow in intense TCs. The 500 mb level was examined for synoptic patterns steering a TC. This level is the primary steering level in the NIO. The 700 mb and 850 mb levels were the primary steering levels for very weak storms. Archived satellite imagery consisting of a mix of hemispheric and global images for 1991 to 1997 was also reviewed. More detailed images were available between 1998-2001 from the European Organisation for the Exploitation of Meteorological Satellites (EUMETSAT) archive. Despite the special flow structures in the NIO, the three common synoptic patterns found in the four previously discussed TC basins are also found in the NIO and are discussed below.

The TC Motion Meteorology Knowledge Base for the North Indian Ocean is summarized in Fig. 2.5. Focusing on the Environment Structure in the upper left-hand corner, only the three common (Standard, Poleward, and Midlatitude—see Chapter II A.1-3 above) synoptic patterns were found to exist in the NIO. Tropical cyclone structure will only be briefly discussed, and Transitional Mechanisms will be discussed in Chapter III.

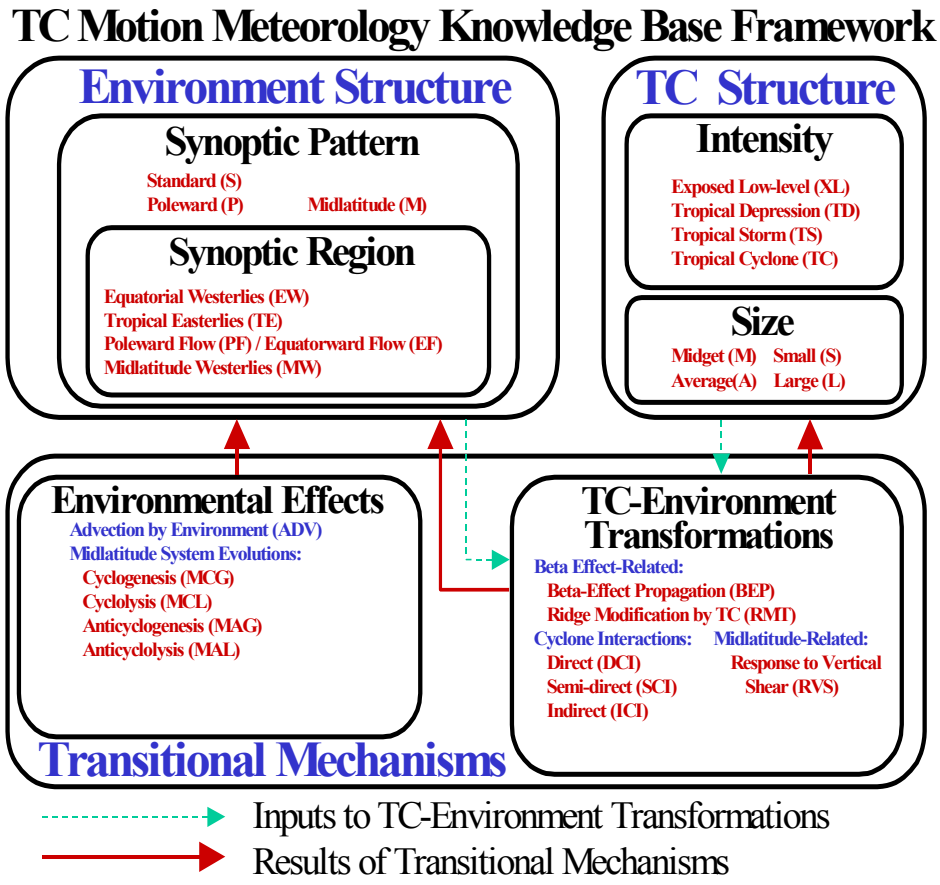

Figure 2.5. TC Motion Meteorology Knowledge Base as in Fig. 2.1 for the North Indian Ocean, and thus includes only those synoptic pattern/regions and Transitional Mechanisms that apply to the North Indian Ocean TCs.

C. ENVIRONMENT STRUCTURE IN THE NIO

The Environment Structure in the NIO is significantly different from other global regions so far examined, mainly as a result of the structure of the oceanic basin. The NIO covers an area equivalent to 4,500,000 sq n mi from the equator to 25 deg. N and from 50 deg. to 100 deg. E. The basin is made up of the Bay of Bengal to the east

and the Arabian Sea to the west of the Indian subcontinent. The Asian continent to the north of the NIO makes the basin unique to the previous four basins. Extremely high elevations occur over the Himalayan mountain range, and even the Tibetan Plateau elevations reach to the 700 mb level, so that the atmospheric boundary layer extends to higher elevations. During the spring and fall, midlatitude weather systems may extend to lower latitudes, especially over the Arabian Sea. Cold air outbreaks farther east are impeded by the Himalayas.

Two subtropical anticyclone cells are present throughout the year with an average ridge axis at 500 mb near 20 deg. North. The western cell of the subtropical anticyclone is centered over east Africa, and is separated from the eastern cell over southwest Asia by a col typically located over northern India. The locations of these two subtropical anticyclone cells and the central col shift to the east and west along the 20 deg. latitude line. Their positions will tend to shift westward with TCs in the Arabian Sea and eastward with TCs in the Bay of Bengal.

During the pre- and post-monsoon periods when TCs exist, the monsoon trough extends zonally from East Africa and across the South Arabian Sea, across southern India and the Bay of Bengal, and then southwest to northeast into the South China Sea. Large (radius as large as 600 km) monsoon depressions often form in the Bay of Bengal within the monsoon trough.

The TC season is nearly year-round in the NIO, with TCs during 1991-2001 occurring in every month except August. Two frequency maxima occur in the months of May to June and October through December. During the summer monsoon period, large vertical wind shear between lower-tropospheric westerlies and upper-tropospheric easterlies is unfavorable for TC formation.

D. SYNOPTIC PATTERNS AND REGIONS IN THE NIO

No unique synoptic pattern as in Fig. 2.4 was identified for the period 1991-2001, which covered 64 TCs and 656 cases. Within the three common patterns (Fig. 2.2), two synoptic regions were not found to exist in the NIO region: the ME region of the Midlatitude Pattern and the EF region of the Poleward Pattern. Further discussion will be provided in the following sections.

The TC tracks in the NIO (Fig. 2.6) rarely cross the Indian subcontinent, which essentially divides the NIO region into two subregions of the Bay of Bengal (BOB) and the Arabian Sea (AS). In the BOB, a TC typically forms in the southeast to south-central portion of the BOB, travels in a general westward direction and dissipates over central India, or recurves to the northeast and makes landfall in northern India, Bangladesh, or Myanmar. In the AS, TC formation generally occurs off the west coast of India. The subsequent tracks are then westward and the cyclones either dissipate over the open ocean or make landfall in Somalia or Oman. Only a few TCs recurve to the north-northeast and make landfall in northern India.

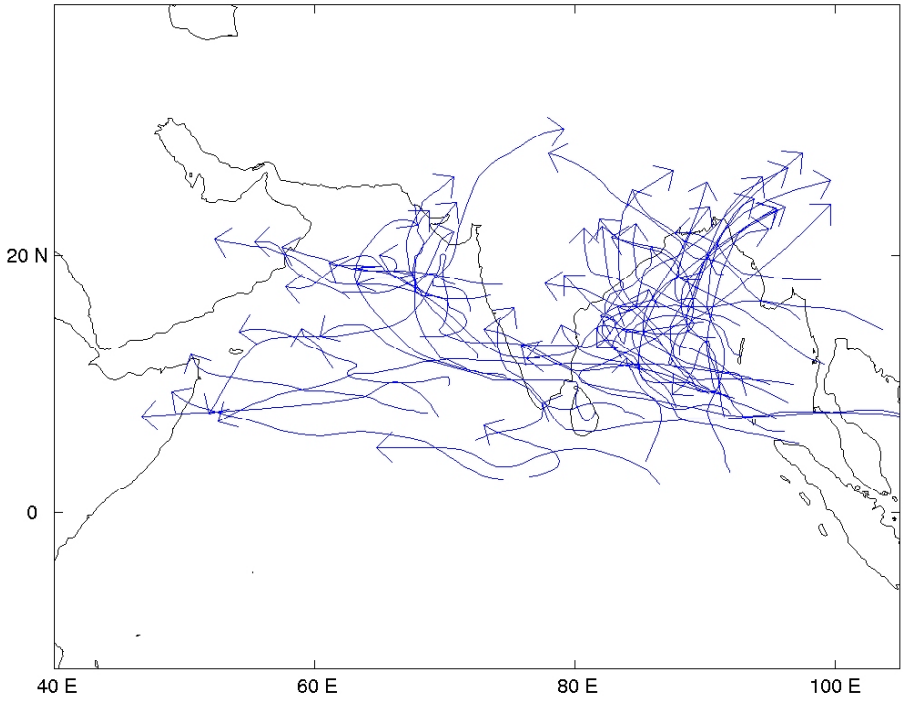

Figure 2.6. All TC tracks in the North Indian Ocean in all synoptic pattern/regions during 1991-2001.

1. NIO Standard Pattern

The Standard (S) pattern conceptual model from the western North Pacific (Fig. 2.7) is found to apply in 74.7% of the 656 NIO cases studied between 1991-2001 (Fig. 2.8). The high percentage of Standard pattern cases is because most TCs are formed in the monsoon trough and then are steered by prevailing tropical easterly winds, and these TCs are of only moderate intensity and size so that a P pattern is not common. The western and eastern subtropical anticyclone cells and the zonally oriented monsoon trough to the south are the primary synoptic features that steer the TC tracks in this S pattern.

a. S/TE Pattern/Region

The S/TE pattern/region is the most common in the NIO and occurs in 44.2% of the 656 cases considered (Fig. 2.8). Tropical cyclone tracks in the S/TE pattern/region are predominantly from east to west (Fig. 2.9), and generally are parallel to the subtropical anticyclone axis. Only one TC during 1991-2001 actually crossed the

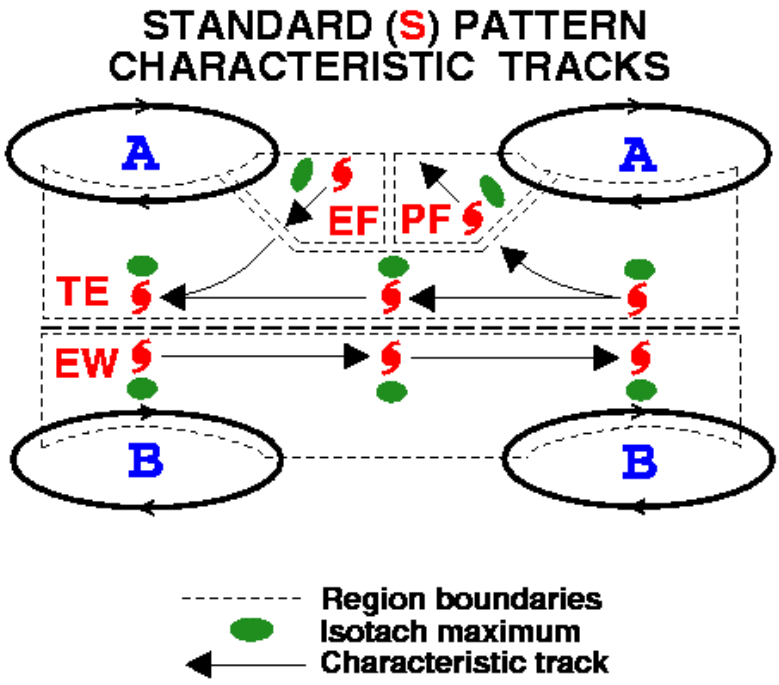

Figure 2.7. Schematic of the Standard pattern in the North Indian Ocean, which is the same as the Standard pattern common to previously examined oceanic basins as in Fig. 2.2.

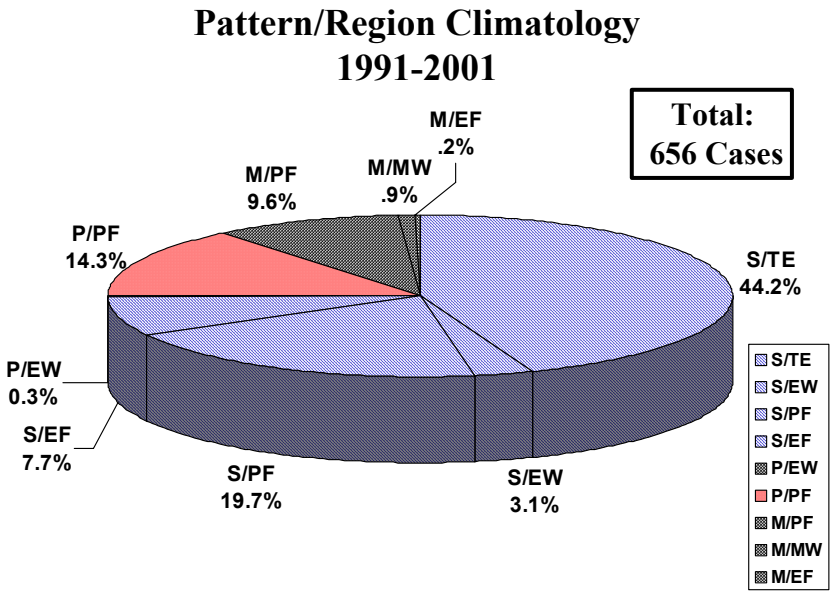

Figure 2.8. Climatology of synoptic pattern/regions in the NIO environment for 656 cases during 1991-2001.

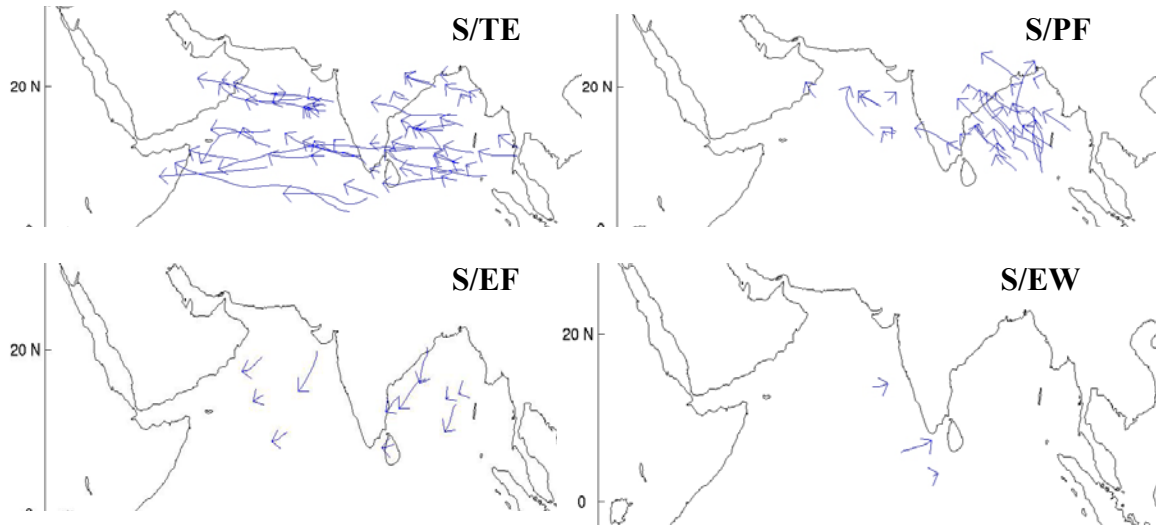

Figure 2.9. Standard pattern TC tracks in the NIO during 1991-2001: (upper left) S/TE pattern/region; (upper right) S/PF pattern/region; (lower left) S/EF pattern/region; and (lower right) S/EW pattern/region.

southern tip of India from the BOB to the AS while in this pattern/region. This pattern/region is also most frequent in the months of May to June and October through December (Table 2.1), which corresponds to the two maxima in the NIO tropical cyclone season.

	JAN	FEB	MAR	APR	MAY	JUN	JUL	AUG	SEP	OCT	NOV	DEC
S/TE	10	4	0	3	25	35	4	0	19.5	46	79	65
S/EW	0	2	0	0	4	3	1	0	1.5	1	7.5	0
S/PF	0	0	0	11	15.5	15	0	0	9	32	39.5	7
S/EF	0	0	4.5	0	0	0	0	0	1	17	19.5	9
P/EW	0	0	0	0	0	0	0	0	0	2	0	0
P/PF	0	2	4.5	2	34	14	0	0	6	17	10.5	4
M/PF	0	0	0	4	26.5	10	0	0	3	5.5	14	0
M/MW	0	0	0	0	0	1	0	0	0	0	4.5	0
M/EF	0	0	0	0	0	0	0	0	0	0	1.5	0

Table 2.1. Occurrences of synoptic pattern/regions defined in Fig. 2.2 by month in the North Indian Ocean for 1991-2001. Each transition occurrence on either a 00 and 12 UTC analysis is counted as a value of 1 if the TC intensity was >25 kt. A value of 0.5 was assigned when a TC was in a transition between two synoptic pattern/regions.

b. S/TE Pattern/Region Case Study

The relatively small (300 n mi diameter) storm TC 04A during 1998 formed in a fairly zonal monsoon trough in the AS. The storm reached tropical storm strength, which was the maximum intensity, at 00 UTC 30 September. Due to the small size and low intensity, the TC tracked westward from 29 September to 1 October (Fig. 2.10a) essentially as a "cork in the stream" in the predominantly westward steering south of the east-west oriented subtropical anticyclone (Fig. 2.10b). The isotach maximum to the north of the TC as illustrated in the S/TE pattern/region schematic (Fig. 2.7) and

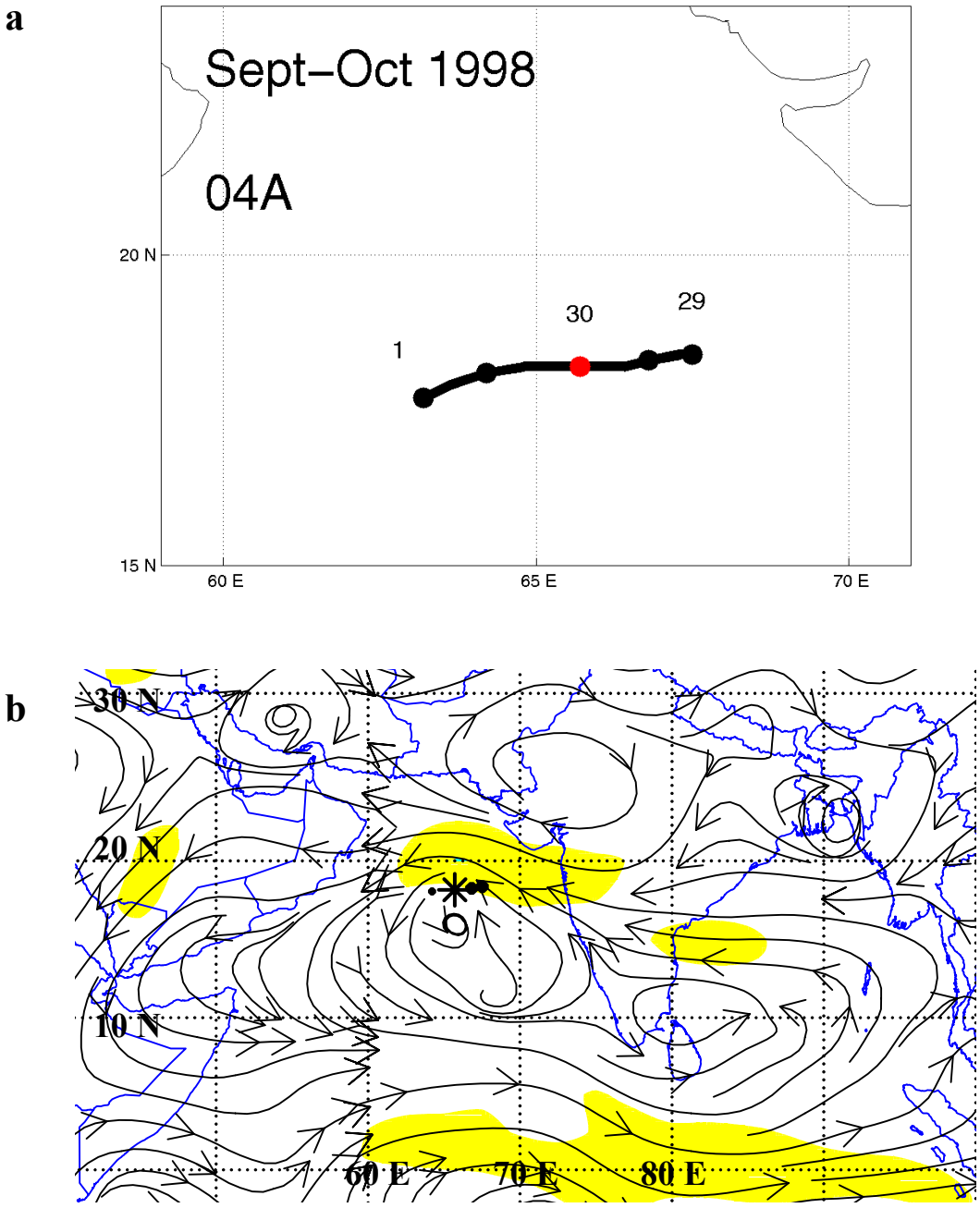

Figure 2.10. (a) Track of TC 04A from 00 UTC 29 September through 00 UTC 1 October 1998; (b) NOGAPS 500-mb streamlines (thin solid) and isotachs (shaded) at 10-kt intervals beginning at 20 kt for 00 UTC 30 September.

depicted in the NOGAPS analysis (Fig. 2.10b) is consistent with the westward track in Fig. 2.10a. The track deflection to the south of west on 1 October (Fig. 2.10a) is consistent with a similar northeast-southwest orientation in the subtropical anticyclone axis in that area on that date (not shown). This is an example of how the conceptual model in Fig. 2.7 should be regarded as a template to be adjusted when the subtropical anticyclone is not oriented east-west.

c. S/PF Pattern/Region

The S/PF pattern/region was the second-most common in the NIO and occurred in 19.7% of 656 cases (Fig. 2.8). Tropical cyclone tracks in the S/PF pattern/region (Fig. 2.9) are northwestward, as the TC advects along the southwest periphery of a subtropical anticyclone cell to the northeast (Fig. 2.7). Tropical cyclones in the PF region of the S (also for the P and M) pattern are often the most damaging as their northwestward (northeastward) tracks result in landfall along the poleward margin of the NIO. When the coastal water is shallow, these TCs can result in extreme flooding due to storm surge. Most TCs in the S/PF pattern/region occur in October and November (Table 2.1) with another peak in May and June.

d. S/PF Pattern/Region Case Study

After TC 06B formed in the southern BOB, the TC was steered northwestward from 13 - 16 November 1998 (Fig. 2.11a) under the influence of the large amplitude subtropical anticyclone cell to the northeast (Fig. 2.11b). The northwestward track (Fig. 2.11b) might be considered to have resulted from northwestward flow on the southwestern side of the subtropical anticyclone or the northeastward flow on the southeastern side of an approaching midlatitude trough to the west of the TC. The isotach maximum to the east-northeast of the TC is similar to the S/PF pattern/region of the S pattern (Fig. 2.7), which indicates that the subtropical anticyclone is the dominant steering influence. That is, the TC position in relation to the subtropical anticyclone, along with the position of the isotach maximum, supports an S/PF pattern/region classification. As TC 06B advected around the subtropical anticyclone, the intensity increased and reached a maximum of 85 kt at landfall on 15 November (Fig. 2.11a).

a

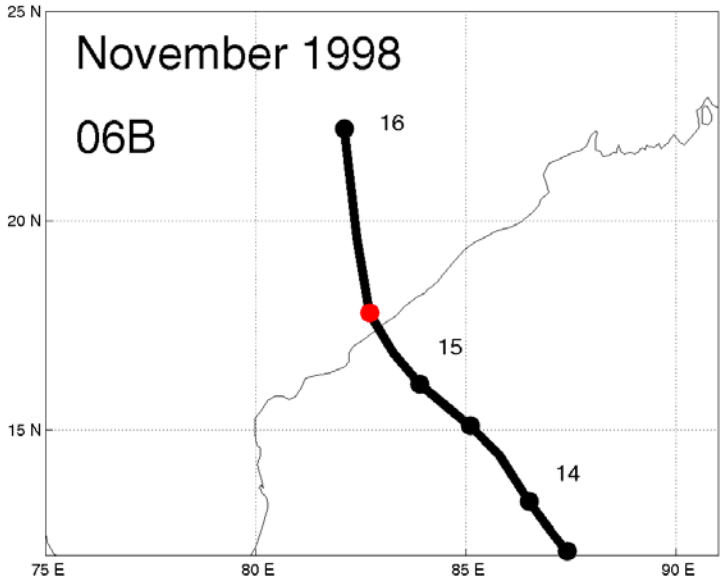

b

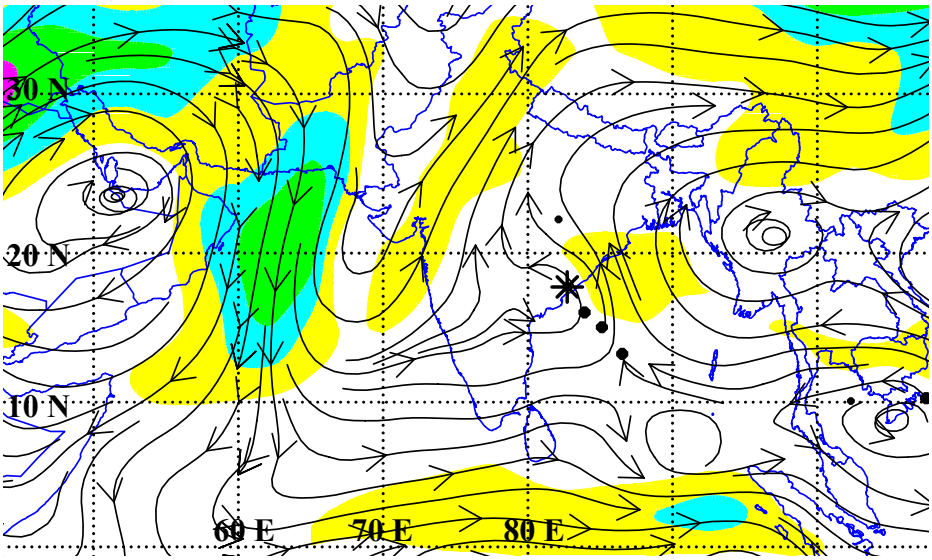

Figure 2.11. (a) Track of TC 06B from 12 UTC 13 November through 00 UTC 16 November 1998; (b) NOGAPS analysis field as in Fig. 2.10b except for 12 UTC 15 November 1998.

e. S/EF Pattern/Region

The S/EF pattern/region occurred in 7.7% of the 656 cases (Fig. 2.8), with most of the S/EF cases from October to December (Table 2.1). Strong midlatitude circulations in the Northern Hemisphere summer result in greater zonal shifts in the subtropical anticyclones, which allows the western subtropical anticyclone cell to become dominant and "take over" steering control from the eastern subtropical anticyclone cell. Tropical cyclones in the S/EF pattern/region move toward the southwest and have relatively short tracks (Fig. 2.9) and on average last only 36 h before dissipating or undergoing a transition to the S/TE pattern/region.

f. S/EF Pattern/Region Case Study

Tropical Cyclone 04B formed to the east of Sri Lanka on 23 December 2000 (Fig. 2.12a). From 12 UTC 26 December to 00 UTC 27 December, TC 04B was in the S/EF pattern/region as it crossed northern Sri Lanka with maximum winds of 65 kt. The western subtropical anticyclone cell centered over the Gulf of Aden extends far to the east and is stronger than the small anticyclonic cell to the east of the TC at approximately 10 deg. N and 90 deg. E (Fig. 2.12b). Thus TC 04B is in the southeastern quadrant of the western subtropical anticyclone cell. Because of the strength of the subtropical anticyclone to the northwest, the TC is being steered south of west after previously having moved westward (Fig. 2.12a). The now southwestward track is supported by the isotach maximum to the west of the TC (Fig. 2.12b), which is consistent with TC 04B being in the S/EF pattern/region as in Fig. 2.7.

g. S/EW Pattern/Region

The least common region in the Standard pattern (Fig. 2.7) is the Equatorial Westerlies (EW), which occurs in only 3.1% of the 656 cases examined (Fig. 2.8). Tropical cyclones in this S/EW pattern/region are typically found in the AS only and move eastward in the prevailing westerly flow (Fig. 2.9). The S/EW pattern/region occurs most frequently in November when the monsoon trough is returning to the equator (Table 2.1). Tropical cyclones remain in this pattern/region for a short time before stronger tropical easterlies in the S/TE pattern/region become the predominant steering flow.

a

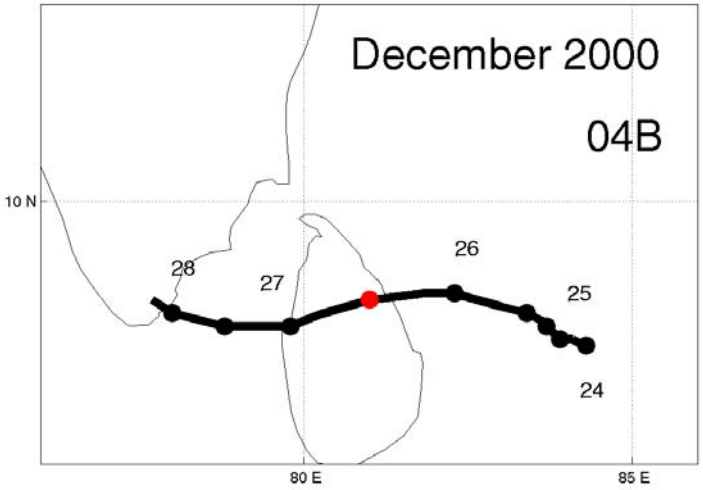

b

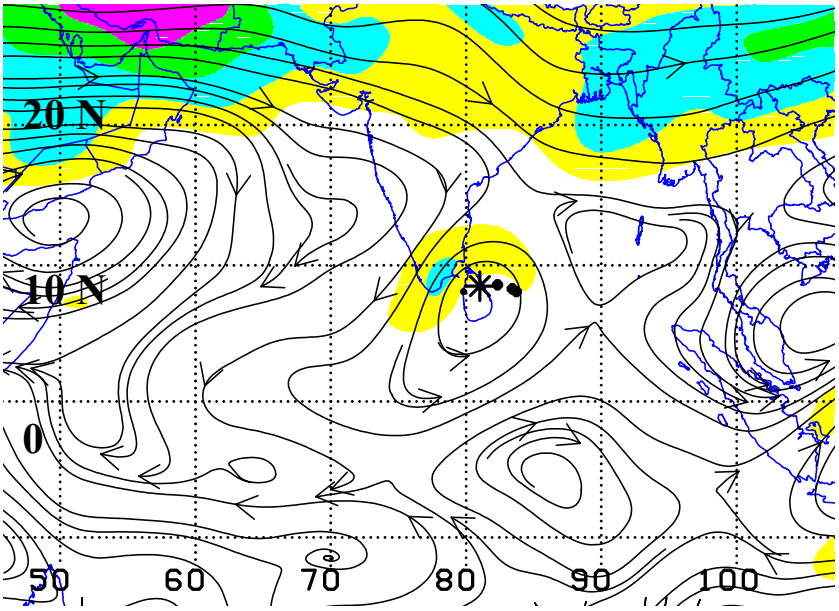

Figure 2.12. (a) Track of TC 04B from 00 UTC 24 December through 06 UTC 28 December 2000; (b) NOGAPS analysis field as in Fig. 2.10b except for 12 UTC 26 December 2000.

h. S/EW Pattern/Region Case Study

Tropical Cyclone 01A of 1993 formed in a weak monsoon depression to the southwest of India at approximately 6 deg. N (Fig. 2.13a). As illustrated in Fig. 2.13b, TC 01A was embedded in a weak westerly flow in association with a cross-equatorial flow induced by the monsoon trough to the northwest and a buffer cell to the southeast of the TC. The isotach maximum to the south and southeast of the TC is stronger and more extensive than the isotach maximum to the north, which is consistent with an eastward track from 12 UTC 5 November to 12 UTC 7 November 1993 (Fig. 2.13a). The relatively weak intensity of the TC at this time (Tropical Disturbance strength) allows the steering to be controlled by the stronger eastward flow at the beginning of the storm. The storm would later experience a transition to the S/TE pattern as a result of a growing subtropical anticyclone to the north, which is known as Midlatitude Anticyclogenesis (to be discussed in Chapter III).

2. NIO Poleward Pattern

The Poleward (P) pattern circulation in the NIO (Fig. 2.14a) is essentially the same as in the western North Pacific basin except that no TC was identified in the Equatorward Flow (EF) region during the 11 years examined in this study. Recall that it is a second TC in the P/EF region that is to the southeast of a larger TC in the P/EW or P/PF pattern/region. Two TCs very rarely occur in the NIO in close enough proximity for this P/EF pattern/region to occur.

Another difference lies in how the P pattern in the NIO is formed relative to the western North Pacific, where the P pattern usually takes place when a large TC forms a peripheral anticyclone through Rossby wave dispersion (to be discussed in Chapter III). This peripheral anticyclone then grows large enough to connect with the eastern subtropical anticyclone cell, which creates a southwest-to-northeast oriented anticyclone to the east of the TC. In the NIO, the P pattern may form in two additional ways. The first is a variation of the western North Pacific method, except the large TC intensifies an equatorial buffer cell (anticyclone if the circulation is clearly in the Northern Hemisphere) to cause a connection with the subtropical anticyclone, without a separate

a

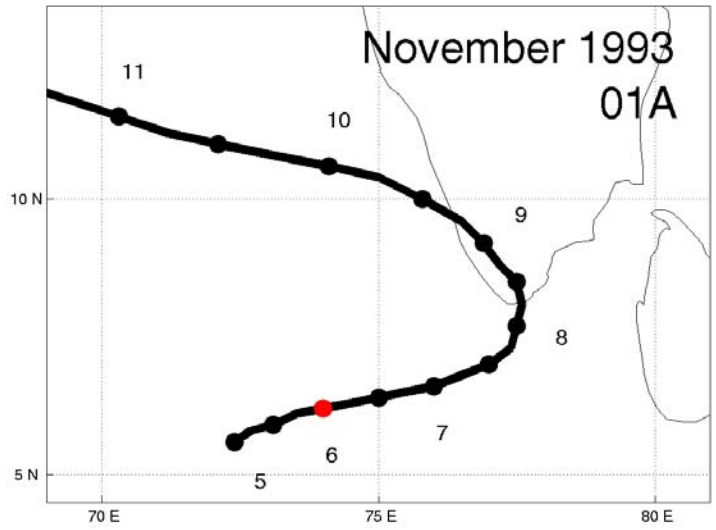

b

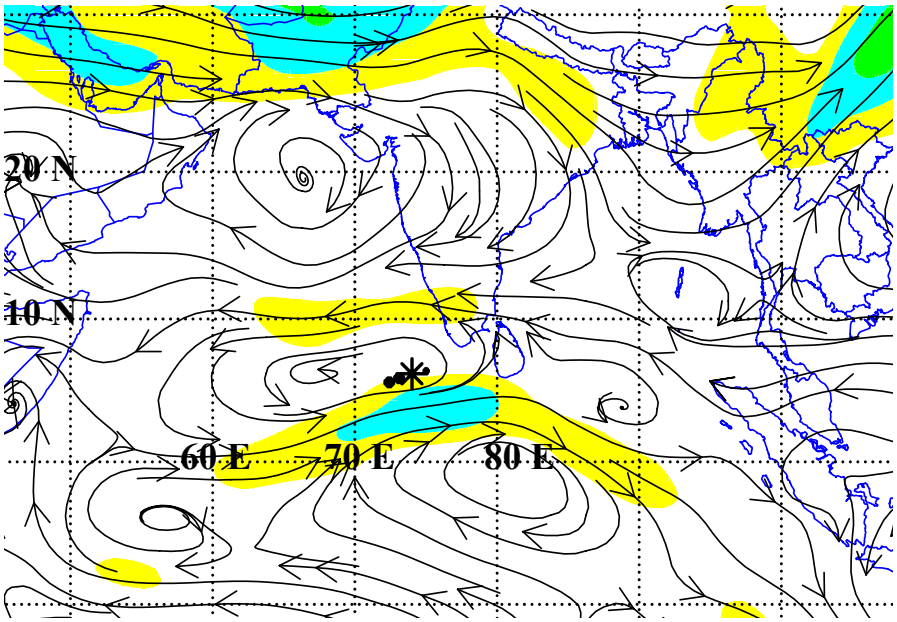

Figure 2.13. (a) Track of TC 01A from 00 UTC 5 November through 06 UTC 11 November 1993; (b) NOGAPS analysis field as in Fig. 2.10b except for 00 UTC 6 November 1993.

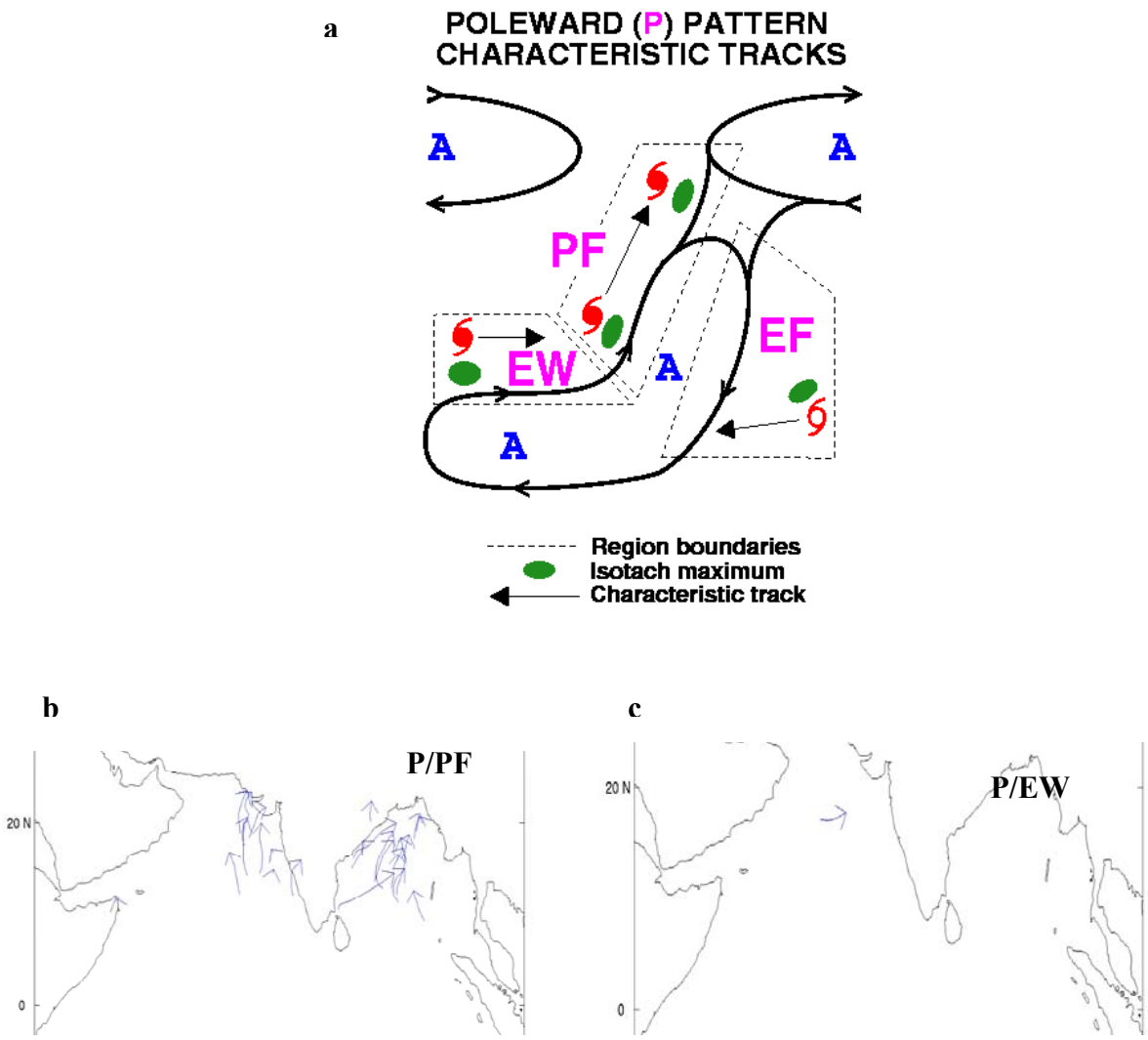

Figure 2.14. (a) Schematic of the Poleward pattern in the North Indian Ocean, which is the same as the Poleward pattern common to previously examined oceanic basins as in Fig. 2.2. Poleward pattern TC tracks in the NIO during 1991-2001 included: (b) P/PF pattern/region; and (c) P/EW pattern/region.

peripheral anticyclone formation. Second, intense heating over southeast Asia may cause an anticyclone formation aloft over the Malay Peninsula. Either a peripheral anticyclone associated with a large TC or an equatorial buffer cell will connect with the Malay Peninsula anticyclone (versus with the subtropical anticyclone) and thereby create a meridional anticyclone. The Poleward pattern occurred in 14.6% of 656 cases between 1991-2001 (Fig. 2.8), and most commonly occurs in May (Table 2.1).

a. P/PF Pattern/Region in NIO

The PF region was the most common in the Poleward (P) pattern of the NIO and occurried in 14.3% of 656 cases (Fig. 2.8). Tropical cyclones in the P/PF pattern/region have a characteristic northward or northeastward track (Fig. 2.14b) parallel to the axis of the meridional anticyclone to the east. These poleward-moving TCs are often the most destructive TCs in the NIO since they bring intense winds and high storm surges to the low-lying areas in northern India and Bangladesh. As discussed in the previous paragraph, the P pattern may form in three different ways. The method of formation affects the appearance of the P/PF pattern/region and two of the three methods are presented in the following case studies.

b. Malay Peninsula Anticyclone P/PF Case Study

At 00 UTC 18 October 1999, the main synoptic feature affecting the track of TC 04B (Fig. 2.15a) is an anticyclone over Thailand to the southeast and an equatorial buffer cell at approximately 2 deg. N and 83 deg. E (Fig. 2.15b). The two anticyclonic circulations are connected in a southwest-to-northeast orientation. Tropical Cyclone 04 B is a large TC to the northwest of the anticyclones and is moving toward the north (Fig. 2.15a). The isotach maximum to the east-northeast of TC 04B in Fig. 2.15b supports the northward steering influence of the northern portion of the P pattern in association with the Malay Peninsula anticyclone. This meridional ridge formation occurred when TC 04B was already so far north that only the north-northeastward steering flow associated with the Malay Peninsula anticyclone (not the equatorial buffer cell) was affecting the track of TC 04B. Also, ridging is still present to the north of TC 04B, and yet it is moving due north. The TC may be classified in the S/PF pattern/region. However, due to the ridging associated with the Malay Peninsula anticyclone to the north, the TC is still in the P/PF pattern/region. That is, the strong Malay anticyclone is required for TC 04A to move toward the north as in Fig. 2.15a.

a

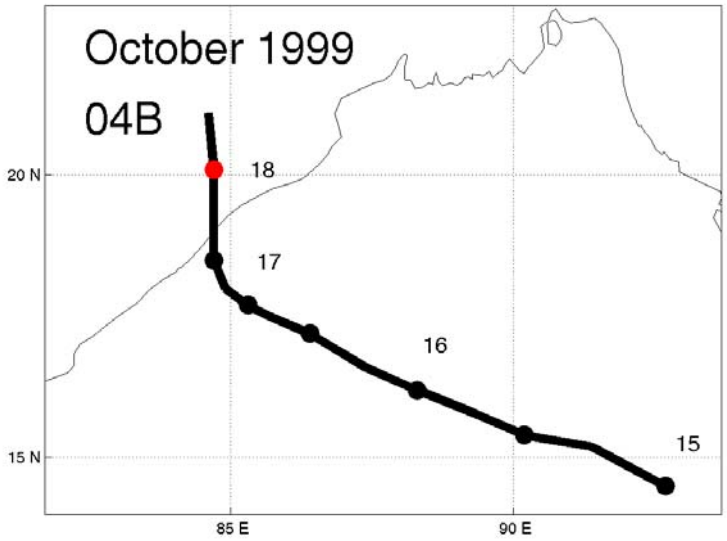

b

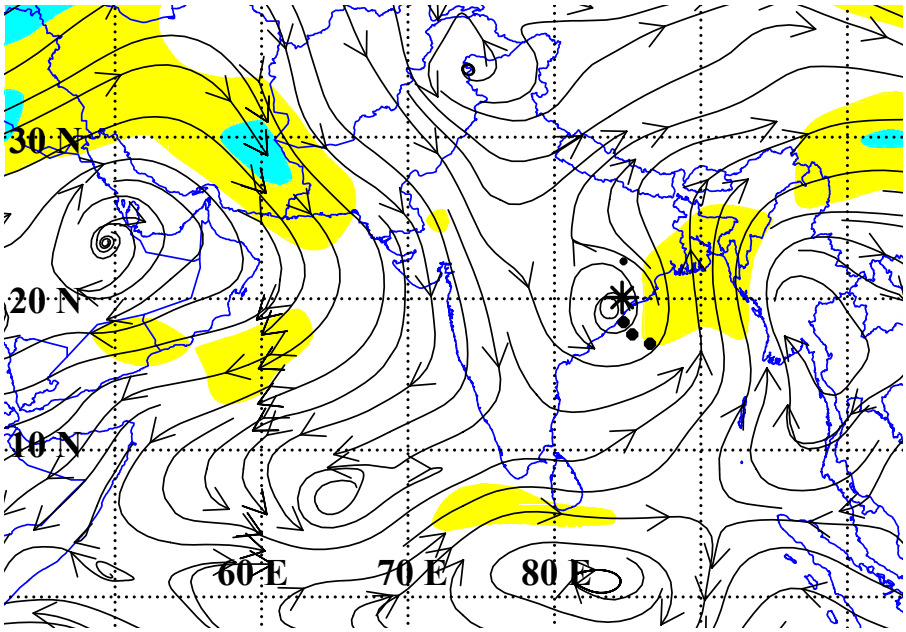

Figure 2.15. (a) Track of TC 04B from 00 UTC 15 October through 06 UTC 18 October 1999; (b) NOGAPS analysis field as in Fig. 2.10b except for 00 UTC 18 October

c. Northern Anticyclone P/PF Case Study

Tropical Cyclone 02A formed in the AS southwest of India on 15 May 1999 (Fig. 2.16a). A subtropical anticyclone was to the north over northwestern India and an extensive equatorial buffer cell was directly to the south of TC 02A (Fig. 2.16b). The TC analyzed in the NOGAPS 500 mb streamline analysis was relatively large as shown in Fig. 2.16b. Initially the TC was moving toward the northwest (Fig. 2.16a) under the influence of the northern subtropical anticyclone. As the TC moved to the northwest, it began forming a peripheral anticyclone to the southeast. The peripheral anticyclone connected to the subtropical anticyclone to the north, which was now extending to the east-southeast (Fig. 2.16c). The equatorial buffer cell was also being extended to the northeast with the development of the peripheral anticyclone. In Fig. 2.16d, the peripheral anticyclone, northern anticyclone, and equatorial buffer cell now form one meridional anticyclone. The position of the strongest nearby isotach maximum is to the east-southeast of the TC, which is consistent with the northeastward track.

d. P/EW Pattern/Region in NIO

The P/EW pattern/region was the least common (Fig. 2.8) of all the pattern/regions examined, and it occurred in only two of the 656 cases in association with only one TC. The EW region is associated with the eastward flow on the northern zonal side of the anticyclone in the Poleward pattern (Fig. 2.14a), which causes the TC to move toward the east (Fig. 2.14c). Due to the infrequency of this pattern/region, no case studies will be presented.

3. NIO Midlatitude Pattern

The midlatitudes are significantly different in the NIO compared to other TC basins of the world because of the presence of land poleward of 25 deg. N throughout the NIO. As TCs are advected around the subtropical anticyclone in the NIO they often dissipate over land prior to entering the Midlatitude (M) pattern. When a TC is able to move north of the subtropical anticyclone axis, it is often because the subtropical anticyclone axis has been displaced to lower latitudes, which provides the TC with a longer “over-water” time and subsequent low-level moisture and heat to sustain its

a

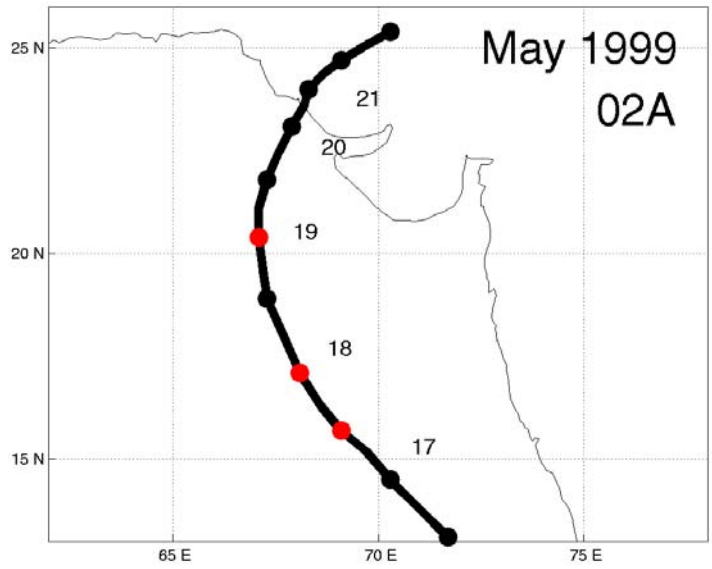

b

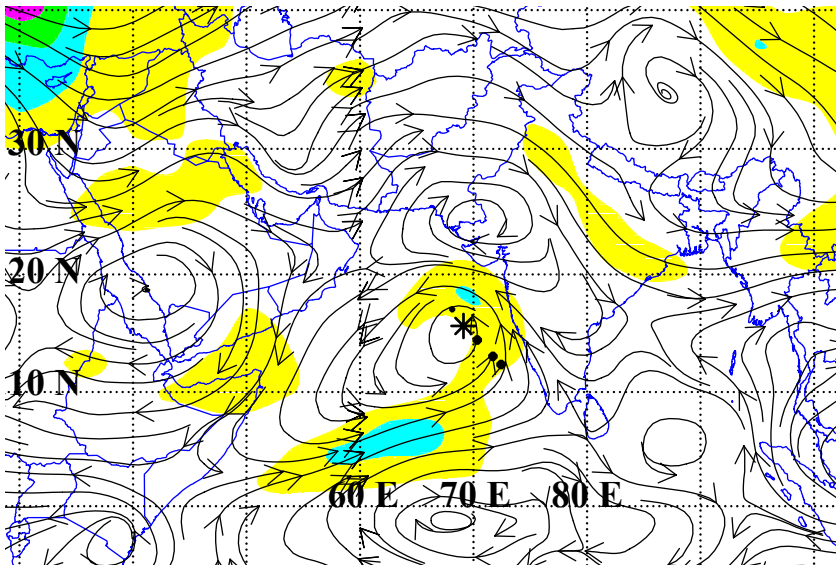

Figure 2.16. (a) Track of TC 02A from 12 UTC 16 May through 12 UTC 21 May 1999; (b) NOGAPS analysis field as in Fig. 2.10b except for 12 UTC 17 May; (c) 00 UTC 18 May; and (d) 00 UTC 19 May.

c

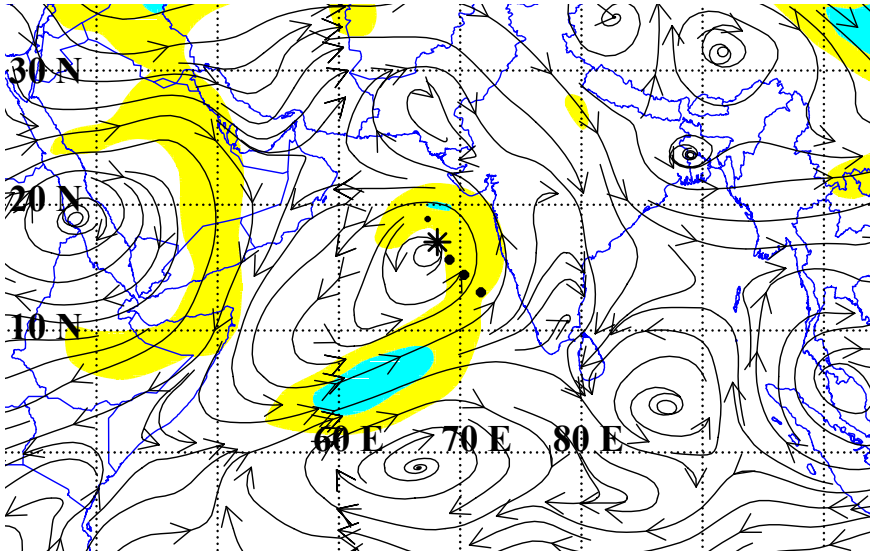

d

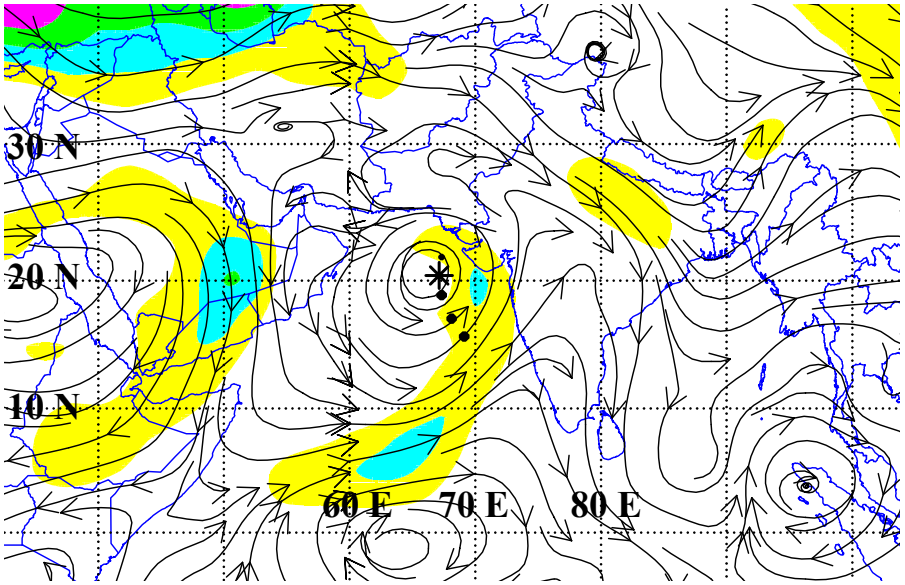

Figure 2.16. (continued)

existence. As a result, the M pattern (Fig. 2.17a) is the least frequent of the three common patterns as it occurred in only 10.7% of the 656 cases examined (Fig. 2.8).

a. M/PF Pattern/Region in NIO

The Poleward Flow (PF) region is the most common in the Midlatitude pattern because it is the first region encountered by a TC as it is advected through the subtropical anticyclone axis from either the Standard or Poleward pattern into the M pattern. Predominant tracks in the Midlatitude pattern are toward the northeast (M/PF) or east (M/MW) in the NIO (Fig. 2.17b). The length of time the TC remains in the Midlatitude pattern is primarily dependent on the latitude at which it transitions into the

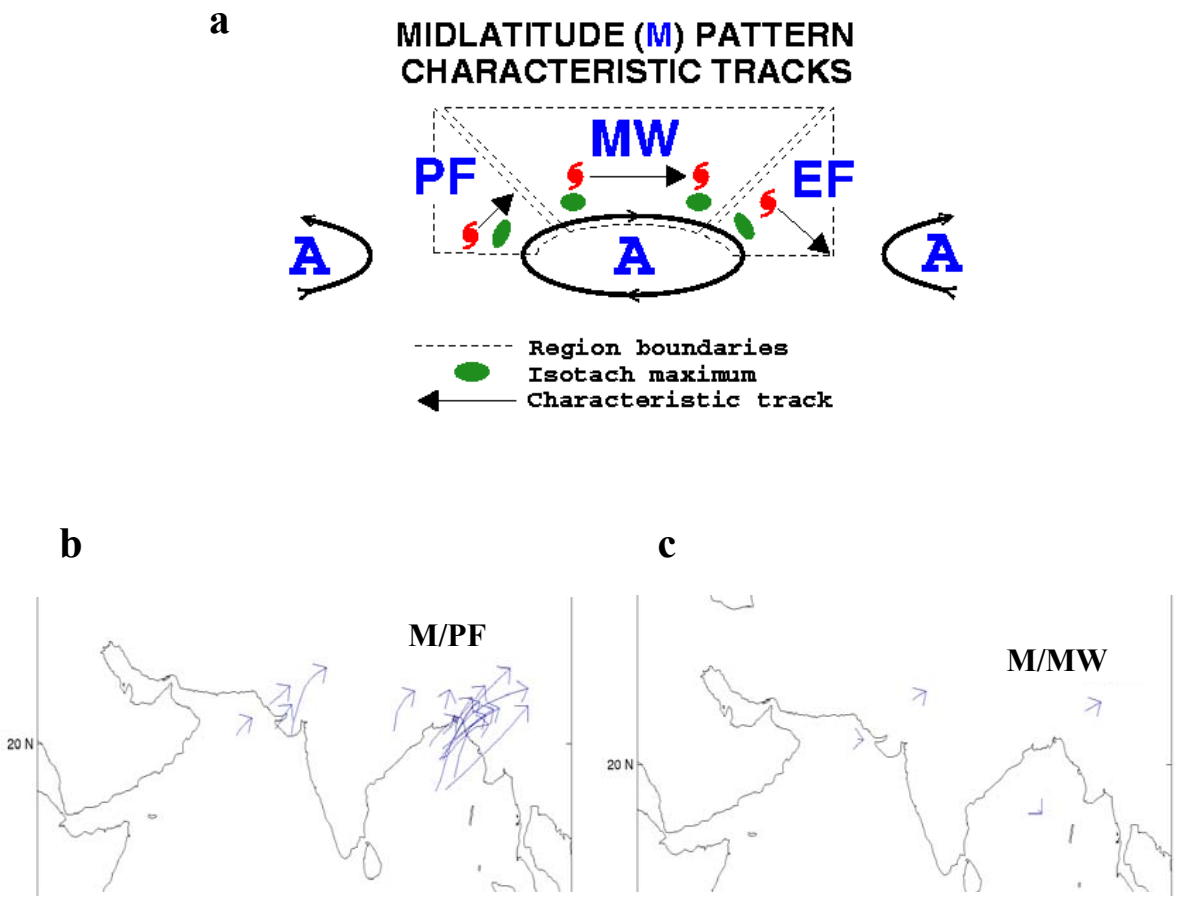

Figure 2.17. (a) Schematic of the Midlatitude pattern in the North Indian Ocean, which, except for the absence of the ME region, is the same as the Midlatitude pattern common to previously examined oceanic basins as in Fig. 2.2. Midlatitude pattern TC tracks in the NIO during 1991-2001 including: (b) M/PF pattern/region; and (c) M/MW pattern/region.

pattern. The lower the latitude of the subtropical ridge axis, the sooner the TC will have a transition into the Midlatitude pattern. A TC may also have a transition to the M/PF pattern/region following landfall. The M/PF TC tracks are toward the northeast in both the AS and BOB basins (Fig. 2.17b) before dissipating over mountainous terrain. The M/PF pattern/region occurs in 9.6% of 656 cases in the NIO (Fig. 2.8), and is most common in May and November (Table 2.1). Similar to TCs in the S/PF and P/PF pattern/regions, TCs in the M/PF pattern/region can be the most damaging as they tend to make landfall in low-lying areas.

b. M/PF Pattern/Region Case Study

At 00 UTC 19 May 1998 (Fig. 2.18a), TC 01A is in the Midlatitude (M) pattern, embedded in a weak midlatitude trough centered between a northwest-southeast oriented subtropical anticyclone axis (Fig. 2.18a). The strongest jet streak maximum is to the east of TC 01A. However, northeastward steering flow exists between TC 01A and the subtropical anticyclone so that the TC moves toward Bangladesh (Fig. 2.18a). Tropical Cyclone 01A is moving northward between two anticyclones and into midlatitude flow. The western anticyclone centered over the Pakistan coast and the eastern anticyclone over the Mekong Delta form a northwest-southeast oriented ridge axis. As mentioned in Section 2, an anticyclone over the Malay Peninsula is quite common, and often acts as the boundary between the tropics and midlatitudes for TCs in the BOB. This is not necessarily the subtropical ridge axis, which usually delineates the M pattern from the other patterns. Since TC 01A has passed north of this "subtropical anticyclone axis" with nothing but westerly midlatitude flow to the north and is currently moving toward the north-northeast is evidence that TC 01A is in the M/PF pattern/region.

c. M/MW and M/EF Pattern/Regions in NIO

The Midlatitude Westerlies (MW) and Equatorward Flow (EF) regions of the M pattern each occur in less than 1% of the cases examined due to the presence of land north of 25 deg. N in the NIO. The M/MW pattern/region does occur more often than the M/EF pattern/region, and is most common in the month of November (Table 2.1)

a

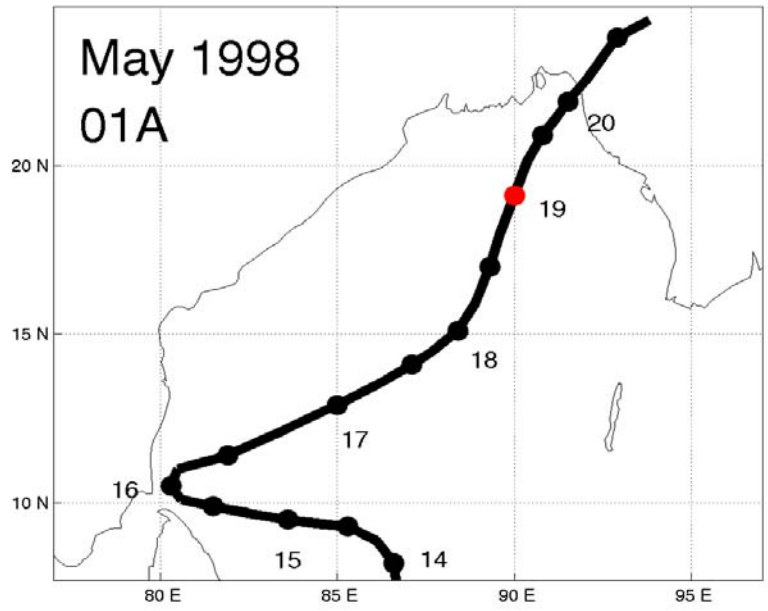

b

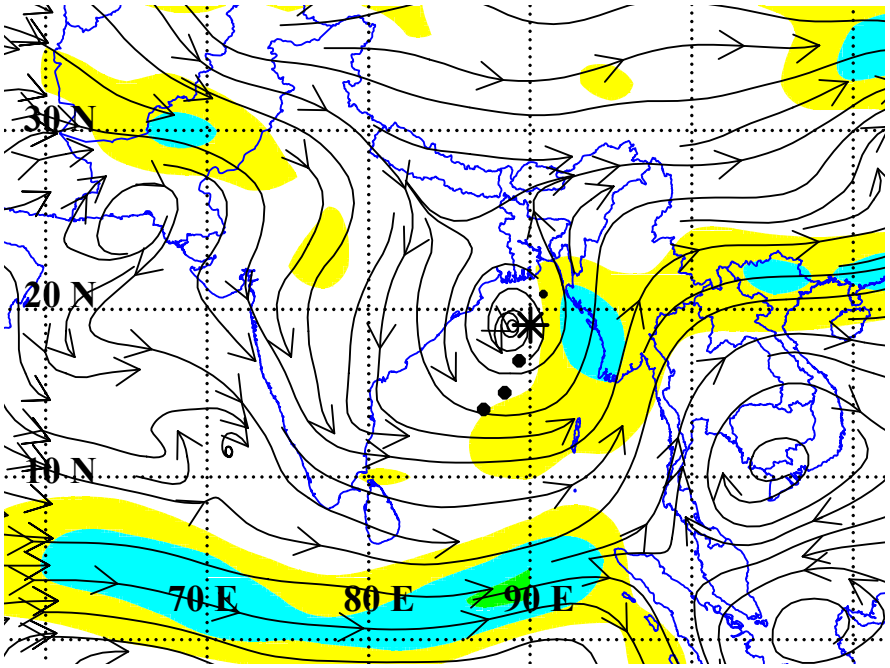

Figure 2.18. (a) Track of TC 01A from 00 UTC 14 May through 18 UTC 20 May 1998; (b) NOGAPS analysis field as in Fig. 2.10b except for 00 UTC 19 May.

when the subtropical anticyclone has shifted equatorward. Tropical cyclones in the M/MW pattern/region move in an eastward direction and are extremely short in duration (Fig. 2.17c), with a period of 12 h or less in the cases examined. The M/EF pattern/region will not be discussed due to its infrequency.

d. M/MW Case Study

The western North Pacific TC 30W crossed over the Malay Peninsula into the NIO (Fig. 2.19a) and became a strong TC in the BOB (reaching an intensity of 125 kt). By 12 UTC 21 November 1992 (Fig. 2.19b), TC 30W is in the M/MW pattern/region. Tropical Cyclone 30W is north of the eastern subtropical anticyclone cell and is being steered by the corresponding eastward flow. The eastward track (Fig. 2.19a) is consistent with the presence of the stronger winds to the south of the TC than to the north. This track brings TC 30W to a landfall on Myanmar, which causes TC 30W to dissipate over the next 12 h.

E. TC STRUCTURE

In the TC Motion Meteorology Knowledge Base Framework (Fig. 2.1), the two factors in the TC Structure are intensity and size. In the Systematic Approach, the intensity of a TC determines which steering level should be used to evaluate the TC motion. A tropical depression or tropical storm tends to be steered by the 700 mb or 850 mb flow. Stronger TCs will generally be steered by a deeper layer, so that the pattern/region is usually determined by the 500 mb analysis. The size of the TC is an important factor in determining if the TC will influence, or be influenced by, the existence of adjacent cyclonic and anticyclonic circulations in the environment structure. Here the size is defined in terms of the gale-force (35 kt) wind radius. The other important structure consideration is that the beta effect is proportional to the outer wind structure, which is related to TC size. Not much research has been done yet on TC Structure for the Systematic Approach. However, it is important because the TC interaction with the environment structure is dependent also on the structure and size of the TC. The TC Structure and its relation to TC-Environment Transformations will be discussed in Chapter III.B.

a

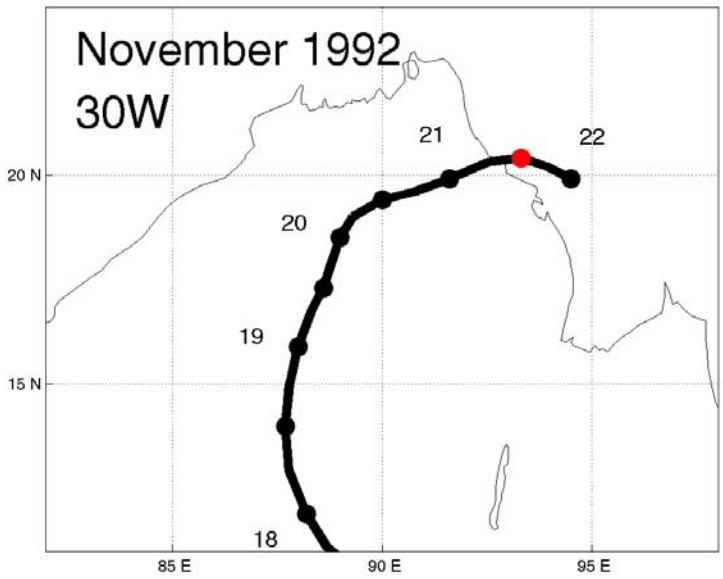

b

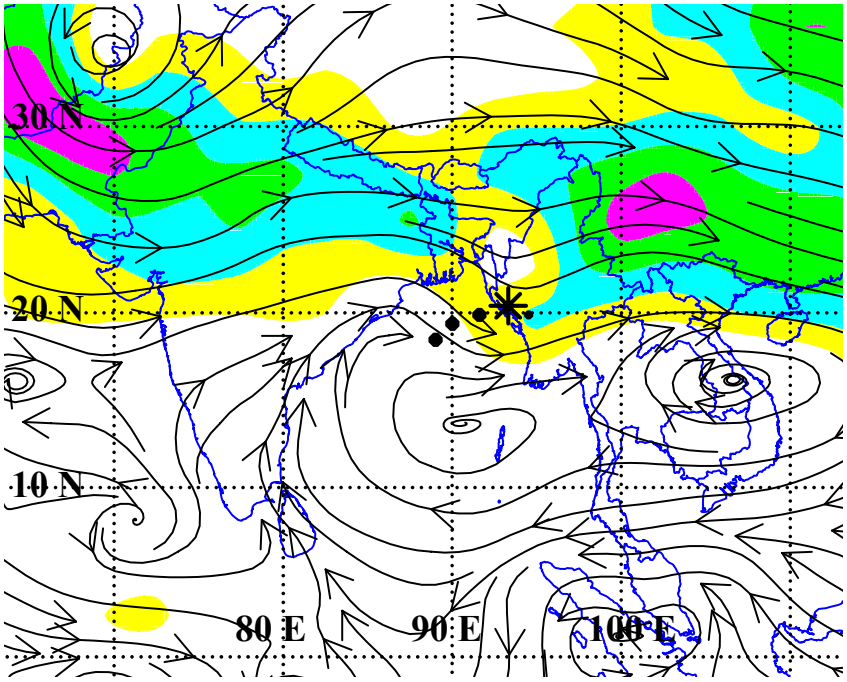

Figure 2.19. (a) Track of TC 30W from 18 UTC 17 November through 00 UTC 22 November 1992; (b) NOGAPS analysis field as in Fig. 2.10b except for 12 UTC 21 November

THIS PAGE INTENTIONALLY LEFT BLANK

III. GLOBAL TC MOTION METEOROLOGY KNOWLEDGE BASE – TRANSITIONAL MECHANISMS

As demonstrated in Chapter II, the synoptic environment is the primary steering influence over TC motion, and may be identified by mentally "removing" the TC from the environment and visualizing the background flow. For a tropical cyclone to change from one synoptic pattern/region to another, there must be a Transitional Mechanism, which is identified in the Systematic Approach as either an Environmental Effect or a TC-Environment Transformation (Fig. 2.1). Several common and basin-specific transitional mechanisms have been identified in each of the basins considered. In the case of Environmental Effects, the environment structure (steering) is changed somewhat independent of processes related to the TC. By contrast, TC-dependent processes are involved in TC-Environment Transformations in which the environment structure (steering) and sometimes the TC structure are changed, and the motion of the TC is changed. Both of these transitional mechanisms will be described as they apply to the NIO.

A. ENVIRONMENTAL EFFECTS

1. Advection (ADV)

The most basic Environmental Effect (Fig. 2.5, bottom) that causes either a transition from one region to another within the same pattern or between two pattern/regions is advection of the TC around major synoptic features. This "cork in the stream" concept implies a TC will move in the direction of the main steering flow with little deviation. Although the magnitude will vary, advection always has some effect on the steering of a TC. For example, it is the primary transitional mechanism for the classic TC recurvature track from S/PF or P/PF to the M/PF and then to the M/MW pattern/region as the primary steering flow of the anticyclone to the east controls the motion of the TC toward the north. Because of the straight-forward nature of this transition, no case study will be presented.

2. Midlatitude System Evolutions

a. Midlatitude Cyclogenesis/Cyclolysis (MCG/MCL)

(1) Conceptual Model**.** Zonal and meridional orientations and amplitudes of the subtropical anticyclone are usually the dominant factors in determining the synoptic influence in every TC region. However, the orientation and amplitude of the anticyclonic circulations may be affected by troughs and ridges traveling eastward in the midlatitude flow. An Environment Structure (Fig. 2.5) transition associated with Midlatitude Cyclogenesis (MCG) occurs when a midlatitude trough weakens the subtropical anticyclone such that the anticyclone takes on a more meridional orientation, which may include a break in the subtropical anticyclone cells (Fig. 3.1). As the anticyclone becomes more meridional, TC A in the S/TE pattern/region in Fig. 3.1a may then experience a transition to the S/PF pattern/region (Fig. 3.1b), or a TC already in the S/PF pattern region will remain there, but travel in a more northward track. Interaction with the midlatitude trough may also cause the TC speed to increase as it moves around the more meridional anticyclone, because of the strengthening northward flow between the east side of the trough and the west side of the subtropical anticyclone.

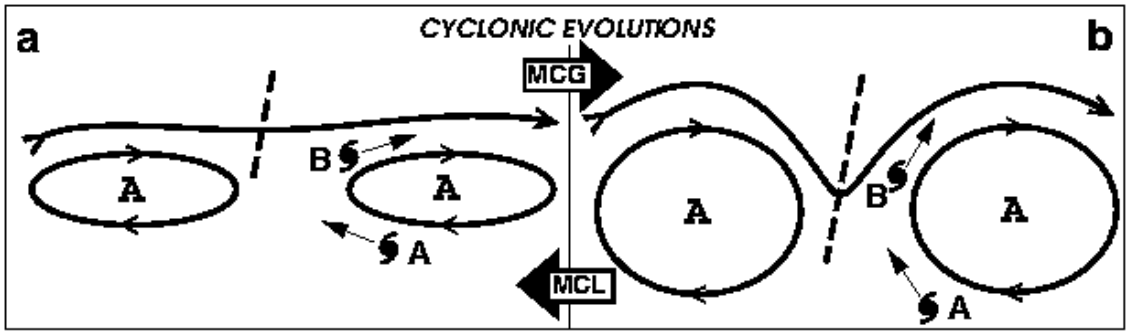

Figure 3.1. Schematics of the Midlatitude System Evolutions that may lead to large track errors. The deepening of the midlatitude trough from (a) to (b) depicts Midlatitude Cyclogenesis (MCG) and the reverse order [(b) to (a)] implies Midlatitude Cyclolysis (MCL).

An Environment Structure transition (Fig. 2.5) associated with Midlatitude Cyclolysis (MCL) occurs when the transiting midlatitude trough weakens such that the subtropical anticyclone circulation becomes more zonal. This MCL has the opposite effect as MCG on the TC motion (Fig. 3.1) and may cause a TC approaching the col region between the two anticyclone cells to turn from a northward track in the S/PF pattern/region to a more westward track in the S/EF or S/TE pattern/region.

(2). NIO MCG/MCL case studies**.** Tropical Cyclone 07B crossed the Malay Peninsula and into the BOB at approximately 03 UTC 17 November 1998 (Fig. 3.2a) under the steering control of the eastern cell of the subtropical anticyclone to the north. It moved westward in a S/TE pattern/region until 12 UTC 18 November (Fig. 3.2b) when a deep midlatitude trough approached TC 07B from the west.

A small ridge over Sri Lanka associated with the deep trough does not appear to have any steering influence over the TC track. Instead, the subtropical anticyclone to the north maintains steering control as supported by the isotach maximum location. By 00 UTC 19 November (Fig. 3.2c), TC 07B has turned to the northwest (Fig. 3.2a) and undergone a transition to the S/PF pattern/region, which characterizes the MCG Transitional Mechanism in Fig. 3.1. Notice in Fig. 3.2c that the subtropical anticyclone to the east has increased in amplitude. Advection of the TC around the subtropical anticyclone, coupled with the approaching deep midlatitude trough, has caused TC 07B to change direction. During the next 12 h, TC 07b will increase speed from 7 kt to 10 kt as it continues to move toward the northwest (Fig. 3.2a).

At 12 UTC 25 October 2000, TC 02B is moving toward the northwest at a speed of 11 kt (Fig. 3.3a) in the S/PF pattern/region (not shown). By 00 UTC 26 October (Fig. 3.3b), a midlatitude trough is passing north of the subtropical anticyclone to the northeast of TC 07B. The approach of this trough tends to shift the axis of the subtropical anticyclone southward and closer to the TC, which causes the TC to turn to a more westward track, and decrease the translation speed from 8 kt to 5 kt (Fig. 3.3a). At 12 UTC 26 October (Fig. 3.3c), the short-wave trough has moved

a

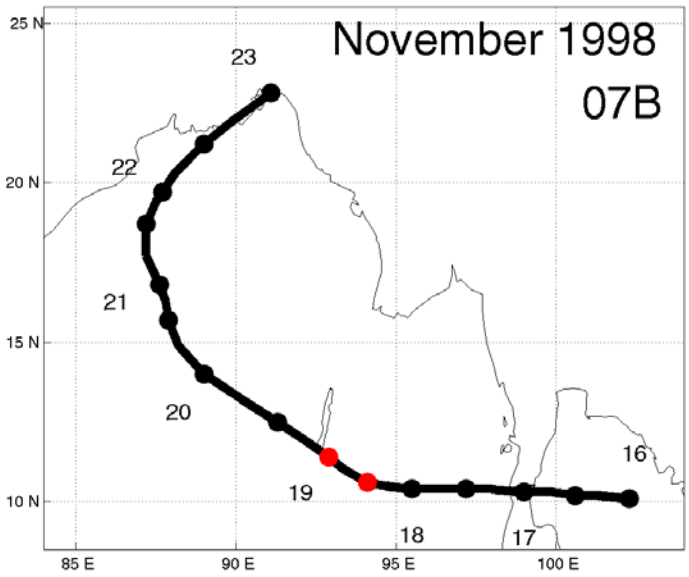

b

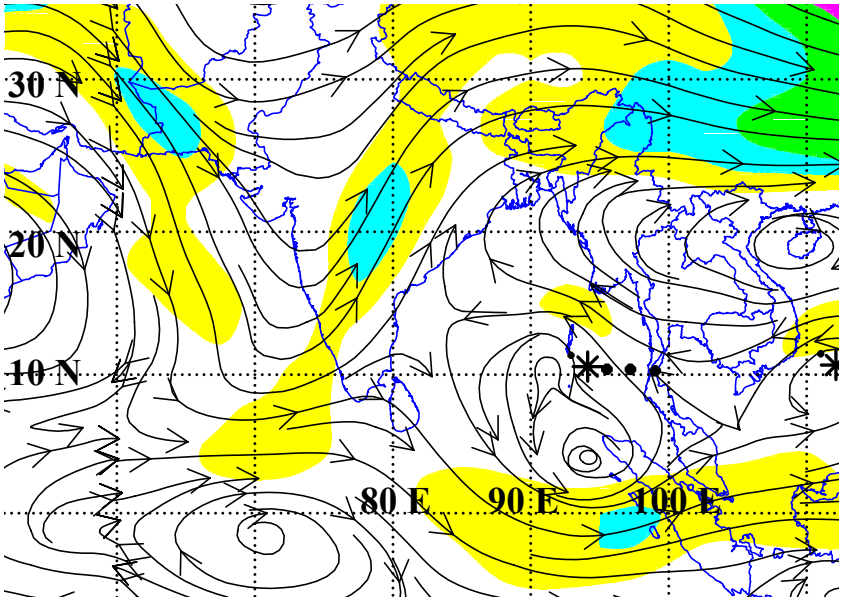

Figure 3.2. (a) Track of TC 07B from 00 UTC 16 November through 00 UTC 23 November 1998; (b) NOGAPS analysis field as in Fig. 2.10b except for 12 UTC 18 November and (c) 00 UTC 19 November.

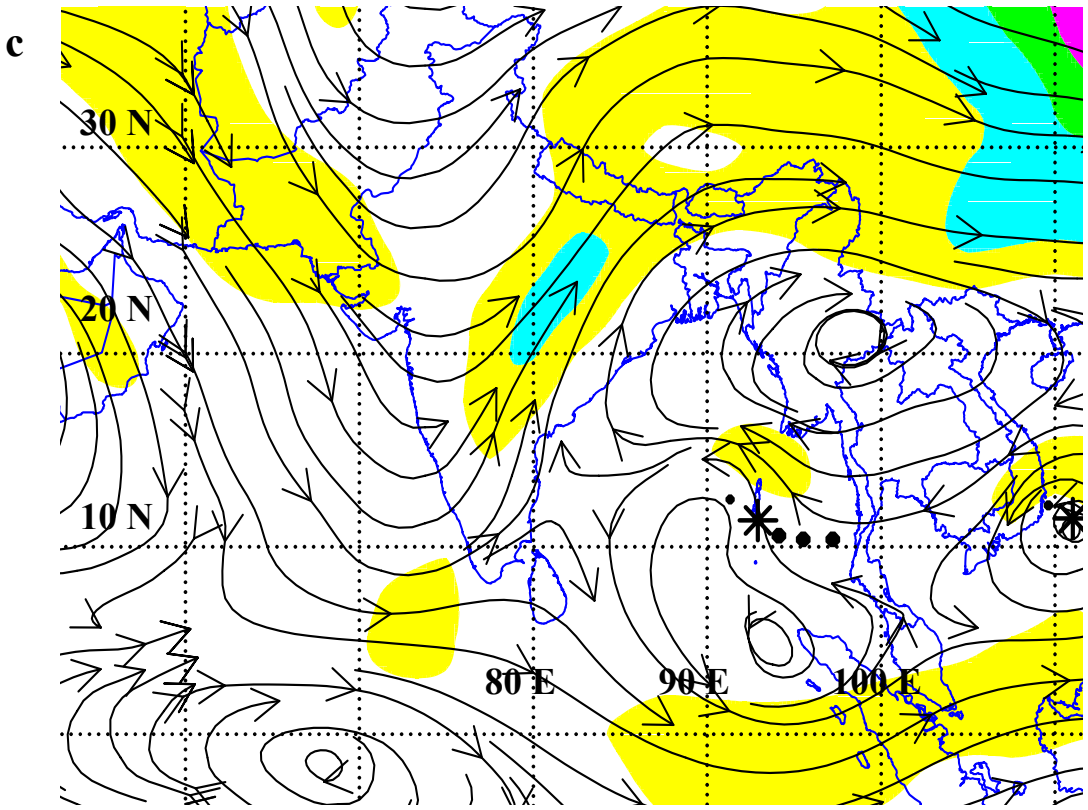

Figure 3.2. (continued)

northeastward and the steering flow associated with the eastern subtropical anticyclone cell becomes more northwestward, which allows TC 07B to turn back toward the northand increase in latitude. Midlatitude Anticyclogenesis/Anticyclolysis (MAC/MAL)

(1) Conceptual Models. The MAC/MAL may occur as a result of the midlatitude trough/ridge interaction with a tropical cyclone affecting the shearing flow in which the TC may be changed in strength and orientation via superposition of a transiting midlatitude ridge. If this causes a weak subtropical anticyclone to be strengthened, the transitional mechanism in Fig. 2.5 will be specified as Midlatitude Anticyclogenesis (MAG). The MAG may also occur as a result of a midlatitude trough increasing the amplitude of the subtropical anticyclone, such that the anticyclone is displaced as opposed to being weakened as in MCG. For example,TC E in the S/PF

a

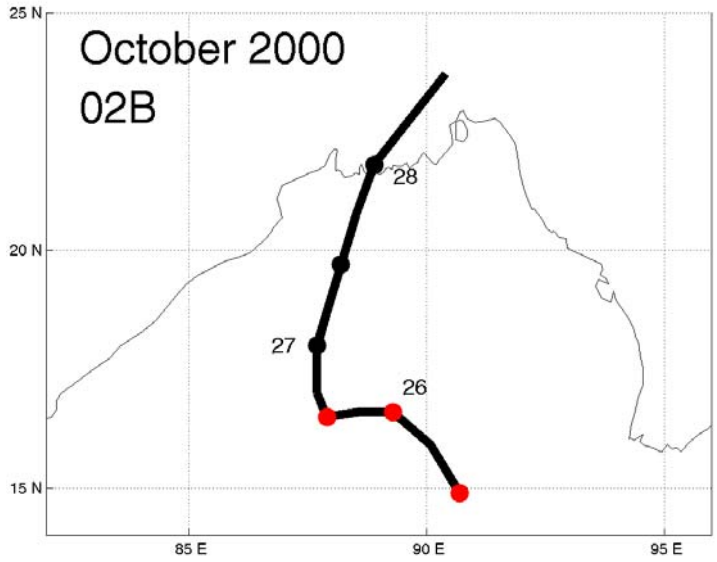

b

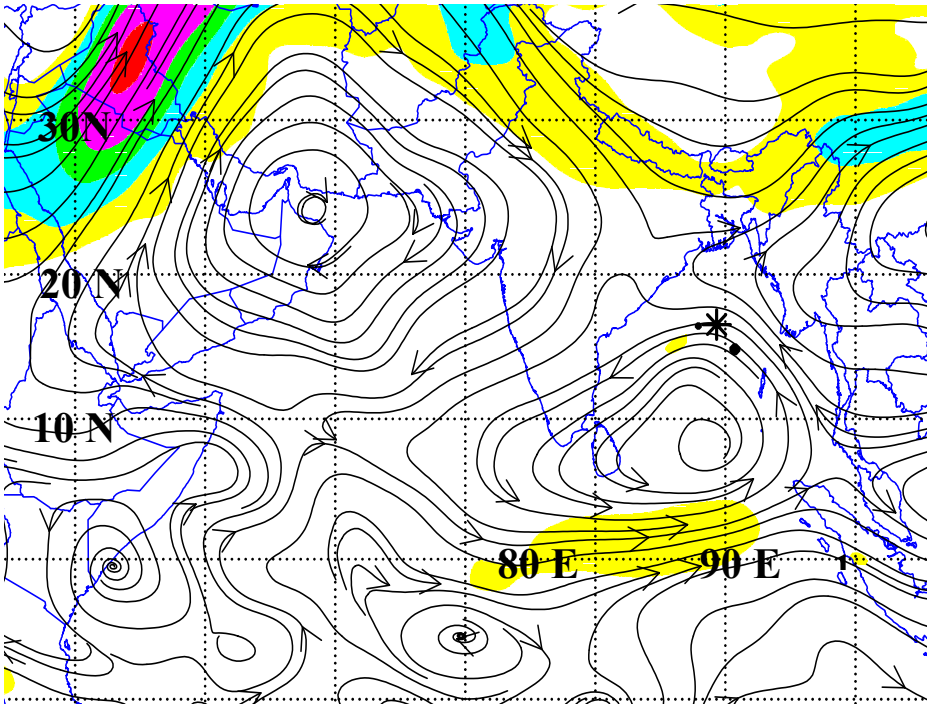

Figure 3.3. (a) Track of TC 02B from 12 UTC 25 October through 06 UTC 28 October 2000; NOGAPS analysis field as in Fig. 2.10b except for (b) 00 UTC 26 October and (c) 12 UTC 26 October.

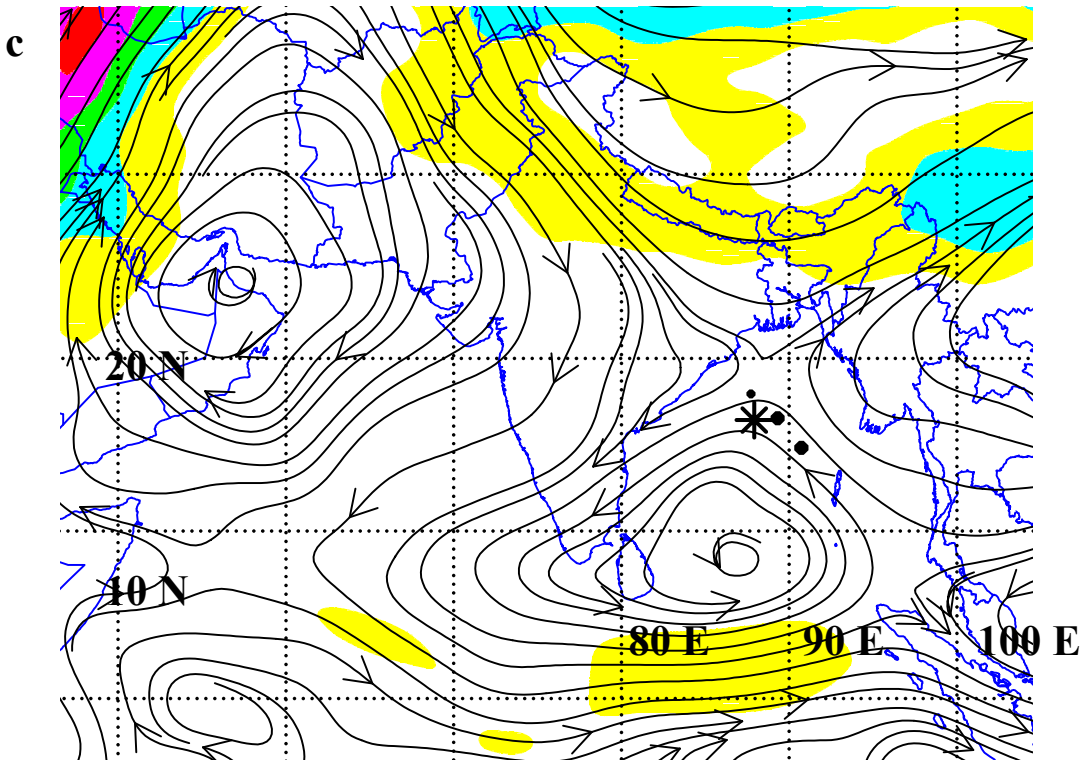

Figure 3.3. (continued)

pattern/region (Fig. 3.4a) tracking poleward through a break in the subtropical anticyclone will turn westward into the S/TE pattern/region (Fig. 3.4b) as a result of MAG. The Environmental Effects transition labeled Midlatitude Anticyclolysis (MAL) in Fig. 2.5 will occur if a subtropical anticyclone weakens and causes a TC to "push" through the anticyclonic circulation and move poleward through the col. Thus, MAL will result in a transition for TC E in Fig. 3.4b changing from a westward track in S/TE to a northward track in the S/PF pattern/region around the now separate subtropical anticyclone cells (Fig. 3.4a).

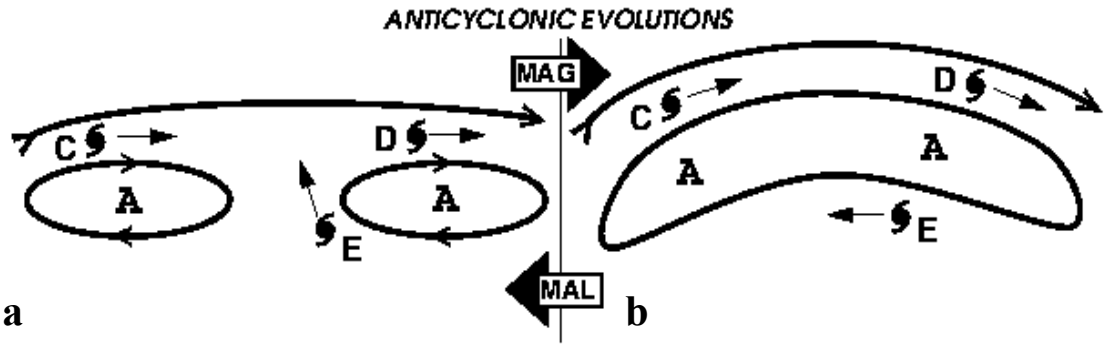

Figure 3.4. As in Fig. 3.1, except the change of the midlatitude anticyclone poleward of the TC from (a) to (b) depicts Midlatitude Anticyclogenesis (MAG) and the reverse order [(b) to (a)] implies Midlatitude Anticyclolysis (MAL).

(2) MAG/MAL Case Studies**.** Tropical Cyclone 07B of 1992 formed in the eastern BOB (Fig. 3.5a) as a part of a loosely organized monsoon depression. Notice in Fig. 3.5b that the stronger isotach maximum is to the north of TC 07B. Tropical Cyclone 07B moved toward the northwest in the S/TE pattern/region between 06 UTC 6 October and 06 UTC 7 October due to the westward steering plus the beta-effect propagation (to be discussed in Chapter III.B.1). Although TC 07B is moving toward a col region, it is still too far south of the subtropical anticyclone cells to be in the S/PF pattern/region. By 00 UTC 8 October (Fig. 3.5c), a midlatitude short-wave ridge near 29 deg. N, 68 deg. E in Fig. 3.5b has moved north of the col region between the two cells of the subtropical anticyclone, which increases its strength. Thus, a MAG transition has occurred as the subtropical anticyclone is now continuous (no col region exists). In response, TC 07B has turned to the west (Fig. 3.5a) with this re-orientation of the steering flow to a S/TE pattern/region. By 12 UTC 8 October (Fig. 3.5d), the midlatitude ridge has moved to the east and the subtropical anticyclone has weakened with a col again to the northwest of the TC. Tropical Cyclone 07B has experienced a transition from the S/TE to the S/PF pattern/region as a result of the MAL Transitional Mechanism (Fig. 3.4). That is, the eastern cell of the subtropical anticyclone has gained steering control, and TC 07B resumes a northwestward track toward the col.

a

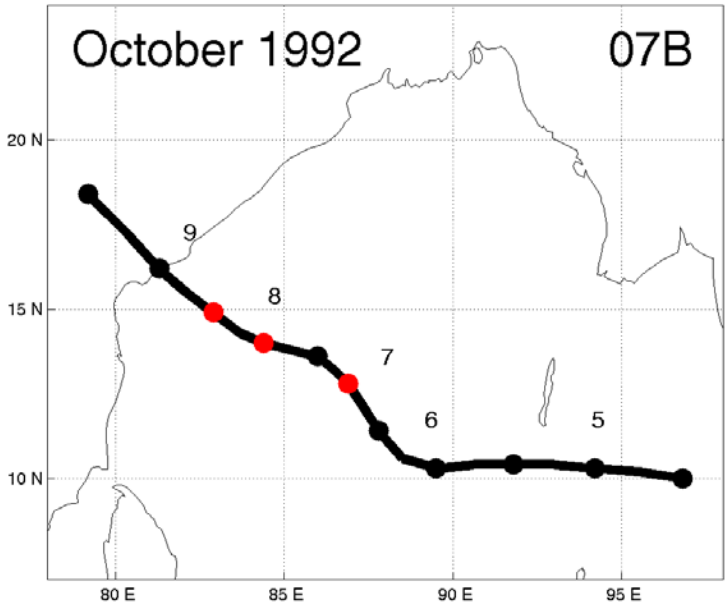

b

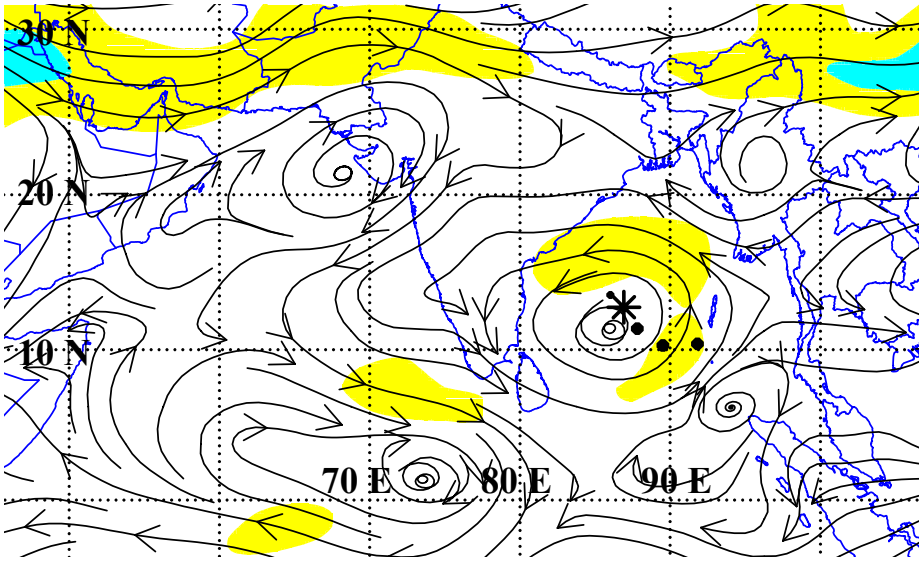

Figure 3.5. (a) Track of TC 07B from 12 UTC 4 October through 12 UTC 9 October 1992; (b) NOGAPS analysis field as in Fig. 2.10b except for 00 UTC 7 October; (c) 00 UTC 8 October; and (d) 12 UTC 8 October.

c

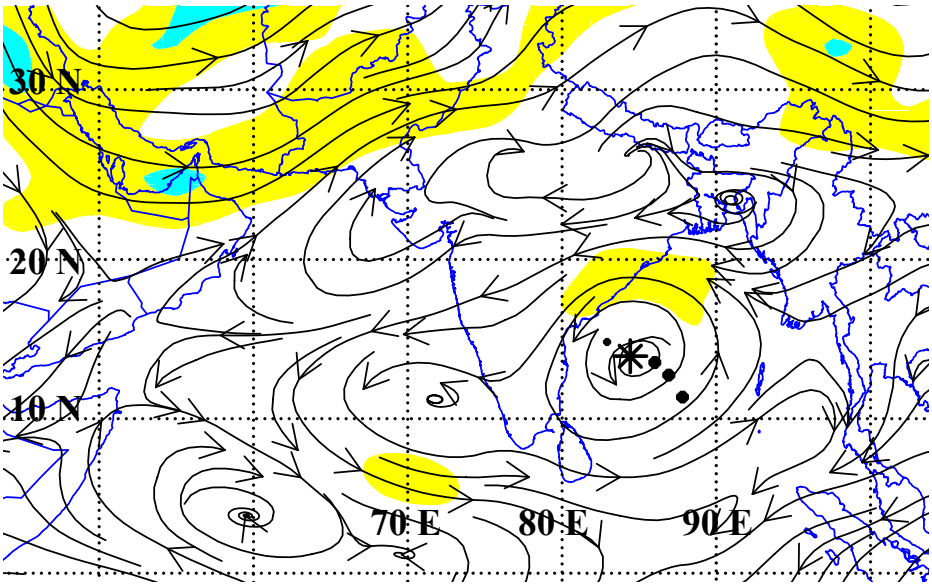

d

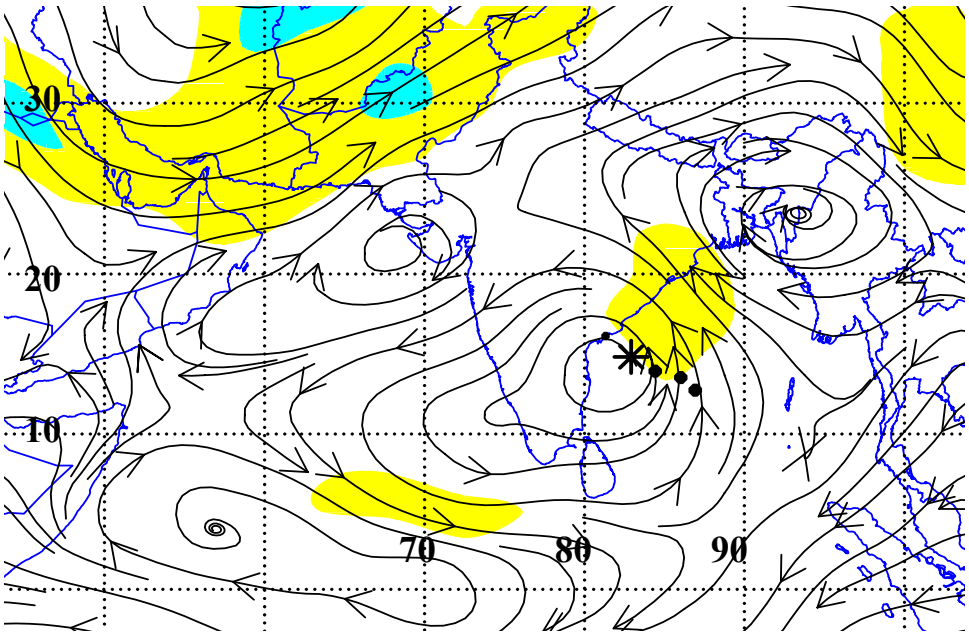

Figure 3.5. (continued)

B. TC –ENVIRONMENT TRANSFORMATIONS

1. Beta-effect related transformations

a. Beta-Effect Propagation (BEP)

The first of three categories of TC-Environment Transformations in Fig. 2.5 deals with the beta-effect phenomena, which ultimately arise because the Coriolis force increases as a function of latitude from a zero value at the equator. This Coriolis dependence on latitude is often linearly approximated on a beta plane. Carr and Elsberry (1994, 1997) described the beta-effect propagation on TC motion as it affects forecasting with the Systematic Approach. Nonlinear beta effects on a TC result in an east-west asymmetry and vorticity advection. The beta adjustment is an attempt by the advection to re-establish circular flow with concentric vorticity isolines by transporting vorticity from high to low values. The net effect of the so-called beta gyres is that the maximum vorticity associated with the vortex center is then advected toward the northwest.

Storm size is also a major factor in beta-effect propagation. If there is a larger radius of 35 kt winds, it follows that there will be larger velocity (v) components at outer radii, and therefore there will be a larger beta effect and stronger adjustment by nonlinear advection. The result is a more rapid advection toward the northwest for larger cyclones. This northwestward (Northern Hemisphere) steering mechanism acting even in a quiescent background environmental flow is termed in Fig. 2.5 as Beta-effect Propagation (BEP). This BEP is the common Transition Mechanism involved in steering a TC from the S/TE to the S/PF pattern/region.

Tropical Cyclone 07B formed in the BOB and began moving toward the northwest (Fig. 3.5a) on 6 October. The subtropical anticyclone axis to the north of the TC is east-west oriented (Fig. 3.6a). Although the isotach maxima to the north and south of the TC in Fig. 3.6a are approximately the same size, the TC is moving toward the northwest due to BEP. Tropical Cyclone 07B was no more intense (maximum intensity of 35 kt) than 04A (Fig. 2.10) at this time. However, its larger size (Fig. 3.6b) leads to a larger beta-effect propagation that causes the TC to move toward the northwest (Fig. 3.5a) vice due west with the environmental flow (Fig. 3.6a).

a

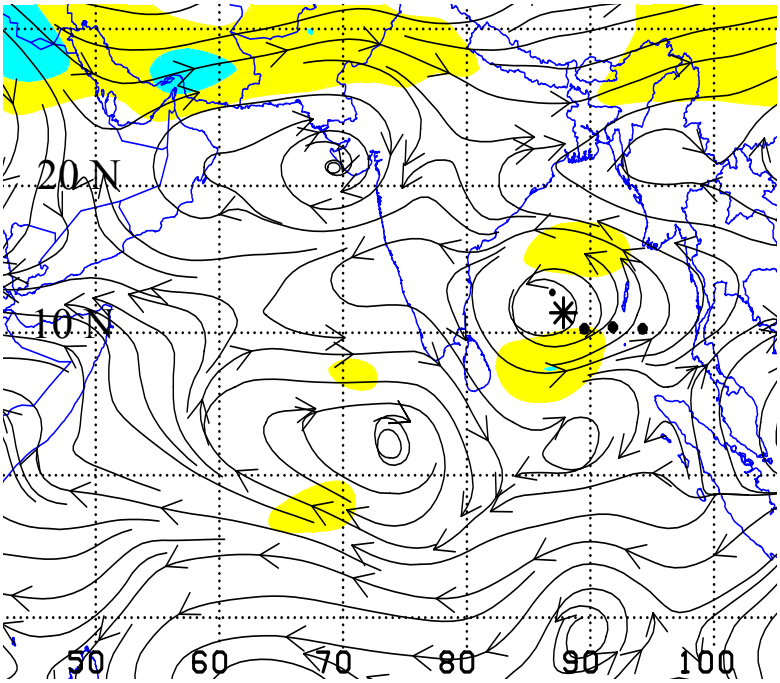

b

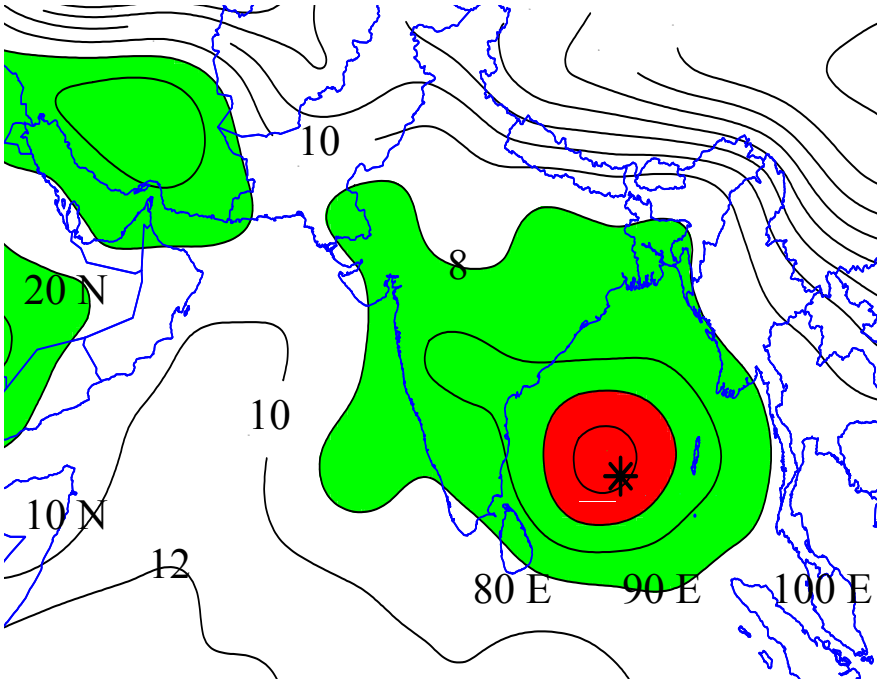

Figure 3.6. NOGAPS analysis field as in Fig. 2.10b except for 12 UTC 6 October at (a) 500 mb; and (b) Mean sea-level pressure contoured every 2 mb. Shading begins at 1008 mb, which is labelled as 8.

b. Ridge Modification by a TC (RMT)

The Ridge Modification by a TC (RMT) Transitional Mechanism (Fig. 3.7) often causes forecasters to be caught by surprise when a TC moving toward the west suddenly recurves to a northerly track. As noted above, the beta effect causes a large TC to self-propagate northwestward relative to the environmental steering. In addition, the Rossby wave dispersion associated with a sufficiently large TC will result in the formation of a peripheral anticyclone to the southeast (Northern Hemisphere) of the TC. If the peripheral anticyclone grows large enough to gain steering control over the TC, the TC track will have a turn to the north or northeast under the influence of the peripheral anticyclone, which is a transition to the Poleward (P) synoptic pattern. A sudden recurvature to the north-northeast and a transition from an S/TE to a P/PF pattern/region is a characteristic of the RMT Transitional Mechanism in Fig. 2.5.

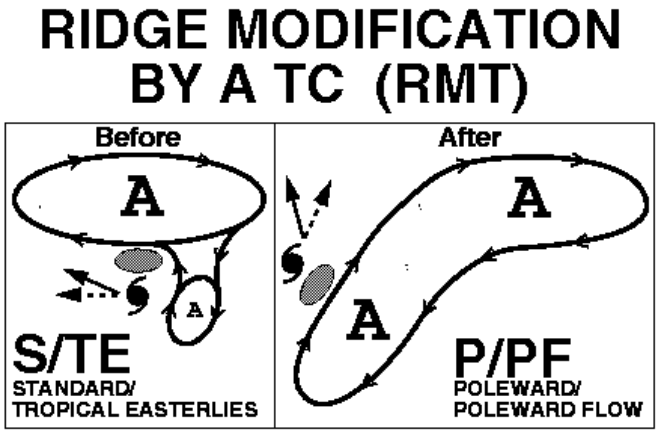

Figure 3.7. Conceptual model of Ridge Modification by a TC (RMT). A small peripheral anticyclone southeast of the TC grows, attaches to the subtropical anticyclone, and modifies it. The TC typically undergoes a transition from the S/TE to the P/PF pattern/region.

A high-amplitude subtropical anticyclone centered over the northern AS is the dominant feature in the NIO at 00 UTC 12 November 1992 (Fig. 3.8b). Tropical Cyclone 10B is moving toward the west-southwest at a relatively low latitude of 7 deg. N (Fig. 3.8a) in the S/EF pattern/region due to steering by the southwestward flow of the large subtropical anticyclone to the northwest. By 12 UTC 13 November, TC 10B is moving toward the northwest (Fig. 3.8a). A buffer cell in the Southern Hemisphere to the

a

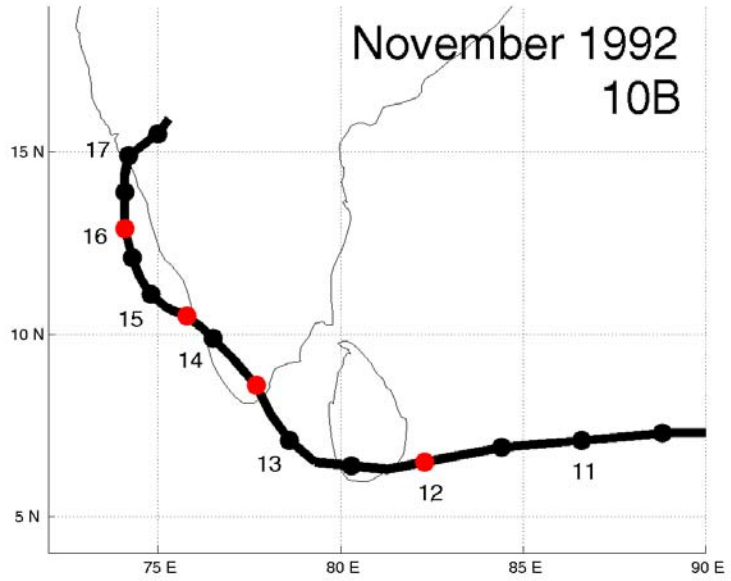

b

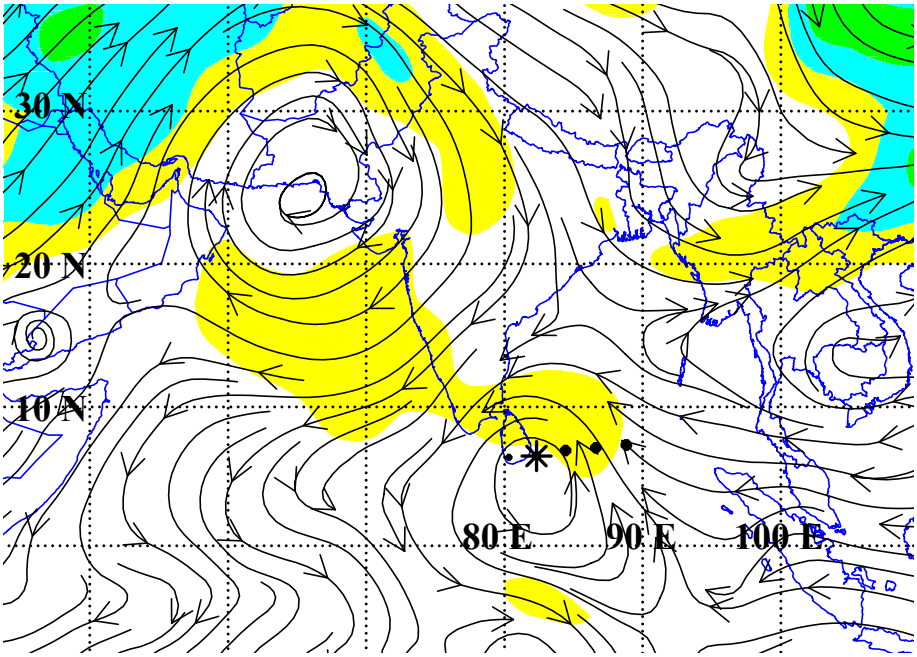

Figure 3.8. (a) Track of TC 10B from 06 UTC 10 November through 18 UTC 17 November 1992; (b) NOGAPS analysis field as in Fig. 2.10b except for 00 UTC 12 November; (c) 12 UTC 13 November; (d) 12 UTC 14 November; and (e) 00 UTC 16 November.

c

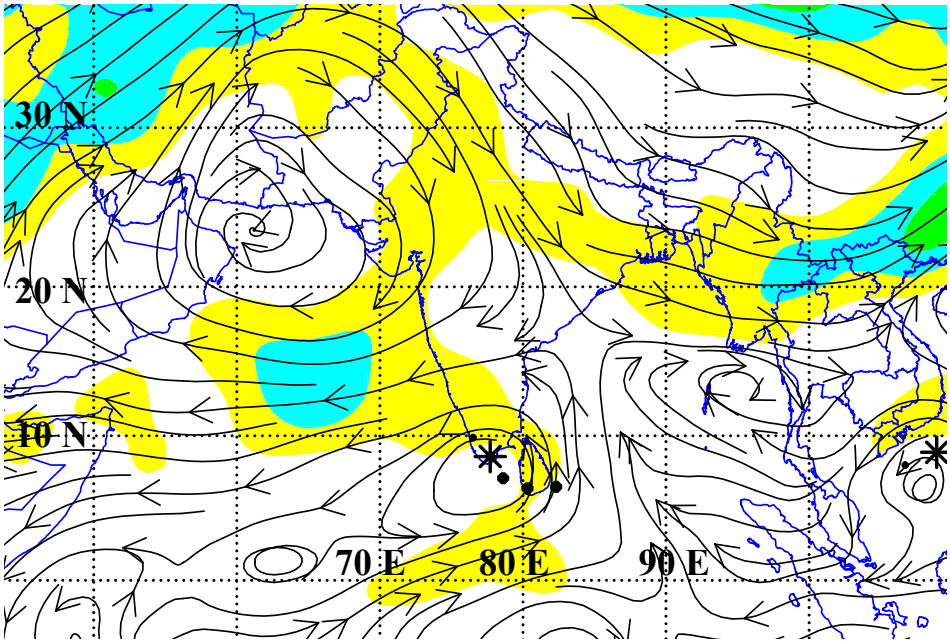

d

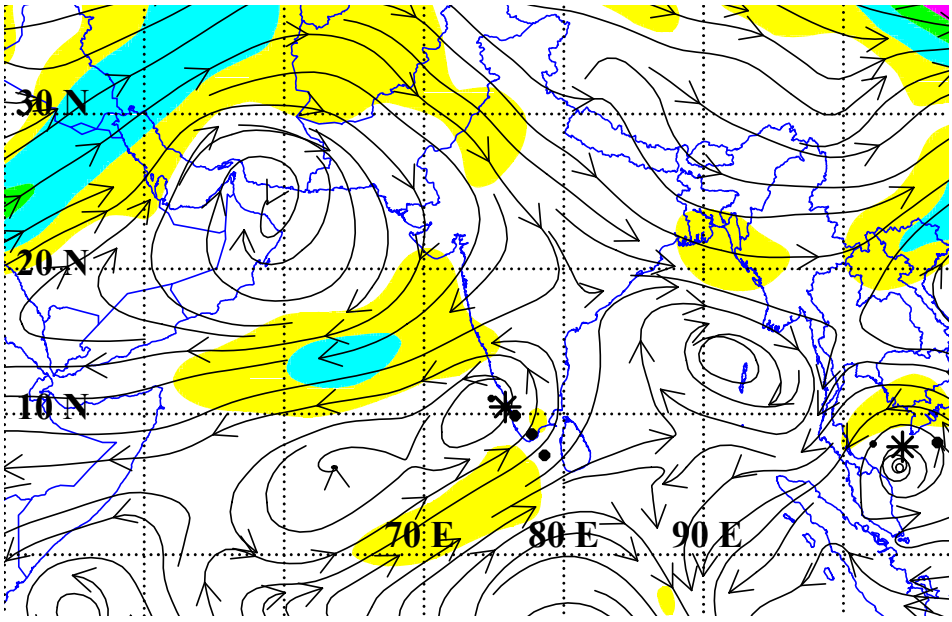

Figure 3.8. (continued)

e

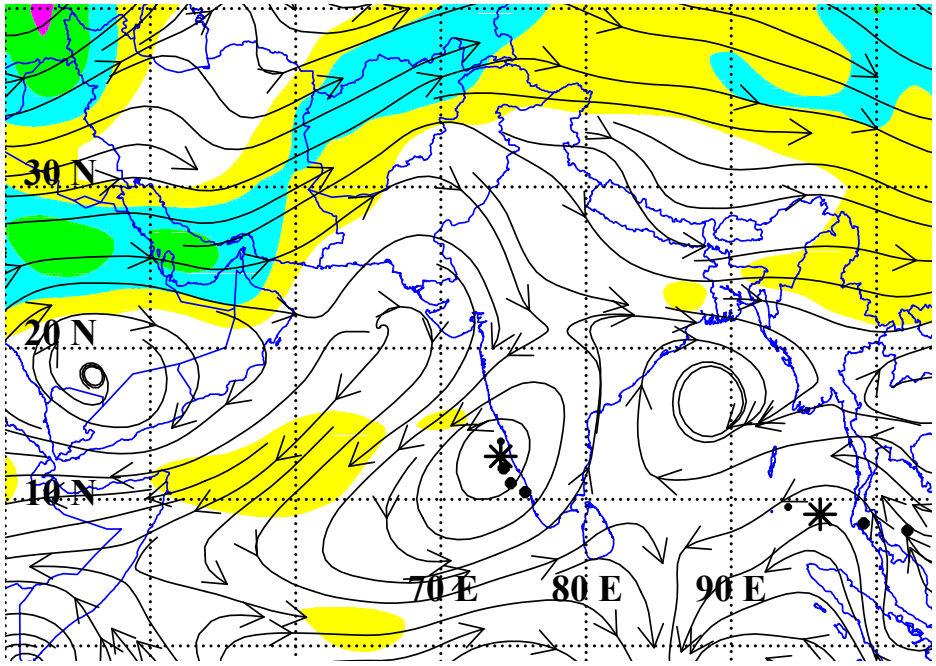

Figure 3.8. (continued)

south-southeast of TC 10B is beginning to amplify (Fig. 3.8c), which creates a northeastward cross-equatorial flow. The cross-equatorial flow appears to merge with the southeasterly flow associated with an anticyclone just off the Malay Peninsula. Consequently, the isotach maximum has shifted to the southeast of TC 10B, which supports the existence of an RMT transitional mechanism.

This RMT is different from that illustrated in Fig. 3.7 because the buffer cell is amplifying, possibly due to Rossby wave dispersion, rather than via the appearance of a noticeable peripheral anticyclone. The westward steering flow associated with the high amplitude subtropical anticyclone has also produced an isotach maximum to the northwest of TC 10B. However, the northwestward track of TC 10B (Fig. 3.8a) indicates that neither steering flow is dominant and that the TC is in a transition from the S/EF to the P/PF pattern/region. The amplification of the buffer cell to the southeast continues to contribute to the formation of a Poleward pattern (Fig. 3.8d), but the isotach maximum to the northwest of TC 10B is stronger, which is consistent with the slight turn of the TC track to the west (Fig. 3.8a).

At 00 UTC 16 November (Fig. 3.8e), a midlatitude trough moves east and weakens the high amplitude subtropical anticyclone. The northeastward steering flow of the Poleward pattern is now stronger than the southwestward steering flow of the subtropical anticyclone, and TC 10B is finally able to complete a transition to the P/PF pattern/region. It is a combination of the MCG weakening the western subtropical anticyclone and the RMT that allows the TC to move toward the north (Fig. 3.8a).

Another RMT case study involves a TC that has formed in an established monsoon depression but is then affected by an amplifying buffer cell to the southeast via Rossby wave dispersion. At 12 UTC 22 September 1997, TC 02B is drifting slowly (3 kt) toward the northwest (Fig. 3.9a) in a weak steering flow near the center of the monsoon depression (Fig. 3.9b). The weak steering is a near-balance between the effect of the eastern subtropical anticyclone cell to the northeast that is steering the TC to the northwest and that due to the buffer cell to the southeast, which is steering the TC to the northeast. These opposing flows cause the TC to slow at 00 UTC 23 September (Fig. 3.9a). As the TC remains nearly stationary, Rossby wave dispersion continues to amplify the buffer cell to the southeast, which is a RMT Transitional Mechanism. At 12 UTC 24 September (Fig. 3.9c), a midlatitude trough has approached from the northwest and weakened the subtropical anticyclone to the north, which might be labeled as an MCG Transitional Mechanism. However, the amplifying buffer cell to the southeast is now connected to the subtropical anticyclone, with a southwest-to-northeast orientation as in the Poleward pattern. Because MCG caused the subtropical anticyclone to weaken, the strengthening peripheral anticyclone then gained steering control, which caused a transition into the P/PF pattern/region due to RMT.

2. Cyclone Interactions

The TC-Environment Transformations in Fig. 2.5 include three variations as a result of interactions between two cyclonic circulations. As described in Carr et al. (1997), the cyclonic circulations may be a combination of two TCs, or a TC and a cyclonic circulation such as a low, depression, heat low, or gyre.

a

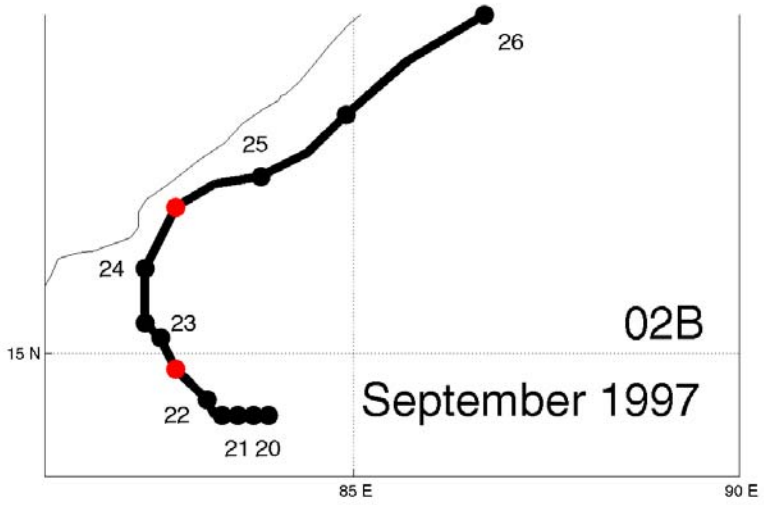

b

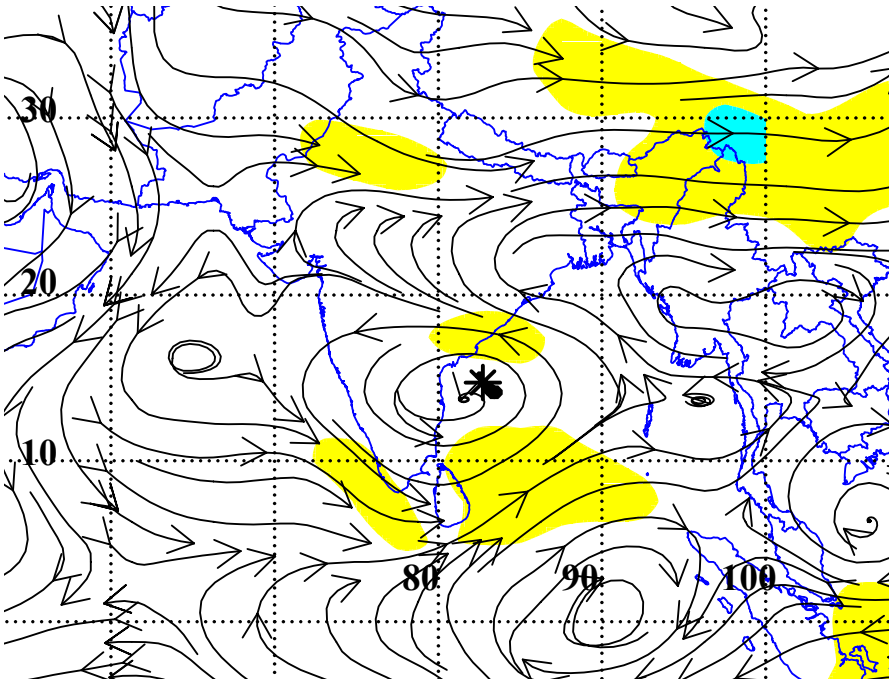

Figure 3.9. (a) Track of TC 02B from 00 UTC 20 September through 00 UTC 26 September 1997; (b) NOGAPS analysis field as in Fig. 2.10b except for 12 UTC 22 September, and (c) 12 UTC 24 September.

c

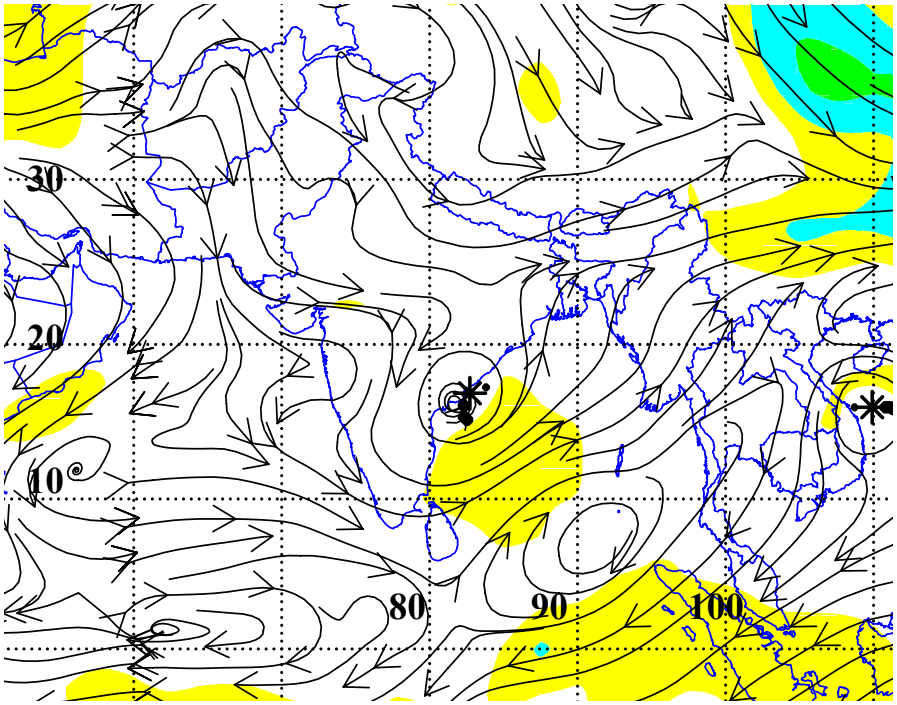

Figure 3.9. (continued)

a. Direct Cyclone Interaction

As illustrated in Fig. 3.10, Direct Cyclone Interaction (DCI) occurs in one of three ways. First, one-way influence (DCI 1) occurs when the track of a much smaller TC is changed as it is steered around the periphery of a much larger and more intense TC or cyclonic circulation. The smaller TC is typically tending to dissipate since it is experiencing vertical wind shear as it advects around the larger circulation. In the second mechanism, called DCI 2, when two TCs of comparable size and intensity interact, the tracks of both TCs are altered such that they rotate around each other until they dissipate or one circulation "escapes" the circulation of the other. The third DCI is similar to the second DCI but the TCs merge into one large TC. The DCI transition is a rare occurrence in every TC basin because the two cyclones have to be close, and the DCI does not generally last long due to the large amount of horizontal and vertical shear encountered between two such circulations. Due to the infrequency at which the DCI Transitional Mechanism occurs (only 4 times during 1991-2001) in the NIO, no case study will be presented.

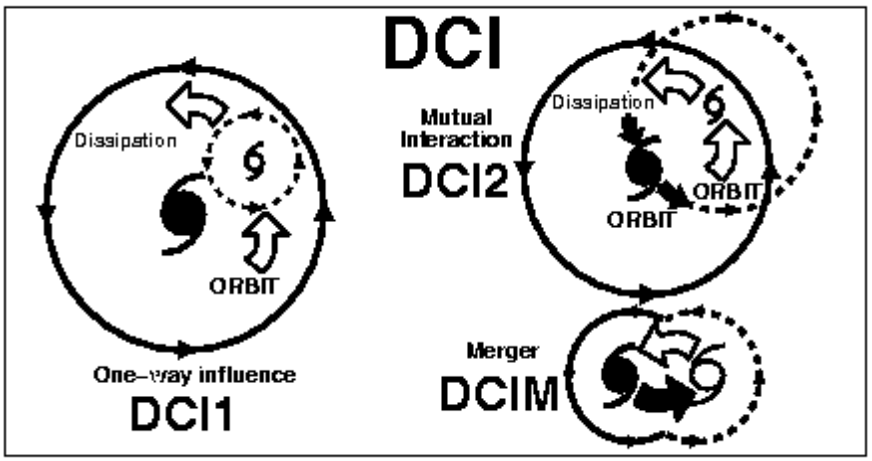

Figure 3.10. Conceptual model of Direct Cyclone Interaction (DCI). Three types of DCI exist owing to the difference in relative sizes of the TCs.

b. Semi-Direct Cyclone Interaction

In the Semi-direct Cyclone Interaction (SCI) Transitional Mechanism in Fig. 2.5, the two cyclones are separated by 10 deg.-20 deg. latitude (Fig. 3.11), yet they still experience a steering influence. This transitional mechanism generally occurs when two TCs or a TC and a cyclonic circulation are both in the S pattern. The SCI-West (W) occurs when the western TC is steered equatorward in the flow between the subtropical anticyclone to the northwest and the second cyclonic circulation to the east (Fig. 3.11a). A small TC will tend to track toward the southwest under the control of this environmental flow, while a large TC will move more toward the west due to the addition of the northwestward tendency of beta-effect propagation. The SCI-East (E) occurs when the TC is in the steering flow between the subtropical anticyclone to the northeast and the second cyclonic circulation to the west (Fig. 3.11b), which produces a poleward track with a more rapid translation than would be expected for a TC in that position on the west-southwest periphery of a subtropical anticyclone cell. The SCI-W (SCI-E) is most likely to be the transitional mechanism when the TC is in the S/EF (S/PF) pattern/ region. A case study in which both the SCI and Indirect Cyclone Interaction (to be presented next) mechanisms occurred will be presented in Section 2.d.

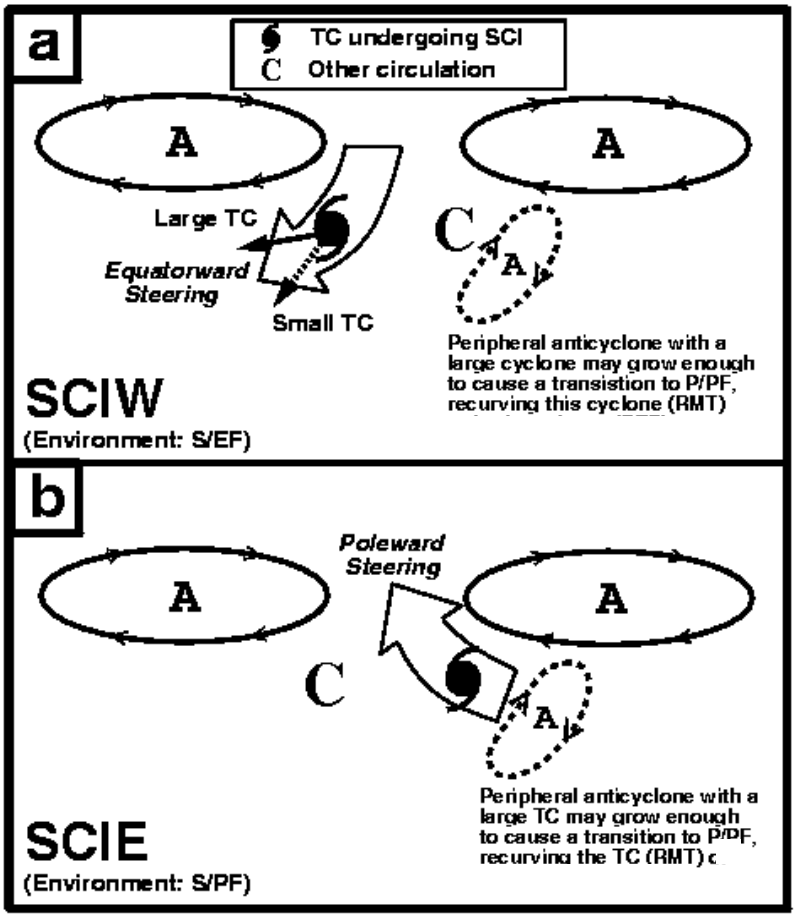

Figure 3.11. Conceptual model of Semi-direct Cyclone Interaction. These SCIs involve a Western (Eastern) TC undergoing SCIW (SCIE), but not necessarily simultaneously.

c. Indirect Cyclone Interaction

The Indirect Cyclone Interaction (ICI) Transitional Mechanism (Fig. 3.12) typically occurs when a TC and a cyclonic circulation are within 15-30 deg. long. of each other (Carr and Elsberry 1997) in an arrangement similar to the Poleward synoptic pattern (Fig. 2.14). In the ICI-East (ICI-E) transition, a large cyclonic circulation and its corresponding peripheral anticyclone exist to the west of an eastern TC, such that the eastern TC steering becomes controlled by the equatorward flow of the eastern side of the peripheral anticyclone. If it is a large TC on the eastern side, it will exhibit a more westward track as a combination of the southwestward steering of the peripheral

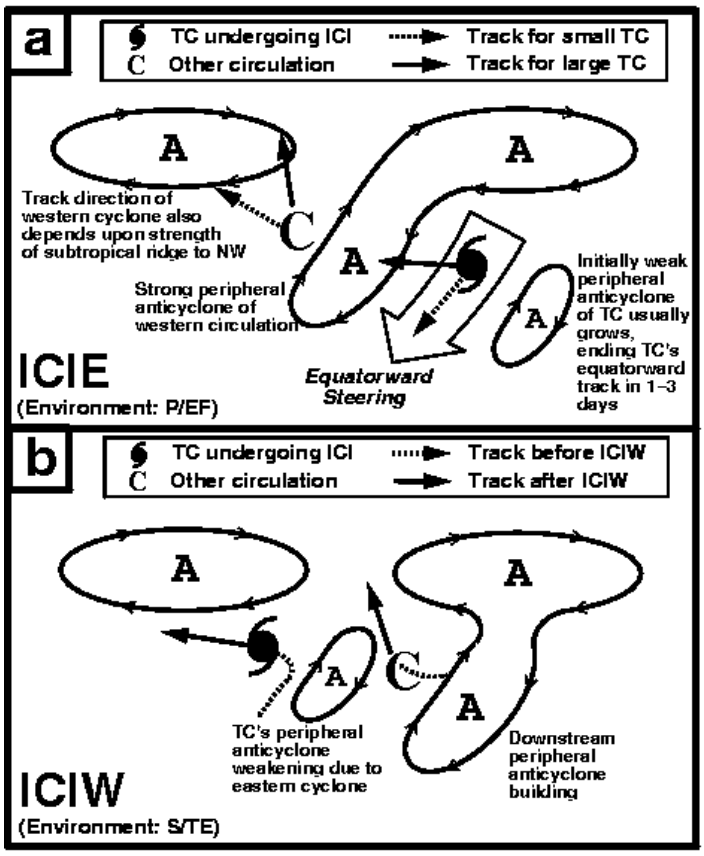

Figure 3.12. Conceptual model of Indirect Cyclone Interaction. Two types of ICI can occur depending upon the size and strength of the TCs. ICIE (ICIW) refers to the TC on the Eastern (Western) side of the peripheral anticyclone.

anticyclone and the northwestward steering due to beta-effect propagation. Without significant beta-effect propagation, a smaller TC will be steered primarily by the southwestward flow of the peripheral anticyclone. The ICI-E Transition Mechanism will cause a TC in the S/TE pattern/region to turn equatorward into the P/EF pattern/region. An equatorward steering component usually lasts for only 1-3 days, as the eastern TC forms its own peripheral anticyclone to the southeast, which causes the eastern TC to turn to a more northward track and disrupt the ICI-E mechanism.

The ICI-W Transitional Mechanism refers to the same environmental situation, with the affected TC being on the west side of the peripheral anticyclone. As shown in Fig. 3.12b, a Rossby wave train develops with the TC and the eastern cyclonic circulation both forming peripheral anticyclones. If the eastern cyclonic circulation

overtakes the peripheral anticyclone of the TC to the west, it will weaken the peripheral anticyclone (see example in Fig. 3.12b,c) and cause a turn of the western TC from a northward track in the P/PF pattern/region to a more westward track in the S/TE pattern/region (Fig. 3.12b).

d. SCI and ICI Case Study

Two TCs are present in the NIO at 12 UTC 24 October 1996 (Fig. 3.13b). Tropical Cyclone 05A in the AS is moving toward the north (Fig. 3.13a) in the P/PF pattern/region. Tropical Cyclone 06B in the south-central BOB is moving toward the west in the S/TE pattern/region. Notice in Fig. 3.13b the peripheral anticyclone that has formed to the southeast of TC 05A. Although this peripheral anticyclone has a weak connection to the subtropical anticyclone, it does not have as strong a steering influence over TC 06B as the eastern subtropical anticyclone cell. At 12 UTC 25 October (Fig. 3.13c), the peripheral anticyclone has been weakened as a result of the approach of TC 06B due to the ICI-W Transitional Mechanism and thus the Poleward pattern steering effect on TC 05A has diminished. As TC 06B continues to strengthen, it generates a peripheral anticyclone between the buffer cell to its southeast and the eastern subtropical anticyclone cell to the northeast, which causes a transition to the P/PF pattern/region by the RMT Transitional Mechanism. Farther to the west, the TC 05A is now in a transition between the P/PF and S/EF pattern/regions as the western subtropical anticyclone begins to steer TC 05A to the southwest (Fig. 3.13a).

By 12 UTC 27 October (Fig. 3.13d), TC 05A has completed a transition to the S/EF pattern/region as a result of the SCI-W Transitional Mechanism (Fig. 3.11a). Tropical Cyclone 06B has recurved to the northeast and had a transition to the P/PF pattern/region primarily as a result of the RMT transitional mechanism. However, the circulation in Fig. 3.13c with TC 05A to the west and the subtropical anticyclone to the east is consistent with SCI-E (Fig. 3.11b). Notice that the translation speed of TC 06B

a

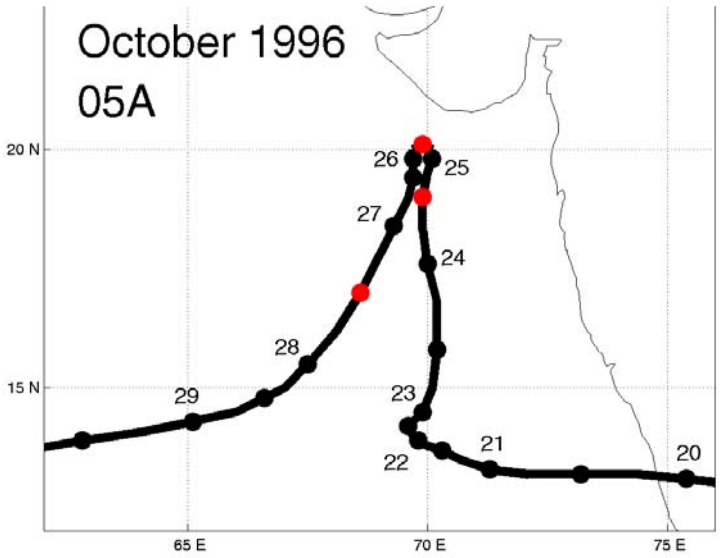

b

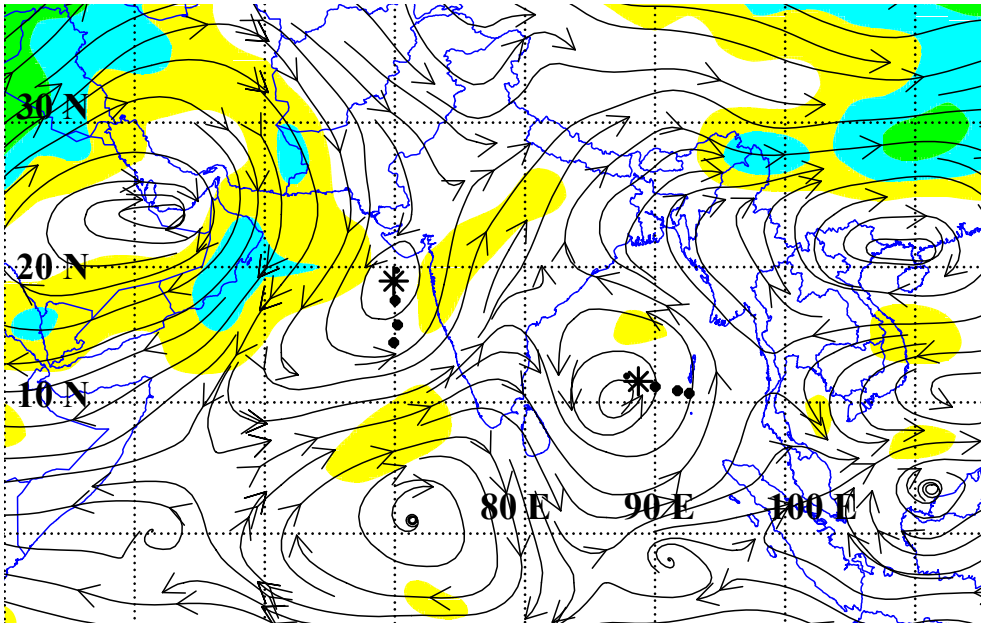

Figure 3.13. (a) Track of TC 05A from 00 UTC 20 October through 12 UTC 29 October 1996; NOGAPS analysis field as in Fig. 2.10b except for (b) 12 UTC 24 October; (c) 12 UTC 25 October; and (d) 12 UTC 27 October.

c

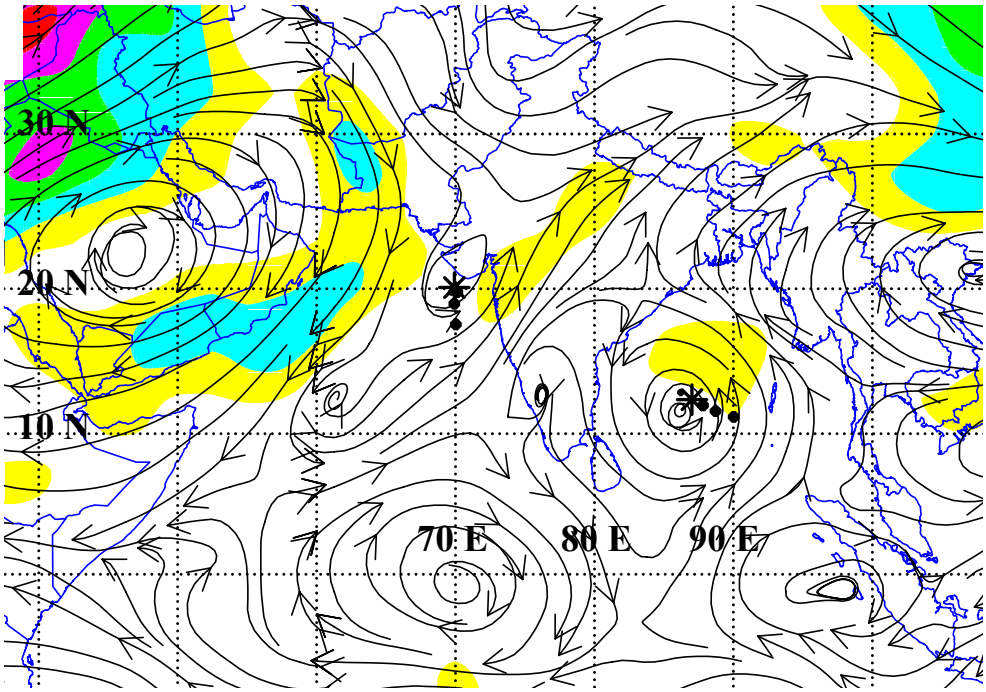

d

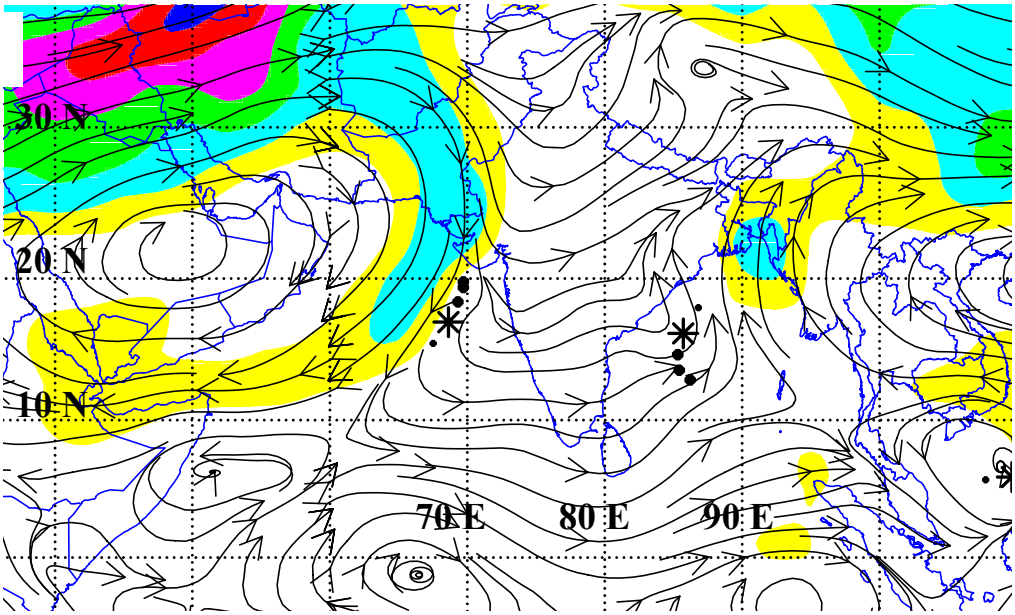

Figure 3.13. (continued)

increased from 4 kt to 8 kt as it recurved, which is also consistent with the SCI-E mechanism.

3. Midlatitude-Related – Response to Vertical Shear (RVS)

In the Systematic Approach, the intensity of a TC is used to determine the pressure level at which the storm is most likely being steered by adjacent synoptic circulations. Most mature TCs are steered at the 500 mb level, while less intense storms may be steered at the 700 mb or even the 850 mb level. When the vertical structure of a TC is compromised sufficiently by environmental vertical wind shear so as to decouple the upper-level warm core from the low-level circulation center, the TC will weaken, and thus its steering level will be at a higher pressure level (Fig. 3.14). For example, winter season TCs in the extreme western North Pacific may experience a combination of strong upper-level southwesterlies associated with an upper-level jet and low-level northeasterlies from the winter monsoon. If this vertical wind shear decouples the warm core aloft from the low-level circulation, the TC will experience a sudden track change toward the southwest in the direction of low-level environmental flow. This is the Response to Vertical Shear (RVS) Transitional Mechanism in Fig. 2.5.

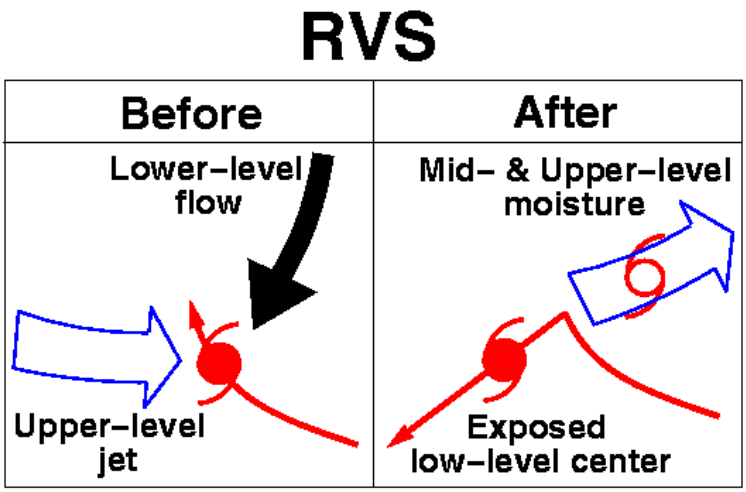

Figure 3.14. Conceptual model for the Response to Vertical Shear (RVS) of a TC in a dynamical model. Upper-level southwesterlies advect the mid- and upper-level moisture northeastward while lower-level northeasterlies advect the exposed low-level center of the TC to the southwest.

Although TC32W of 2001-2002 did not encounter strong vertical shear due to the northeast winter monsoon, it nevertheless underwent a drastic track change due to similar meteorological conditions. Tropical Cyclone 32 W reached an intensity of 65 kt over the South China Sea while on a westward track, and then crossed Malaysia and northern Sumatra into the BOB (Fig. 3.15a). At 12 UTC 31 December 2001 (Fig. 3.15b), the eastern cell of the subtropical anticyclone is over Southeast Asia, and a strong westerly to southwesterly flow dominates the AS and western BOB at 500 mb. At 700 mb (Fig. 3.15c), a weak anticyclone is centered at 12 deg. N, 89 deg. E, and it is connected to a subtropical anticyclone cell over the southern AS. Since the intensity is only 35 kt, TC 32W is being steered by the weak westward flow at 700 mb (Fig. 3.15c) versus the 500 mb flow (Fig. 3.15b). The transitional mechanism RVS is the reason TC 32W did not increase in intensity as it moved across the warm BOB waters between 2 deg. and 5 deg. North.

C. NIO TRANSITIONAL MECHANISMS

A TC is said to have undergone a transition when a change has occurred in the synoptic pattern/region as defined in Chapter II. The transition is most recognizable when there is a significant change in the TC track. These changes are caused by Environmental Effects or TC-Environmental Transformations (Fig. 2.5) as discussed in the previous sections. Each time a TC in the NIO experienced a transition from one pattern/region to another, a transitional mechanism associated with the change has been assigned. A TC may undergo several transitions through its life, and a transitional mechanism may occur multiple times in one TC. Not all transitional mechanisms identified in the four tropical cyclone basins previously studied have been found to occur in the NIO. Additionally, no unique transitional mechanisms were identified in the NIO.

Once a synoptic pattern/region is identified for a particular TC, it is important for the forecaster to know the climatological frequency that a TC may experience a transition from that pattern/region to another, as well as to understand the transitional mechanisms that cause the change. Thirteen (three, one) of the 64 TCs studied between 1991-2001 remained in the S/TE (S/PF, M/PF) pattern/region during their entire life.

a

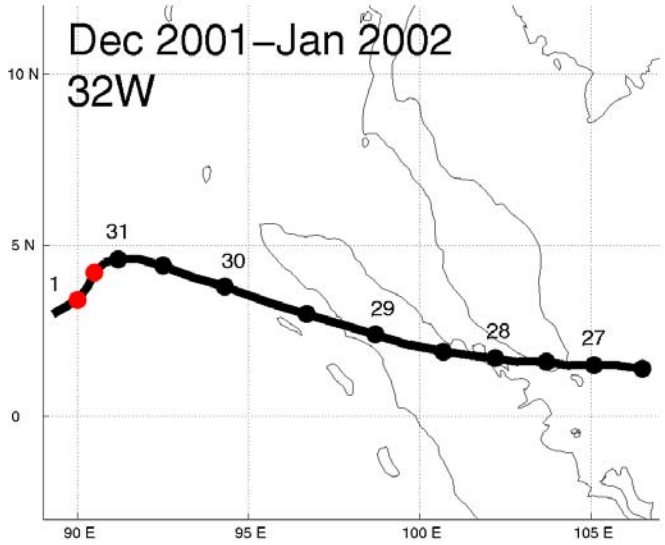

b

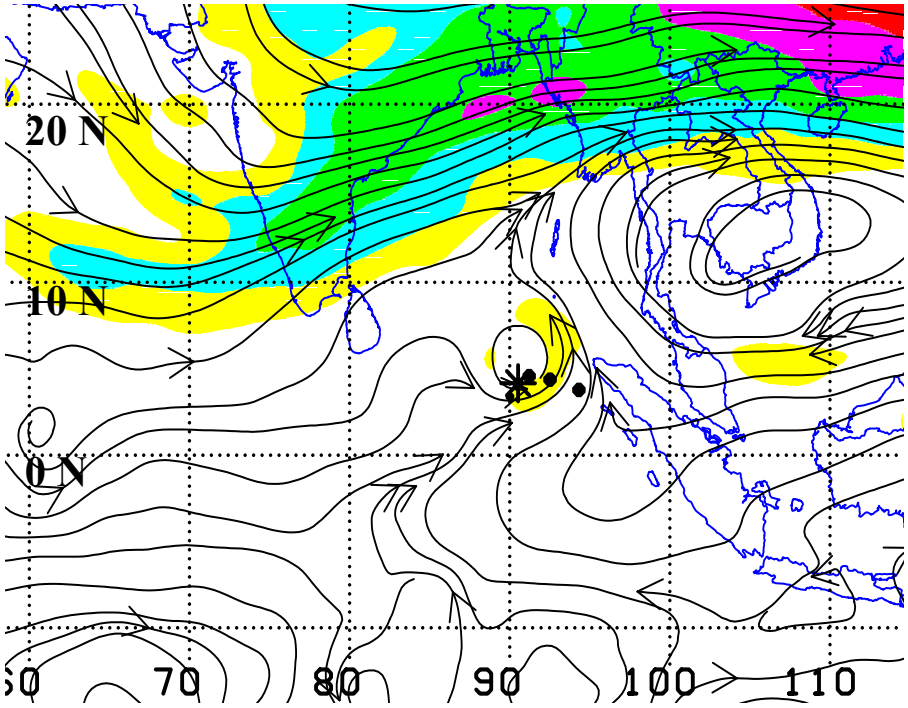

Figure 3.15. (a) Track of TC 32W from 12 UTC 26 December through 00 UTC 11 January; NOGAPS analysis field as in Fig. 2.10b except for (b) 12 UTC 31 December at 500 mb; (c) 12 UTC 31 December at 700 mb; (d) 00 UTC 1 January at 500 mb; and (e) 00 UTC 1 January at 700 mb.

c

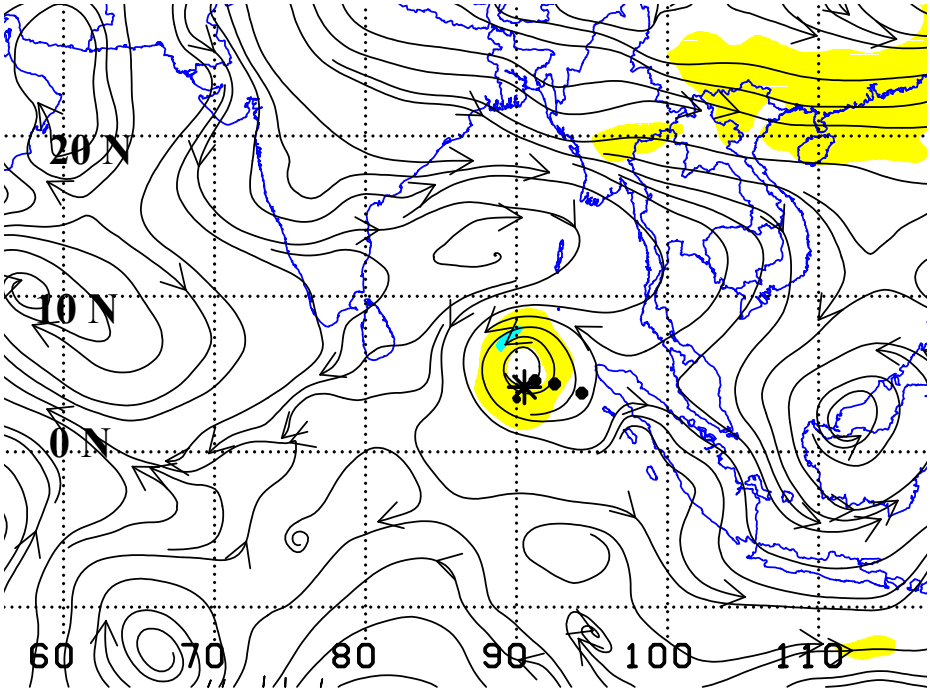

d

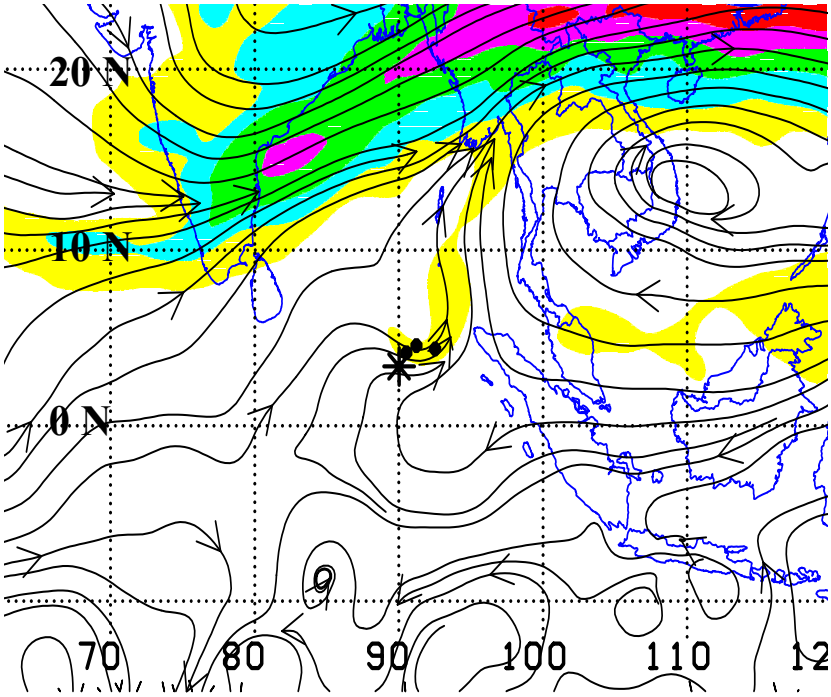

Figure 3.15. (continued)

e

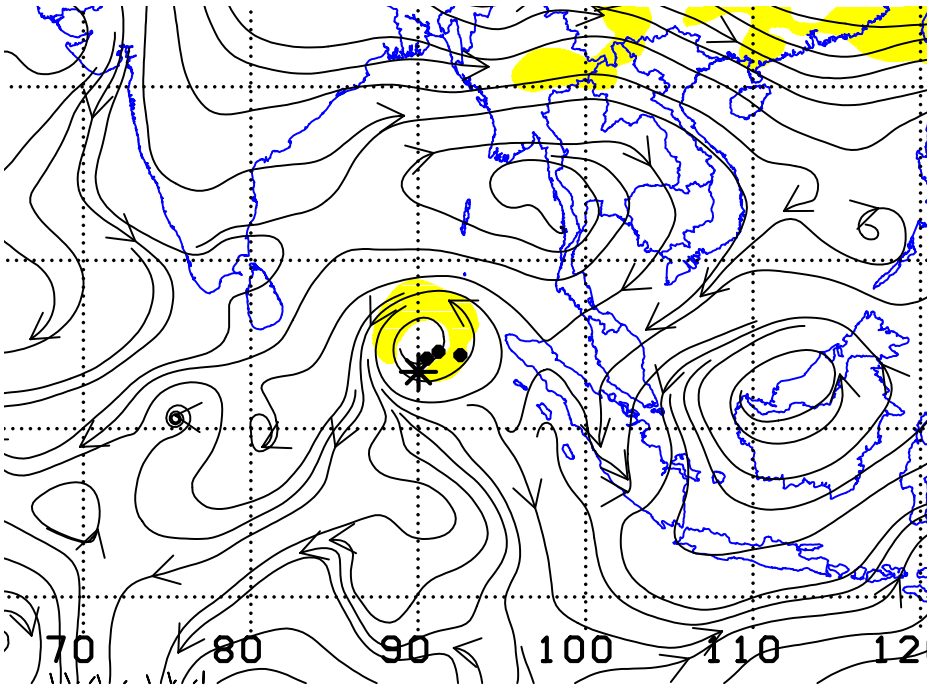

Figure 3.15. (continued)

A total of 86 recurring transitions (meaning the transition occurred more than once) were identified during 1991-2001 (Fig. 3.16). By far the most common transition in the NIO (Fig. 3.16) was from the S/TE to the S/PF pattern/region, which may occur by the ADV, BEP, MCG, or MAL mechanisms. This is not surprising as most TCs in the NIO form in the monsoon trough to the south of the subtropical anticyclone in the S pattern as shown in Fig. 2.2. It is helpful to the forecaster to know that a NIO TC in the S/TE pattern/region was only found to have transitions to the S/PF or the P/PF pattern/region.

Once the TC moves poleward, it is likely to threaten land areas. It is thus particularly important to note the transitions from the S/PF pattern/region. In the four previously examined tropical cyclone basins, it was most common for a TC in the S/PF pattern/region to transition directly into the M/PF pattern/region as the TC advected through the break in the subtropical anticyclone and into the midlatitudes. In the NIO transition diagram (Fig. 3.16), a TC often appears to remain in the S/PF pattern/region

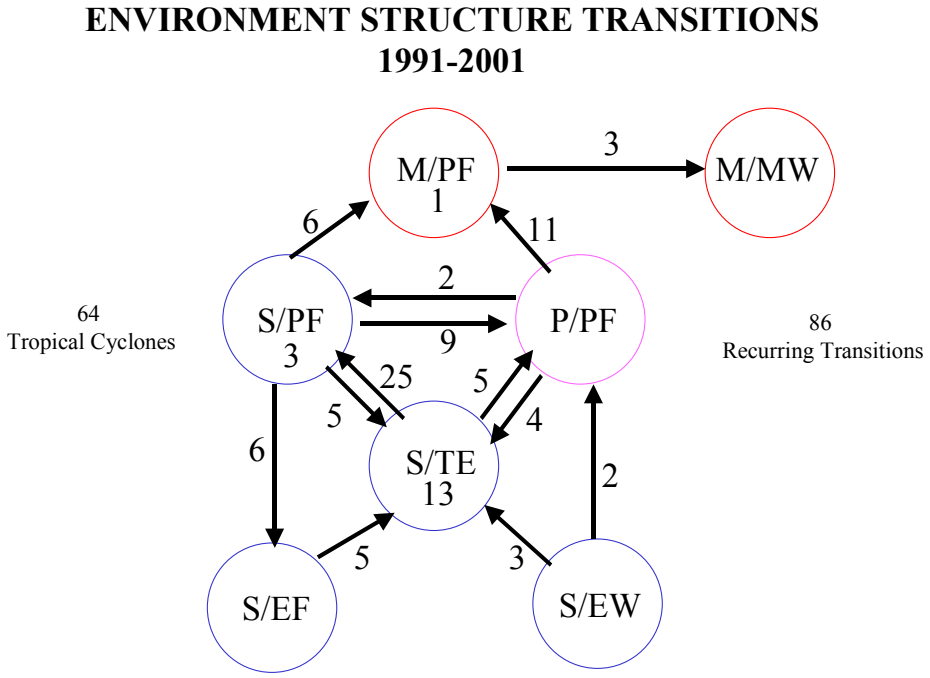

Figure 3.16. Environment structure transitions for the 64 TCs in NIO during 1991-2001. Only recurring transitions that occurred more than once during the period are included, with a total of 86 recurring transitions. Numbers within a pattern/region marker indicate the number of TCs that persisted in that environment structure for their entire lives.

long enough for the TC to form a peripheral anticyclone through the RMT transitional mechanism and experience a transition into the P/PF pattern/region. That is, 9 of 26 (35%) of the transitions from the S/PF pattern/region are into the P/PF pattern/region, while only 6 of 26 (23%) of the S/PF transitions are directly into the midlatitudes (M/PF pattern/region). This relative infrequency of a classical recurvature track is due to the Asian continent to the north of the NIO. That is, the TC dissipates soon after making landfall in the region where a transition into the midlatitudes normally occurs.

Similar to other tropical cyclone basins, a total of 11 of 26 (42%) of the transitions from the S/PF pattern/region are back into the tropics: 6 of 26 (23%) of the S/PF transitions are to the S/EF pattern/region, and 5 of 26 (19%) of the transitions are to the S/TE pattern/region. Both of these transitions may lead to the so-called stair-step track with westward motion in the S/TE pattern/region followed by poleward flow in the

S/PF pattern/region, and then these transitions lead to a more westward track again. Since 42% of the transitions from poleward motion in the S/PF pattern/region are in this category, this is an important scenario for the TC forecaster to be aware of.

Other frequent transitions occurred from the P/PF to the M/PF pattern/region. The P/PF to M/PF pattern/region transition is the second-most common due to the frequent occurrence of the RMT transitional mechanism, which occurred 32 times in the 64 TCs examined between 1991-2001. Sixty-five percent (11 of 17) of the transitions from the P/PF pattern/region are into the midlatitudes, and specifically to the M/PF pattern/region. Another 12% (2 of 17) of the P/PF transitions are to the S/PF pattern/region following a breakdown of the peripheral anticyclone. However, this is still a poleward motion. Another 23% (4 of 17) of the transitions from the P/PF pattern/region are to the S/TE pattern/region and thus are also back into the tropics.

The smaller number of TCs in the NIO compared to previous studies in other tropical cyclone basins obviously limits the number of Environment Structure transitions. Only three synoptic patterns are found in the NIO, and some of these patterns have fewer regions than in other basins. Thus, fewer options exist for transitions among pattern/regions. The TCs in the S/EW pattern/region were observed making only the transition to the S/TE or P/PF pattern/region, while TCs in S/EF were recorded making only the transition into the S/TE pattern/region. This information assists the forecaster in narrowing down the possible track changes a TC will make during its lifetime.

D. CASE STUDIES

The following three case studies describe the frequently occurring transitions and associated transitional mechanisms in the NIO between 1991-2001.

1. S/TE – S/PF – P/PF – M/PF

Tropical Cyclone 02B of 1991 was one of the most intense TCs ever to form in the BOB as it reached an intensity of 140 kt. It made landfall at Chittagong, Bangladesh with an intensity of 130 kt, and caused a 20 ft storm surge that killed 138,000 people and caused U.S. $1.5 billion in damage (JTWC 1991).

Tropical Cyclone 02B of 1991 formed in the eastern extension of the monsoon trough at approximately 10 deg. N (Fig. 3.17a). Initially, the storm was in the S/TE

a

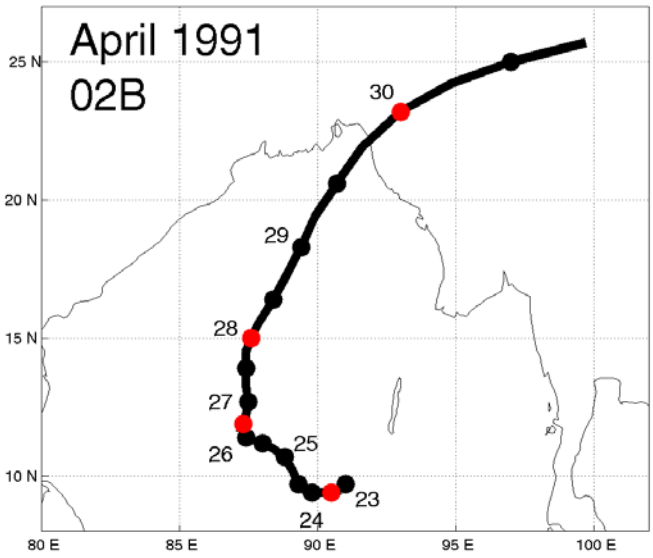

b

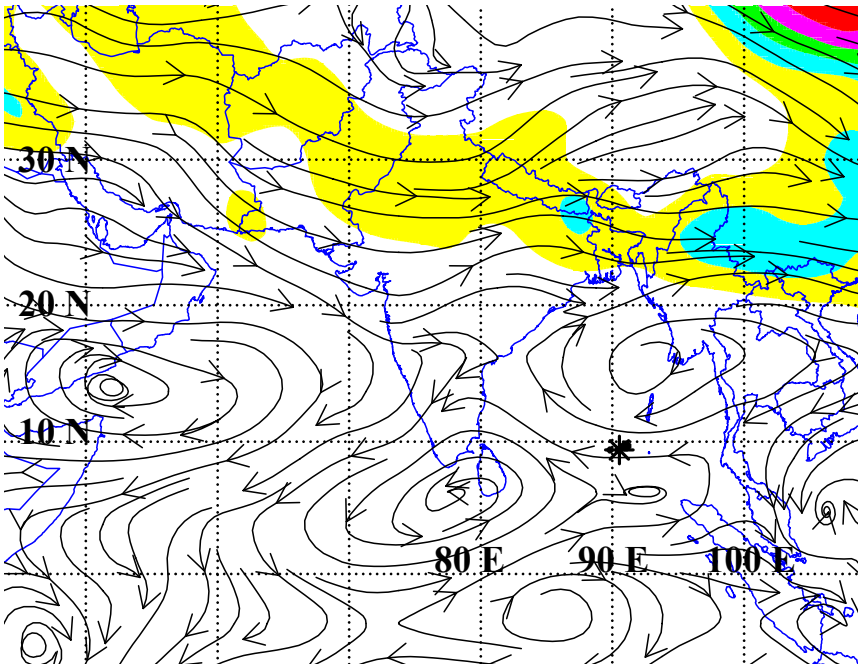

Figure 3.17. (a) Track of TC 02B from 00 UTC 23 April through 00 UTC 1 May 1991; NOGAPS analysis field as in Fig. 2.10b except for (b) 12 UTC 23 April; (c) 12 UTC 26 April; (d) 00 UTC 28 April; and (e) 00 UTC 30 April.

c

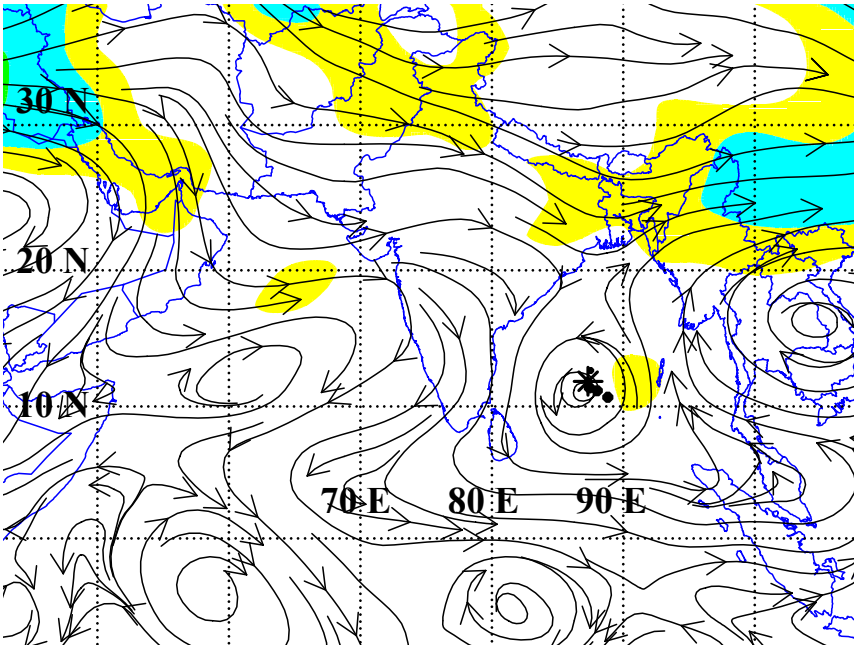

d

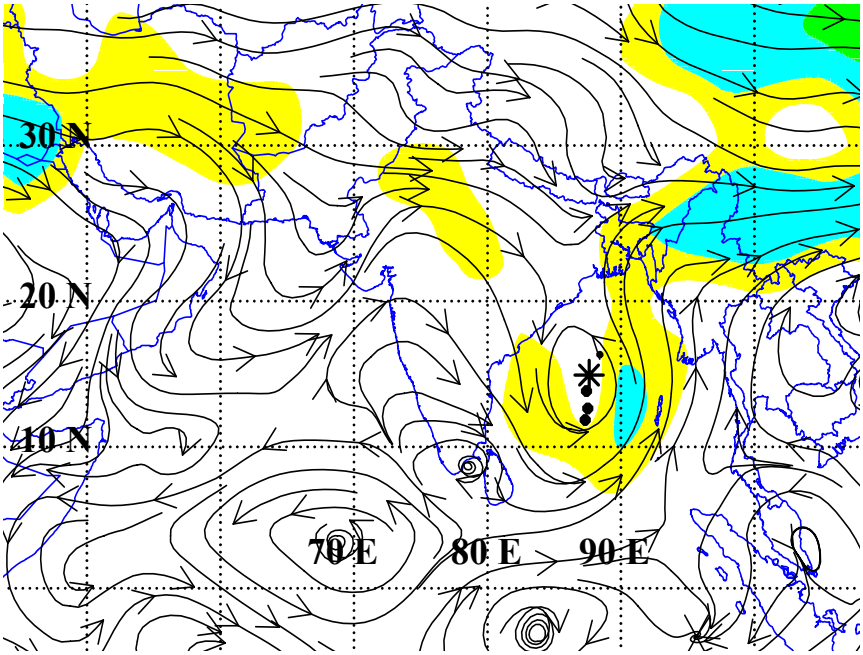

Figure 3.17. (continued)

e

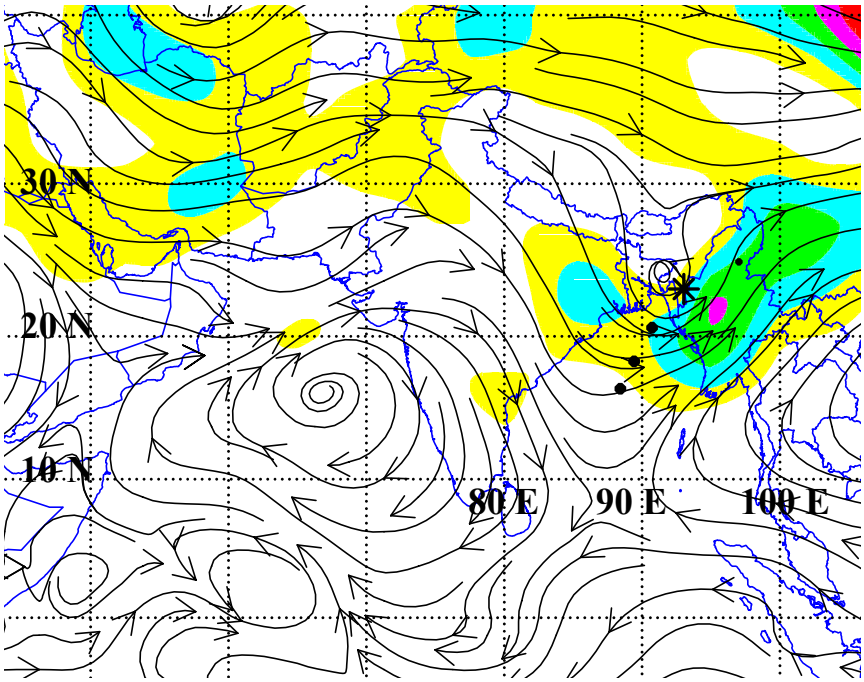

Figure 3.17. (continued)

pattern/region under the steering influence of the eastern subtropical anticyclone cell over the northeast BOB (Fig. 3.17b). Tropical Cyclone 02B was relatively small in extent with an intensity of 25 kt at 12 UTC 23 April. Tropical Cyclone 02B moved westward for 12 h (Fig. 3.17a) when a series of short-wave troughs to the north caused the eastern subtropical anticyclone cell to move to the east (not shown). A Midlatitude Anticyclolysis (MAL) mechanism was then evident as TC 02B began a slow turn to the north with a transition from the S/TE to the S/PF pattern/region. On 25 April, TC 02B began to move toward the west again and the TC translation speed slowed as the eastern subtropical anticyclone cell amplified (not shown) as a result of the Midlatitude Anticyclogenesis (MAG) mechanism. However, TC 02B remained in the S/PF pattern/region in the southwest quadrant of the eastern subtropical anticyclone.

By 12 UTC 26 April (Fig. 3.17c), a midlatitude shortwave trough had approached from the west and began interacting with TC 02B, which is the Midlatitude Cyclogenesis (MCG) mechanism. The combination of northeastward steering from the eastern side of the midlatitude trough and the western side of the subtropical anticyclone resulted in a slight track change toward the northeast and a slow increase in speed. However, the TC

is considered to have remained in the S/PF pattern/region despite these slight track changes because the TC is still in the west-southwest quadrant of the eastern subtropical anticyclone with an isotach maximum to the east-northeast (Fig. 3.17c). As the midlatitude trough moved eastward, the TC 02B track shifted back to the north (Fig. 3.17a). Low environmental shear and significant outflow at upper levels allowed TC 02B to continue to strengthen over the next 24 h.

As the TC grew in size and intensity, the Ridge Modification by a TC (RMT) mechanism caused a peripheral anticyclone to form, which merged with the circulation of the equatorial buffer cell to the south and the subtropical anticyclone to the east. Tropical Cyclone 02B already had started moving to the north-northeast (Fig. 3.17a) and had a transition from the S/PF to P/PF pattern/region. The exact timing of this type of recurvature may be very difficult for forecasters to identify, and is not always handled properly by numerical models (to be discussed in Chapter 4). Recurvature of TC 02B was not as marked a turn toward an eastward component as is normally seen as the TC was primarily moving poleward in the P/PF pattern/region with an eastward component. Had the subtropical anticyclone been less meridionally oriented, a track change toward the northeast would be much clearer. The synoptic situation depicted in Fig. 3.17d supports the P/PF pattern/region. An extensive meridional anticyclonic circulation that extended from the equator to 20 deg. N was steering TC 02B toward the north-northeast with an isotach maximum to the east-southeast, which is consistent with a P/PF assignment. Satellite imagery (not shown) also supports the P/PF pattern/region assignment as an area of clearing caused by subsidence was present east of TC 02B.

A transition into the M/PF pattern/region occurred at 12 UTC 28 April as the TC advected around the subtropical anticyclone. Tropical Cyclone 02B made landfall at about 18 UTC 29 April (Fig. 3.17a) after reaching its maximum intensity while still in the M/PF pattern/region. By 00 UTC 30 April (Fig. 3.17e), TC 02A was to the north of the subtropical anticyclone axis, and with an isotach maximum to the east-southeast. Tropical Cyclone 02B dissipated over the mountainous regions inland, although not before torrential rains associated with the TC had caused severe flooding (JTWC 1991).

2. S/EW-S/TE-S/PF-M/PF-M/MW

This pattern/region transition sequence is primarily a result of advection around the eastern subtropical anticyclone cell in the NIO. Tropical Cyclone 01A was the only TC to form in the AS during 1993 and formed near 6 deg. N in the western half of the monsoon trough. The TC initially moved toward the east (Fig. 3.18a) in the S/EW pattern/region, as supported by the extensive isotach maximum to the south (Fig. 3.18b) The isotach maximum to the north of TC 01A is indicative of an upcoming transition to the S/TE pattern/region.

At 00 UTC 11 November 1993, TC 01A came under the steering influence of a large anticyclone (via MAG) over northern India (Fig. 3.18c). The isotach maximum to the north of TC 01A is stronger and closer than the isotach maximum to the south associated with the cross-equatorial westerlies. By 12 UTC 13 November (Fig. 3.18d), TC 01A had transitioned into the S/PF pattern/region as it advected around the western periphery of the eastern subtropical anticyclone cell and moved north-northwest (Fig. 3.18a). The isotach maximum has shifted to the east-northeast of TC 01A, which now has an intensity of 60 kt.

At 12 UTC 14 November (Fig. 3.18e), TC 01A is just north of the eastern subtropical anticyclone cell axis, which is now oriented northwest-to-southeast from central India to the southeast BOB. Although TC 01A has now recurved with an eastward track component, the isotach maximum is to the northeast of the TC because it is now embedded in the westerly short-wave trough. This is a common feature of TCs in M/PF (namely the isotach maximum is not necessarily to the southeast as in Fig. 2.18a). With strong steering winds to the southeast combined with the typically strong midlatitude winds to the north, the isotach maximum is often analyzed to the east or even northeast of the TC, even though the steering on the TC is still toward the northeast. The transition from the S/PF pattern/region into the M/PF pattern/region was caused by (ADV) advection around the subtropical anticyclone. The transition into the M pattern occurred while TC 01A was still over the northern AS as the subtropical anticyclone was

a

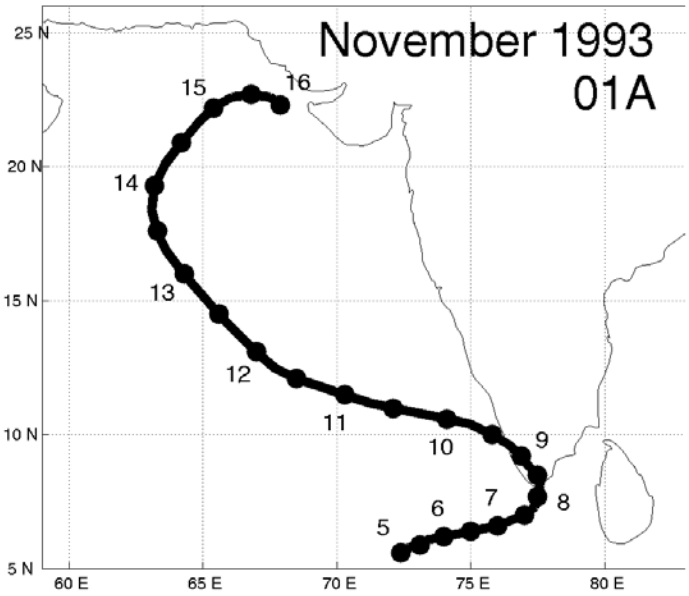

b

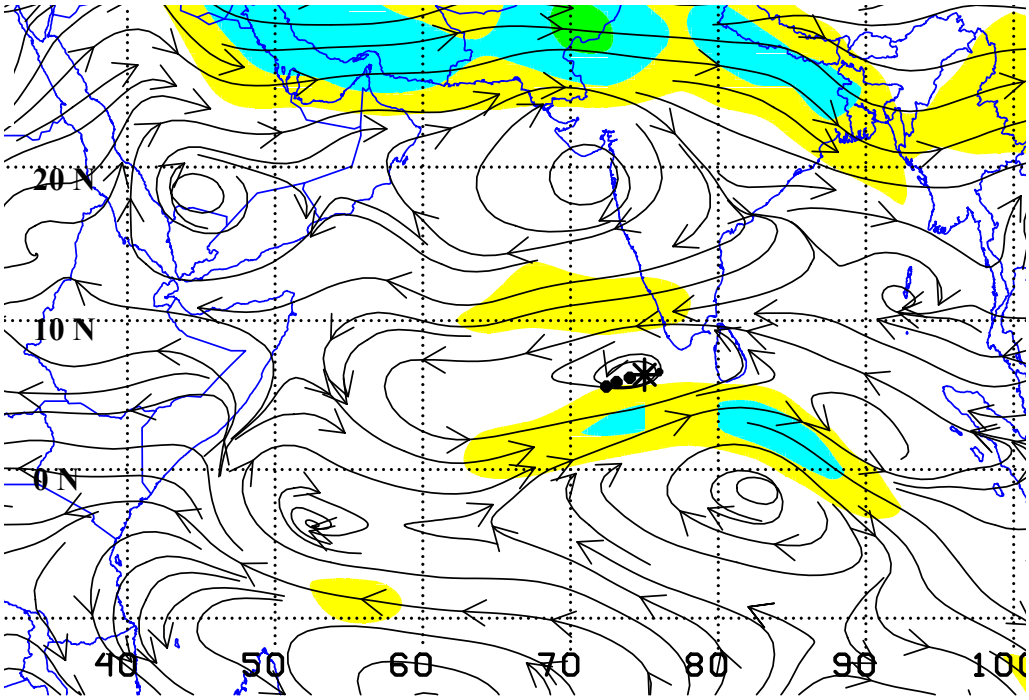

Figure 3.18. (a) Track of TC 01A from 00 UTC 5 November through 00 UTC 16 November 1993; (b) NOGAPS analysis field as in Fig. 2.10b except for 12 UTC 6 November; (c) 00 UTC 11 November; (d) 12 UTC 13 November; and (e) 12 UTC 14 November.

c

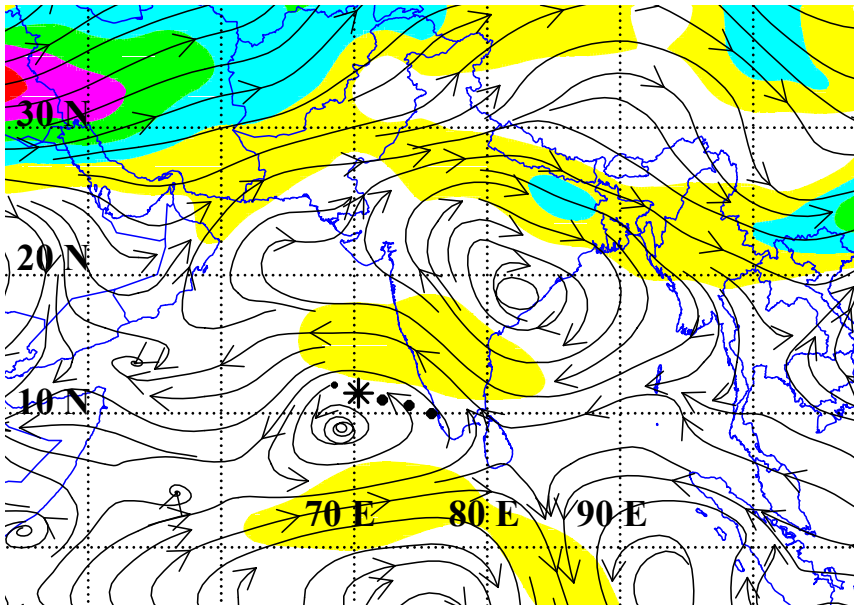

d

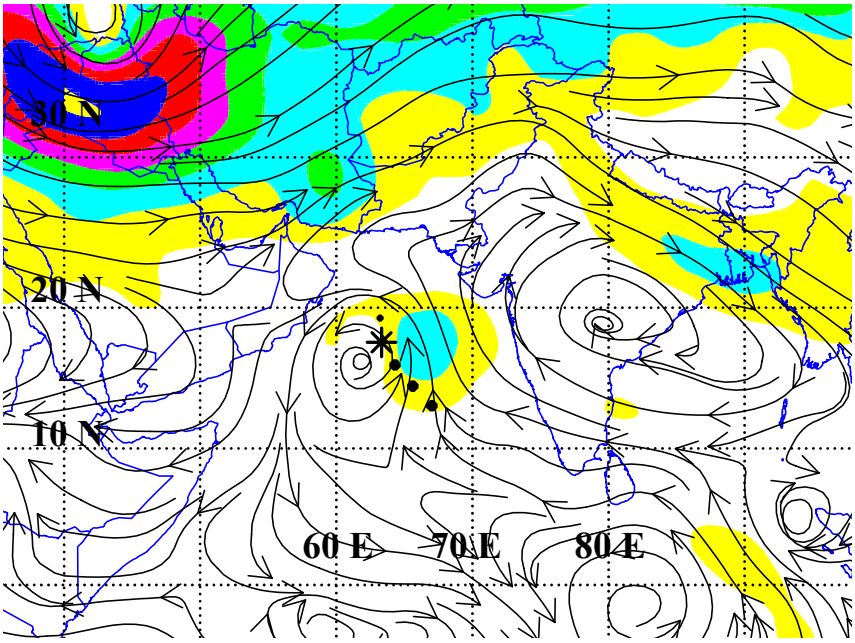

Figure 3.18. (continued)

e

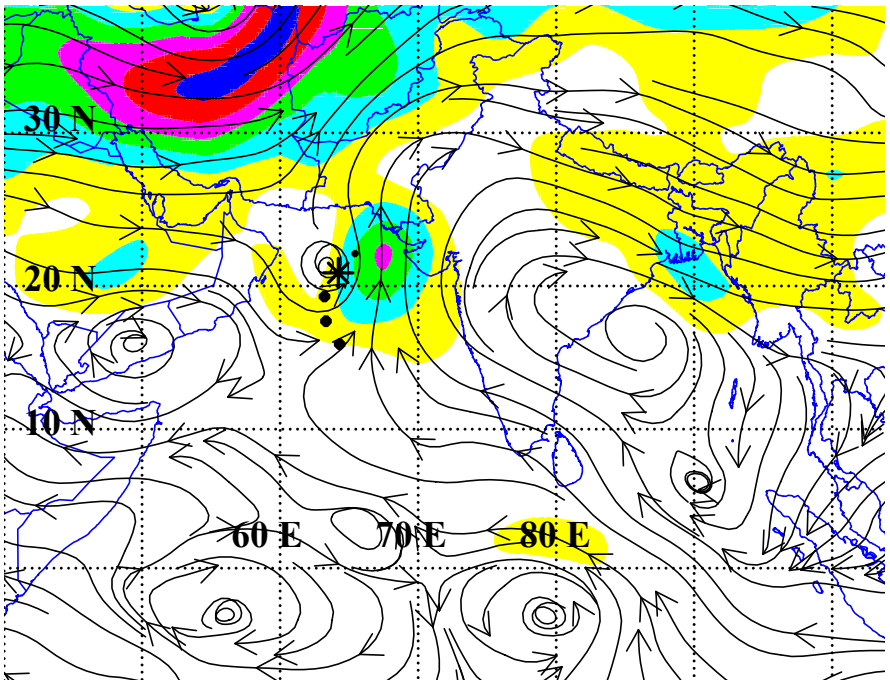

Figure 3.18. (continued)

farther south than usual. Later TC 01A experienced a transition to the M/MW pattern/region for a period of about 12 h before dissipating (Fig. 3.18a).

3. S/TE-S/PF-S/EF

Tropical Cyclone 05B during 1999 was an extremely intense storm for the NIO as it reached a peak intensity of 140 kt. When it made landfall near Bhubaneswan, India nearly 10,000 people were killed, and the region experienced record flooding. It was the worst storm to strike northeastern India since 1971 (JTWC 1999).

Whereas TC 05B formed east of the Malay Peninsula in an area of significant vertical wind shear, it did not begin to intensify until it entered the eastern BOB in the S/TE pattern/region at 00 UTC 25 October 1999 (Fig. 3.19a). The TC was being steered at 500 mb by the easterly flow between a zonally oriented subtropical anticyclone to the north and the monsoon trough (Fig. 3.19b). As TC 05B continued to intensify, it began to advect around the eastern subtropical anticyclone cell toward a col over Myanmar to the north, so that a transition to the S/PF pattern/region occurred due to ADV.

a

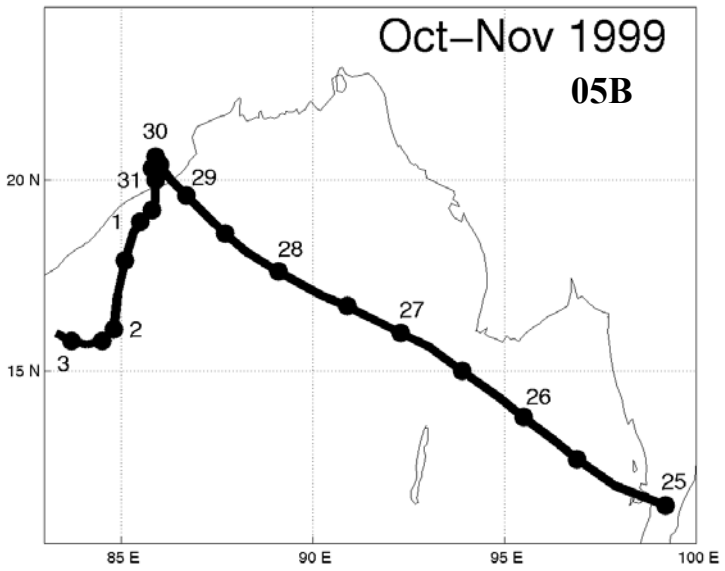

b

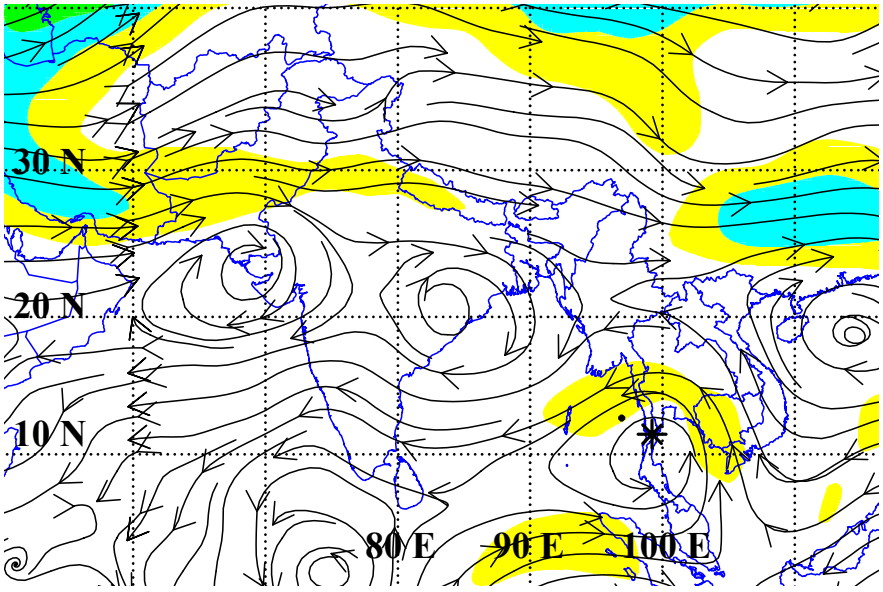

Figure 3.19. (a) Track of TC 05B from 00 UTC 25 October through 00 UTC 3 November; NOGAPS analysis field as in Fig. 2.10b except for (b) 00 UTC 25 October; (c) 12 UTC 26 October; (d) 12 UTC 28 October; and (e) 12 UTC 29 October.

c

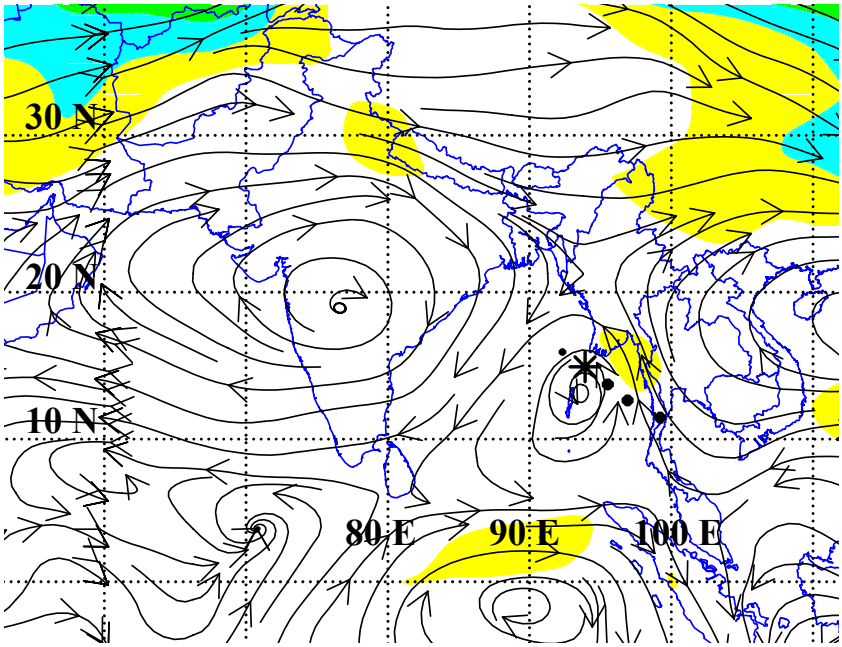

d

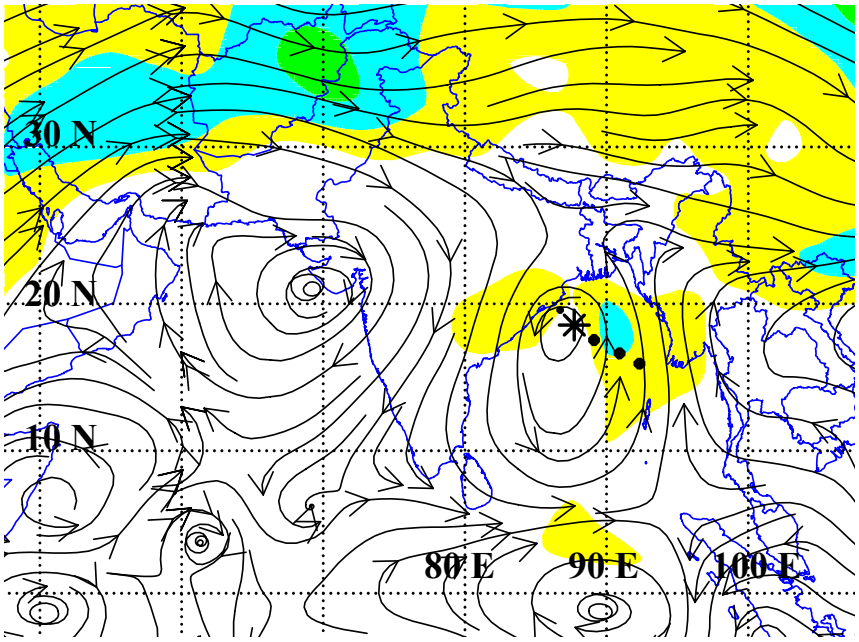

Figure 3.19. (continued)

e

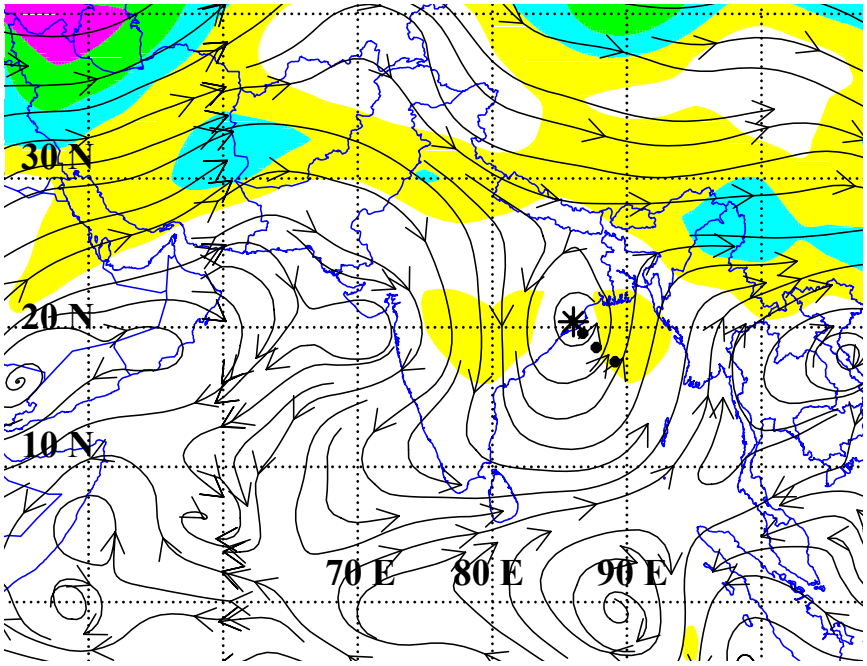

Figure 3.19. (continued)

Over the next 48 h, TC 05B moved toward the northwest (Fig. 3.19a) and closer to the col and the western subtropical anticyclone cell (Fig. 3.19c), which had intensified due to Midlatitude Anticyclogenesis (MAG) over the past several days. As TC 05B moved into the col between the western and eastern subtropical anticyclone cells, the steering of TC 05B was changing as the storm then began a transition to the S/EF pattern/region. Given the opposing southward flow to the west and northward flow to the east (note maximum isotach positions in Fig. 3.19d), TC 05B began to slow (Fig. 3.19a). Since TC 05B was still over warm water and in weak shear, it intensified and pounded the northeast Indian coast with wind and heavy rain. As TC 05B remained in a transitional state between the S/PF and S/EF pattern/regions for the next 36 h, it started to decrease in intensity over land. Although TC 05B was strong enough to form a peripheral anticyclone to the southeast through Rossby wave dispersion that might have lead to RMT (Fig. 3.19e), the western subtropical anticyclone cell started to strengthen even more by MAG due to the short wave ridge passing over the Afghanistan-Pakistan border.

The sharp turn from a northerly to a southerly track over the northeast Indian coast during a 48 h period is a classic "stair-step" track example of a TC transition from the S/PF to the S/EF pattern/region. By 00 UTC 1 November (not shown), the western subtropical anticyclone cell had gained steering control over TC 05B, which moved toward the southwest and out to sea (Fig. 3.19a) in the S/EF pattern/region. Tropical Cyclone 05B then dissipated over the next 54 h.

E. CONCLUSIONS

Once a forecaster understands the transitional mechanisms common to a particular ocean basin, it is important for that forecaster to recognize those patterns in the various models applicable to that basin. As discussed in the introduction, models are initialized with varying initial conditions, which ultimately affect the forecast of the synoptic situation for each ocean basin. It is therefore necessary to identify numerical model traits in accordance with the Systematic Approach (Fig. 1.1) for the NIO. A Dynamical Model Forecast Traits Knowledge Base has been developed by Carr and Elsberry (1999, 2000a, 2000b), Brown (2000), and Reader et al. (2000) for the western North Pacific, Atlantic, and Southern Hemisphere. Chapter IV will be a description of the Dynamical Model Forecast Traits Knowledge Base for the NIO.

IV. NORTH INDIAN OCEAN DYNAMICAL MODEL FORECAST TRAITS KNOWLEDGE BASE

A. OBJECTIVE

As stated in Chapter I.A, the central focus of the Systematic Approach is that forecasters can formulate track forecasts that improve on the accuracy and/or consistency of the dynamical model or other objective guidance if they are equipped with: (i) a TC Motion Meteorology Knowledge Base of dynamically sound conceptual models that classify various TC-environment situations; (ii) a knowledge base of recurring TC track forecast errors attributed to various combinations of TC structure and environment structure, and anticipated changes; and (iii) an implementing methodology or strategy for applying these two knowledge bases to particular TC forecast situations (Carr and Elsberry 1999). Since the TC Motion Meteorology Knowledge Base has already been established in Chapters II and III, the second step in fulfilling the Systematic Approach conceptual framework in Fig. 1.1 lies in defining a Dynamical Model Forecast Traits Knowledge Base for the North Indian Ocean.

B. METHODOLOGY

This study examines large North Indian Ocean TC track errors made by the dynamical models used at the Joint Typhoon Warning Center during the 2000 and 2001 seasons. A model error is defined as "large" if the predicted track exceeds 225 n mi from the TC verifying best track. By contrast, the "large" error has previously been set at 300 n mi (Carr and Elsberry 1999) because it is difficult to identify the cause of the error unless it is fairly large. A smaller error cutoff of 225 n mi for this study reflects the lower average model errors in the NIO as compared to the western North Pacific.

Models used in this study include the Navy Operational Global Atmospheric Prediction System (NOGAPS), UK Met Office global model (UKMO), and the Geophysical Fluid Dynamics Laboratory- Navy Model (GFDN). These three models were used in forecasting TC motion in the NIO during 2000 and 2001. An error mechanism determination was completed by comparing model forecast fields of 200 mb, 500 mb, 700 mb, and 850 mb winds as well as mean sea level pressure that are associated with large forecast track errors to the corresponding analysis fields.

C. TRACK ERRORS OVERVIEW

The distributions of the 72-h NOGAPS, UKMO, and GFDN forecast track errors (FTE) for the 2000 and 2001 North Indian Ocean TC seasons are shown in Fig. 4.1, from which several salient points can be drawn in reference to model performance in the NIO. First, NOGAPS has a significantly higher occurrence of small FTEs at 72 h than the other

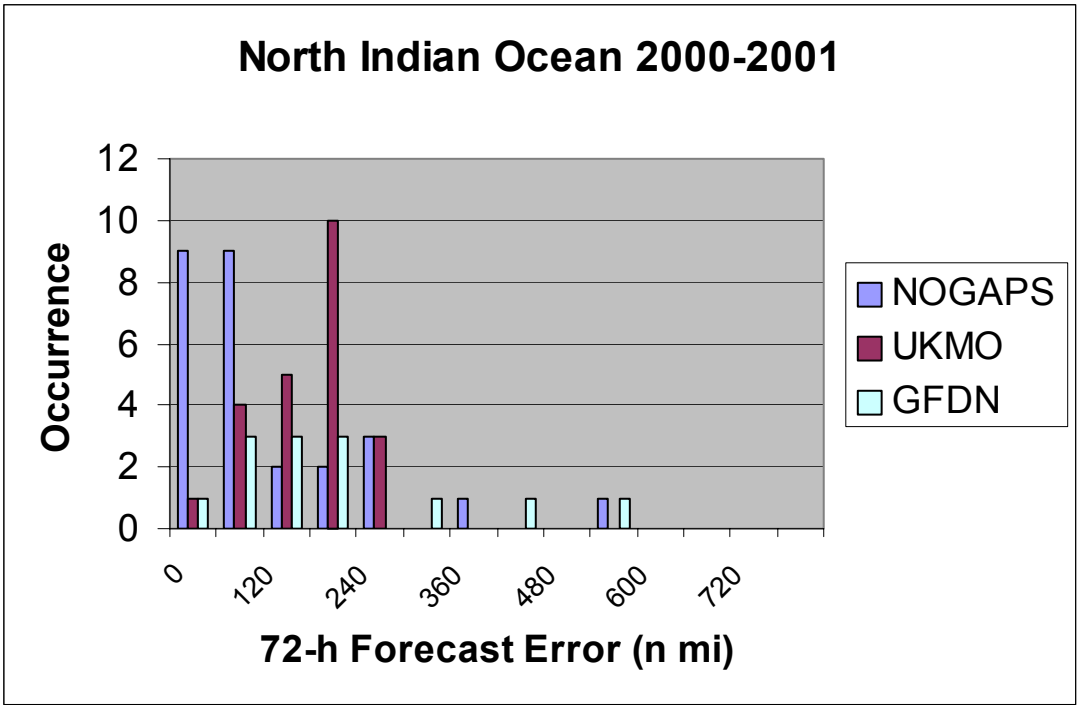

Figure 4.1. Frequency of occurrence of 72-h track errors for the NOGAPS, UKMO and GFDN forecasts during the 2000 and 2001 TC seasons.

models, and thus has a general decrease in occurrence of larger FTEs. The UKMO model has an increase relative to NOGAPS in the occurrence of higher FTEs; however, no very large UKMO outliers occurred during the 2000 and 2001 seasons. Second, notice that the histograms of the NOGAPS and GFDN track errors are not normal distributions, but are skewed toward larger FTEs. Similar distributions have been found in the other oceanic basins. These large errors pose a significant challenge to the

forecaster. The largest FTEs are 573, 560, and 288 n mi for the NOGAPS, GFDN, and UKMO models, respectively.

A non-homogeneous comparison of 24-h to 72-h FTEs for the three models is given in Fig. 4.2. The average non-homogeneous 72-h FTEs are 134, 179, and 216 n mi for the NOGAPS, UKMO, and GFDN models, respectively. Whereas the NOGAPS model has the highest FTE at 24 h, it is the most accurate at the 48-h and 72-h forecast periods. The regional GFDN model has a significantly larger error than the global models due to the errors incurred during the forecasts of TC 01A in 2001. It is expected that a larger sample size would decrease the FTE of the regional model as compared to the global models. The percentage of 72-h forecasts with a 225 n mi or greater FTE is 13% for UKMO, 19% for NOGAPS, and 31% for GFDN. However, an FTE of 225 n mi is 50% above the average 72-h FTE goal of 150 n mi set by the Meteorology Group Pacific Command. The percentage of 72-h forecasts with a 150 n mi or greater FTE is 33% for NOGAPS, 62% for GFDN, and 70% for UKMO. Therefore, NOGAPS appears to consistently be the most accurate of the four models beyond 24 h.

A homogeneous FTE comparison was made for those cases in which both NOGAPS and UKMO models were available (Fig. 4.3a). For the 15 forecasts in which

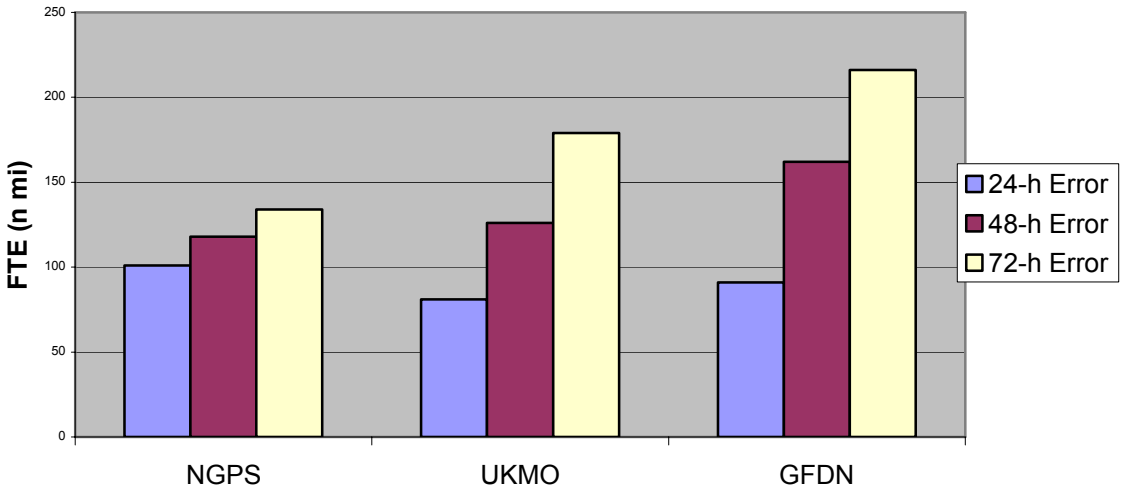

Figure 4.2. Average non-homogeneous FTE for NOGAPS, UKMO, and GFDN during the 2000-2001 TC seasons.

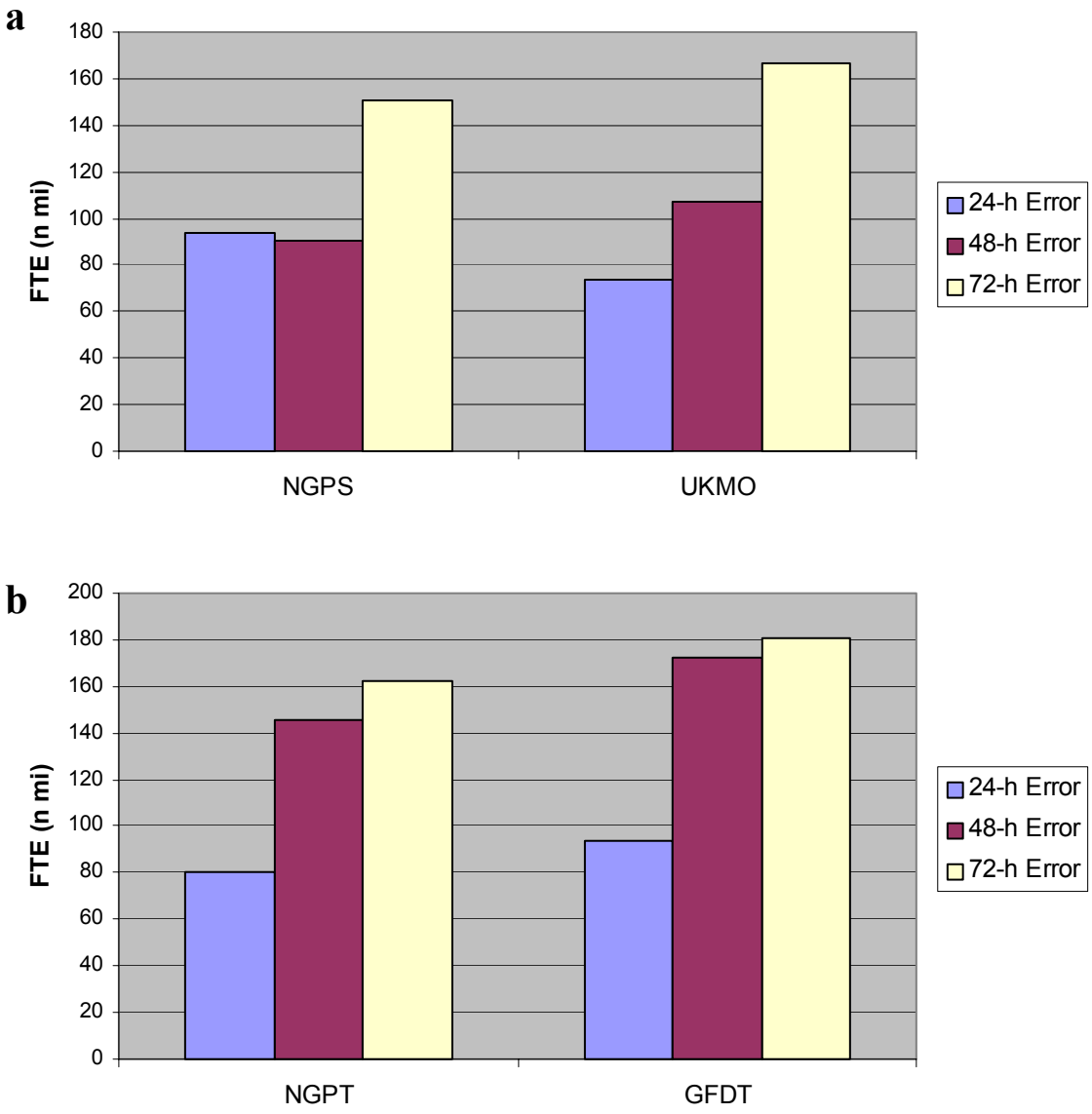

Figure 4.3. Average homogeneous FTE for (a) NOGAPS and UKMO; and (b) translated NOGAPS (NGPT) and GFDN (GFDT) during the 2000-2001 TC seasons

both models tracked a TC to 72 h, the average FTEs were 150 and 167 n mi for NOGAPS and UKMO, respectively. A homogeneous comparison is possible between the NOGAPS and GFDN translated model tracks (NGPT and GFDT) to overcome the differences in model run time. As illustrated in Fig. 4.3b, the average FTE for the 22 forecasts available at 72 h were 162 and 181 n mi for the NGPT and GFDT models, respectively. However, based on a student t-test statistical analysis, there is no significant difference between the average FTEs of the NOGAPS and UKMO models or the NGPT

and GFDT models. Due to the lower average model errors and inherently fewer storms in the NIO, only 12 forecasts during 2000-2001 were found to have a 72-h FTE of greater than 225 n mi.

The twelve large error cases for NOGAPS, UKMO, and GFDN during the 2000-2001 TC seasons were examined following the approach of Carr and Elsberry (1999) to find discernable model error traits. Only six of the eight TCs that formed in the NIO during the 2000-2001 seasons provided the twelve large error cases for this study. Of those twelve cases, six occurred in TC 01A of 2001 and will be discussed in the case studies in section D. The results of the analysis are listed in Tables 1a-c for NOGAPS, UKMO, and GFDN. The frequencies of the phenomena causing the model errors are listed in Table 2.

Six error mechanisms common to the western North Pacific, eastern and central North Pacific, Atlantic, and Southern Hemisphere basins were identified in the NIO, and are listed in Table 2. The first five of the error mechanism names are associated with the mechanisms that cause TC motion. That is, these track errors occur when the model incorrectly handles real physical processes that explain TC motion. The sixth error mechanism is related to a poor initial TC position in the model.

In accordance with the TC Motion Meteorology Knowledge Base Framework (Fig. 2.5) and Table 2, Midlatitude Systems Evolutions (MSEs) account for 7 (58%) of the large FTEs, four of which occurred during TC 01A of 2001 (Table 1). Errors resulting from beta-effect and tropical-related Environmental Effects each resulted in 2 (17%) and 1 (8%) of large FTEs. Initial position errors resulted in 2 (17%) large FTEs as well. Each of these error mechanisms will be discussed below, followed by a corresponding case study.

D. CASE STUDY ANALYSIS

The purpose of the case studies is to provide the forecaster with a general synoptic situation and description of the corresponding error mechanism. Because of the limited number of cases examined during the 2000-2001 TC seasons in the NIO, these case studies may not represent the most common synoptic situations in which these error mechanisms may be found. It is important to note that the error mechanisms detected in

a NOGAPS 72-H FORECASTS EXCEEDING 225 N MI IN 2000-2001

2000				2001			
TC	DATE	FTE	CAUSE	TC	DATE	FTE	CAUSE
03B	112700	255	E-MCG	01A	052312	263	E-RMT
				02A	092412	573	E-EWB
				03A	101000	246	I-MCG
				04B	110900	379	IPE

b UKMO 72-H FORECASTS EXCEEDING 225 N MI IN 2000-2001

2000				2001			
TC	DATE	FTE	CAUSE	TC	DATE	FTE	CAUSE
04B	122500	284	IPE	01A	052500	274	E-RMT
				01A	052512	288	E-MAG

c GFDN 72-H FORECASTS EXCEEDING 225 N MI IN 2000-2001

2000				2001			
TC	DATE	FTE	CAUSE	TC	DATE	FTE	CAUSE
03B	112806	235	E-MCG	01A	052206	560	E-MCG
				01A	052218	459	E-MCG
				01A	052306	322	E-MAL

Table 1. All (a) NOGAPS; (b) UKMO; and (c) GFDN 72-h track forecasts for NIO TCs during 2000-2001 that resulted in a FTE exceeding 225 n mi. The date is the month, day, and hour (UTC) of the initial time for the 72-h forecast. The meanings of the acronyms in the cause column are provided in Table 2.

CAUSE OF NOGAPS, UKMO, OR GFDN 72-H FORECAST TRACK ERRORS GREATER THAN 225 N MI		NUMBER OF FORECASTS		
Phenomenon Name	Acronym	NOGAPS	UKMO	GFDN
Ridge Modification by a TC	RMT	1-0	1-0	0-0
Midlatitude Systems Evolutions				
Midlatitude Cyclogenesis	MCG	1-1	0-0	2-0
Midlatitude Anticyclogenesis	MAG	0-0	1-0	0-0
Midlatitude Anticyclolysis	MAL	0-0	0-0	1-0
Equatorial Wind Burst	EWB	1-0	0-0	0-0
Initial Position Error	IPE	1	1	0
Not Discernable or Explainable		0	0	0
All Cases		5	3	4

Table 2. Meanings and frequencies of the causes of large NOGAPS, UKMO, and GFDN FTEs in the NIO during 2000-2001. When two numbers are listed, the first (second) is the number of times the phenomenon occurred excessively (insufficiently) in the model and corresponds to the E (I) prefixes in Table 1 a-c.

the North Indian Ocean are a subset of the mechanisms originally described in Carr and Elsberry (1999) for cases in the western North Pacific, and then subsequently detected in the Atlantic by Brown (2000), and in the Southern Hemisphere by Reader et al. (2000).

1. Erroneous Midlatitude System Evolutions

According to Carr and Elsberry (1999), Midlatitude System Evolutions (MSEs) are changes to TC steering flow due to midlatitude circulation changes that occur independently of the TC, and include Midlatitude Cyclogenesis/Cyclolysis (MCG/MCL) and Midlatitude Anticyclogenesis/Anticyclolysis (MAG/MAL). Because a model may excessively or insufficiently misrepresent each of the four evolutions, there are a total of eight possible erroneous MSEs.

Erroneous MCG (Fig. 3.1) will cause a TC track predicition that is too far poleward as it advects around the subtropical anticyclone due to an overly deep midlatitude trough in the case of Excessive (E)–MCG, or a track prediction that is not poleward enough as a result of an under-developed midlatitude trough in the case of Insufficient (I)-MCG. Although it did not occur in this small sample (Table 2), in the

case of Excessive (E)-MCL, the midlatitude trough is forecast to dissipate too quickly, which causes the TC track to change from a poleward orientation to either a westward track equatorward of the subtropical anticyclone or an eastward track poleward of the subtropical anticyclone. Insufficient (I)-MCL occurs when the midlatitude trough is not forecast to dissipate quickly enough, which results in the TC track prediction north or south of the subtropical anticyclone axis to be too poleward. Excessive (E)-MAG will occur when the TC is moving toward a break in the subtropical anticyclone and the model over-predicts the development of the midlatitude anticyclone to the north. Consequently, the predicted track has a large error toward the west. Although it did not occur in this small sample (Table 2), insufficient (I)-MAG in a model will be due to an under-prediction of the anticyclone development to the north. Similarly, E-MAL will occur when the TC is moving toward the west (east) to the south (north) of the subtropical anticyclone axis and the model over-predicts the weakening of the subtropical anticyclone to the north (south). Consequently, the predicted track has a large error toward the pole. Although it did not occur in this sample (Table 2), the I-MAL error mechanism is associated with the model failing to predict the weakening of the subtropical anticyclone. Of the eight possible MSE's, only E-MCG, I-MCG, E-MAG, and E-MAL were observed in the NIO during 2000-2001.

Because Tropical Cyclone 01A of 2001 was involved in so many of the erroneous MSEs, this storm will be discussed extensively. Tropical Cyclone 01A formed in the eastern half of the monsoon trough off the west coast of India and reached a maximum intensity of 110 kt. Tropical Cyclone 01A experienced several pattern/region transitions throughout its life, which resulted in corresponding track changes (Fig. 4.4). The storm first had a transition during 22 May 2001 from the S/EW to the P/PF pattern/region due to RMT while near 15 deg. N with an intensity of 60 kt, which was already stronger than the peak intensity of most NIO TCs. The TC soon had a transition from the P/PF to S/TE pattern/region in response to a series of midlatitude-related transitional mechanisms. The steering control of TC 01A alternated between the subtropical anticyclone and a steady peripheral anticyclone throughout this period. A transition back

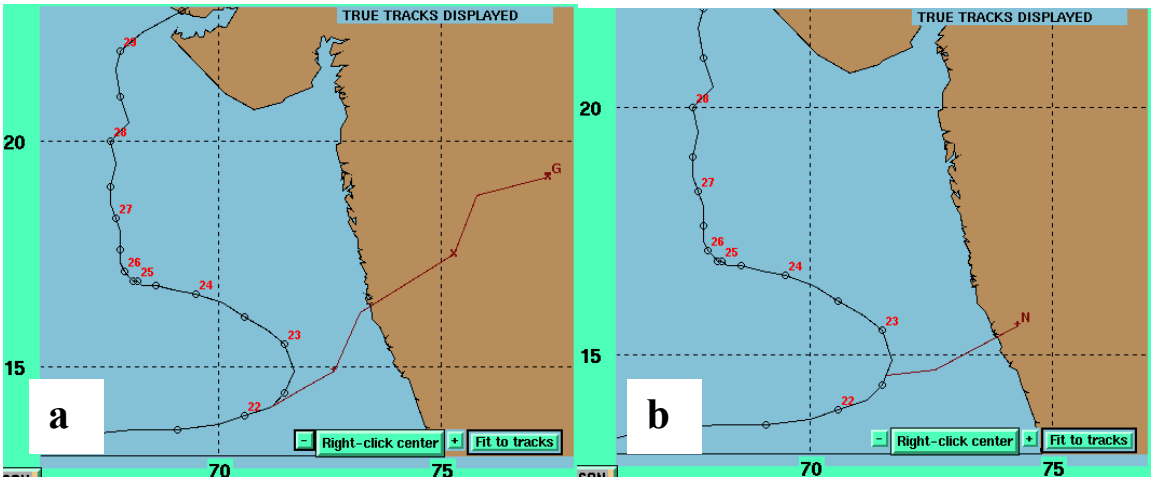

Figure 4.4. Track of TC 01A 2001 with the (a) GFDN (G) and (b) NOGAPS (N) forecast tracks initiated at 06 UTC for the GFDN and at 12 UTC for the NOGAPS on 22 May 2001, respectively. The forecast tracks are marked each 24 h, and the NOGAPS track ended after only 24 h.

to the P/PF pattern/region occurred on 26 May as the peripheral anticyclone regained steering control.

a. GFDN E-MCG Case Study

All three models experienced large FTEs during TC 01A, with the NOGAPS and GFDN models experiencing large FTEs during the initial stages of the storm. However, only the GFDN and UKMO models experienced large MSE-related errors.

The GFDN regional model forecast initiated at 06 UTC 22 May 2001 had a large 72-h FTE of 560 n mi due to E-MCG (Fig. 4.4). The E-MCG in this case is associated with a phenomenon called a spurious Himalayan Plateau-induced jet (Carr et al. 2000), which was first identified during the beta test of the Systematic Approach Forecasting Aid (SAFA) in the western North Pacific. Carr et al. explained that longer-range GFDN track forecasts of a TC approaching China seemed to be affected by an anomalous jet that originated along the Himalayan Mountains. In that case, the erroneous jet was accompanied by an anomalous cyclone to the north over western China that may have contributed to excessive ridging to the east (downstream) to the north of the TC in the GFDN model. It was subsequently determined by GFDN personnel that the

extremely abrupt Himalayan topography slopes in the nested model were the cause of this anomalous jet.

In the case of TC 01A in the NIO, the jet forms over the Himalayan Plateau in northern India, and it then weakens the subtropical anticyclone over the northern Arabian Sea in a manner that mimics Midlatitude Cyclogenesis. The lower panels of Fig. 4.5 present the 24-, 48-, and 72-h GFDN 500 mb wind forecasts initiated at 06 UTC 22 May 2001. The upper panels are the verifying GFDN analyses valid at the times of the corresponding forecast panels below. The verifying analyses (upper panels) will first be used to explain the actual storm track. Then we will compare the GFDN forecast fields with the verifying analyses to find differences, and hence the likely error mechanism that caused the large FTE.

In the 06 UTC 22 May analysis (Fig. 4.5a), TC 01A is moving toward the northeast in a transition from the S/EW to the P/PF pattern/region as the peripheral anticyclone over southern India begins to be the steering flow for the TC. By 06 UTC 23 May (Fig. 4.5b), the peripheral anticyclone that had steered the TC toward the north on the previous day had a weaker steering effect on TC 01A as the storm moves northward toward the northwestern subtropical anticyclone over the Gulf of Oman. The west-southwestward flow around the subtropical anticyclone, in combination with the weakening northward flow of the peripheral anticyclone, turns TC 01A toward the west, and puts TC 01A in a transition between the P/PF and S/TE pattern/regions. A wind maximum over the Himalayan Plateau extends zonally from 50 deg- 70 deg E before turning toward the southeast over northern India. Tropical Cyclone 01A completes the transition into the S/TE pattern/region by 06 UTC 24 May (Fig. 4.5c) as the subtropical anticyclone to the northwest first builds and then later weakens due to a series of shortwave midlatitude troughs to the north. The wind maximum over northern India is now only 20 kt and extends farther east. By 06 UTC 25 May (Fig. 4.5d), a midlatitude trough approaches the northwestern subtropical anticyclone from the northwest. Although the anticyclone grows northward ahead of the trough, it is weakened over

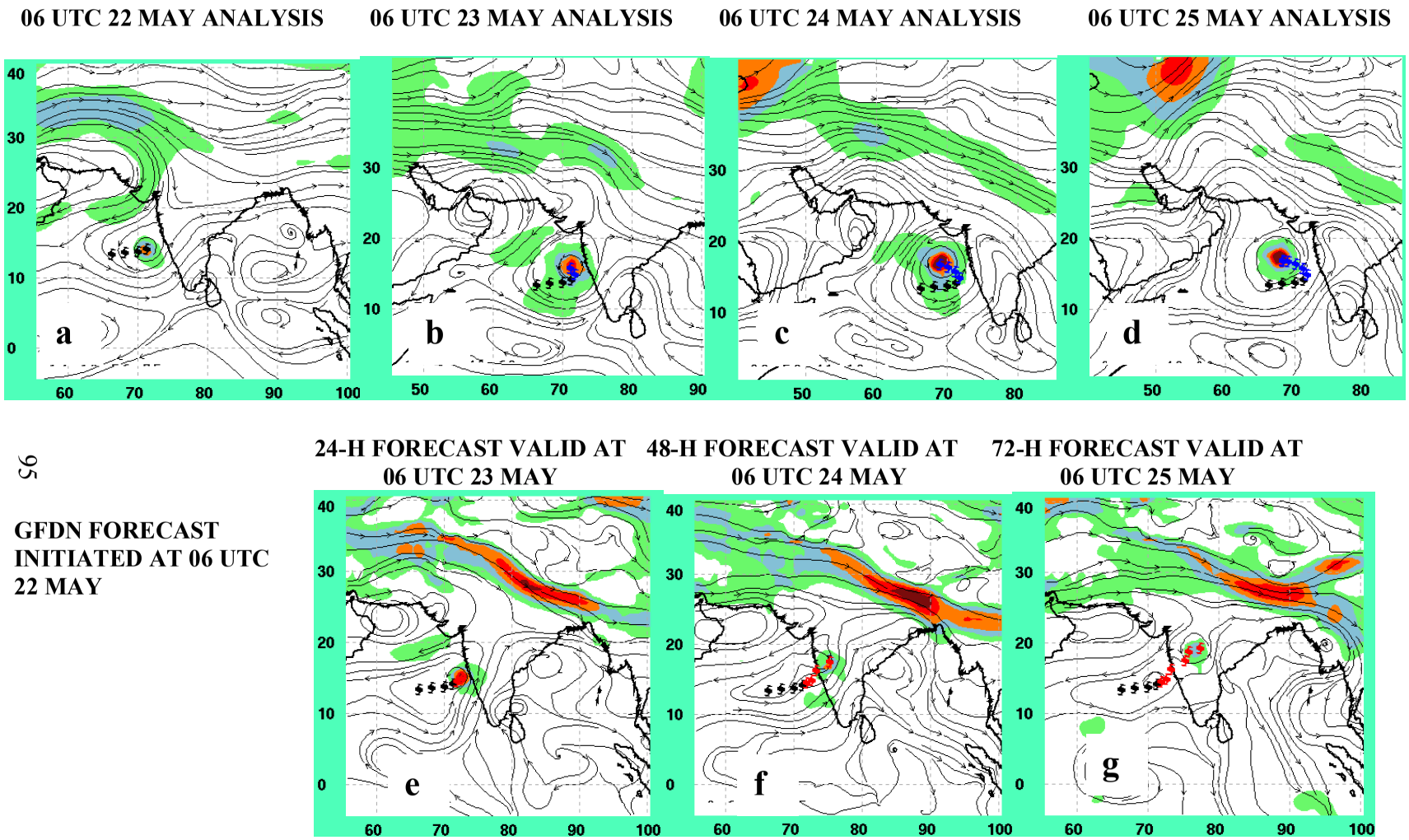

Figure 4.5. A comparison of the GFDN 500 mb verifying analyses and wind forecasts for TC 01A initiated at 06 UTC 22 May 2001. Panels (a)-(d) are the verifying GFDN 500 mb wind analyses, panels (e)-(g) are the 24-, 48-, and 72-h GFDN forecasts. Isotach shading starts at 20 kt in increments of 20 kt.

Oman, where it affects TC 01A. Because the northwestern subtropical anticyclone weakens, the peripheral anticyclone to the east of the TC begins to regain steering control, and TC 01A slows while undergoing a transition from the S/TE pattern/region back to the P/PF pattern/region. Only a finger of the Himalayan wind maximum remains over northern India.

The 24-h forecast field valid at 06 UTC 23 May (Fig. 4.5e) depicts a 100 kt jet along the southern edge of the Himalayas, and the subtropical anticyclone to the northwest of the TC is slightly weakened as compared to the analysis (Fig. 4.5b). A large col between the subtropical anticyclone cells, as well as a strengthened peripheral anticyclone, has developed in the forecast fields (Fig. 4.5e). A stronger isotach maximum is predicted to the east-southeast of the TC, which indicates steering flow for the TC is toward the col to the northeast. Already by 24 h, the GFDN model is degraded by E-MCG as the spurious Himalayan jet is weakening the subtropical anticyclone northeast of TC 01A. In the 48- and 72-h forecasts (Fig. 4.5f,g), the subtropical anticyclone to the northwest of the TC has remained significantly weaker than in the verifying analyses (Fig. 4.5 c,d). Although the Himalayan jet has weakened to 80 kt, it is still 60 kt stronger than the verifying wind maximum. The E-MCG error mechanism created an environment in which the northwestern subtropical anticyclone weakened and the peripheral anticyclone continued to maintain steering control over the TC track throughout the period. By contrast, TC 01A was being steered by the subtropical anticyclone to the northwest. Whereas the TC was predicted by the GFDN model to make landfall on western India, the weakening of the peripheral anticyclone and strengthening of the subtropical anticyclone led to the turn of TC 01A to the northwest during the 72-h forecast period.

This same error occurred in the next GFDN model integration at 18 UTC 22 May (not shown). The forecast fields were compared to the corresponding NOGAPS model integration of 12 UTC 22 May. Although no large 72-h FTE was recorded in the NOGAPS model due to an erroneous dissipation of the TC, the short track (Fig. 4.4b) exhibited similar trends to the GFDN track (Fig. 4.4a) in that the NOGAPS predicted a track to the northeast rather than recurving it to the west. The NOGAPS forecast fields

(not shown) exhibited evidence of E-RMT as opposed to E-MCG in the GFDN fields, as the strength and position of the subtropical anticyclone were similar to those in the analyses, but the peripheral anticyclone was stronger as supported by the isotach position to the southeast of the TC. No spurious Himalayan Plateau-induced jet was detected in NOGAPS as occurred in the GFDN model (Fig. 4.5). One day later, the NOGAPS model was still being degraded by E-RMT, and this erroneous prediction will be covered in Chapter IV.D.3.

b. GFDN E-MAL Case Study

The GFDN model (Fig. 4.6a) forecasts TC 01A to immediately track toward the north, rather than continuing on a west-northwestward track. The 500 mb analysis field shows TC 01A to be in the middle of a transition from the P/PF (steering controlled by the peripheral anticyclone to the southeast) to S/TE (steering controlled by the subtropical anticyclone to the northwest) pattern/region.

At 06 UTC 23 May 2001 (Fig. 4.6a), Tropical Cyclone 01A had already turned toward the northwest under the influence of a combined steering flow around the peripheral anticyclone to the southeast and the subtropical anticyclone to the northwest, which is supported by a small isotach maximum to the northwest (Fig. 4.6b). At 18 UTC 23 May (Fig. 4.7a), TC 01A has continued its northwestward track under the same steering influence. By 06 UTC 24 May (Fig. 4.7b), the subtropical anticyclone to the northwest had started to weaken slightly with the center shifting to the west, while the peripheral anticyclone remained unchanged, and TC 01A continued tracking toward the northwest. After 48 h (Fig. 4.7c), the subtropical anticyclone to the northwest of TC 01A had continued to retrogress. However, a midlatitude trough had approached 50 deg E, which resulted in an amplification and reorientation of the subtropical anticyclone meridionally along 60 deg E (Fig. 4.7c). Meanwhile, the peripheral anticyclone had amplified east of TC 01A such that it was gaining steering control over the TC track. Tropical Cyclone 01A had first slowed, and by 06 UTC 26 May (Fig. 4.7d) it had turned toward the north (Fig. 4.6a) under the steering influence of a well-defined poleward pattern. The subtropical anticyclone had been displaced eastward by the midlatitude

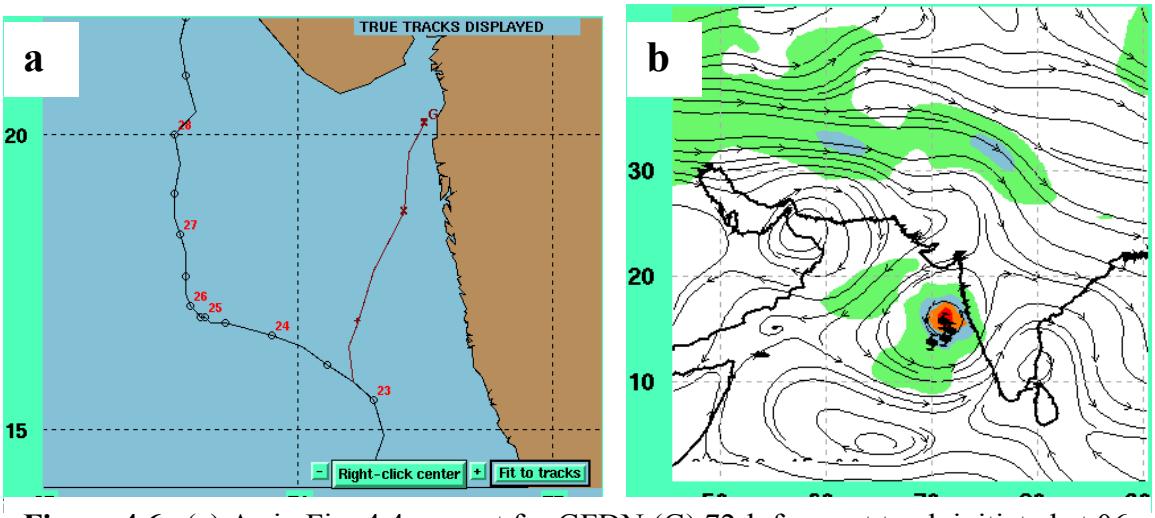

Figure 4.6. (a) As in Fig. 4.4, except for GFDN (G) 72-h forecast track initiated at 06 UTC 23 May 2001; (b) 500 mb wind analysis valid at 06 UTC 23 May 2001.

trough and was now due north of TC 01A at 28 deg N, 67 deg E. However, its steering influence on TC 01A was insignificant compared to the peripheral anticyclone.

The origin of the large GFDN FTE becomes evident in the first two forecast periods. The 12-h forecast (Fig. 4.7e) has the subtropical anticyclone to the northwest of TC 01A extending farther east than in the analysis, but it is slightly weaker. Notice that no peripheral anticyclone is predicted to the southeast of TC 01A. By the 24-h forecast (Fig. 4.7f), the subtropical anticyclone to the northwest of TC 01A has weakened significantly. A peripheral anticyclone has now formed to the east of TC 01A, which created a stronger northeastward steering flow as supported by the position of the isotach maximum to the southeast. Thus, TC 01A is forecast to move toward the northeast. A comparison of this 24-h forecast field with the verifying analysis (Fig. 4.7b) indicates little difference in the depiction of the peripheral anticyclone, but a significant difference in the strength of the subtropical anticyclone to the northwest of TC 01A. The too rapid decay of the northwestern subtropical anticyclone in the GFDN model that results in the incorrect turn to the northeast is attributed to Excessive Midlatitude Anticyclolysis (E-MAL). A weak spurious Himalayan Plateau-induced jet had also formed far to the northeast, which might have again contributed to an error mechanism of

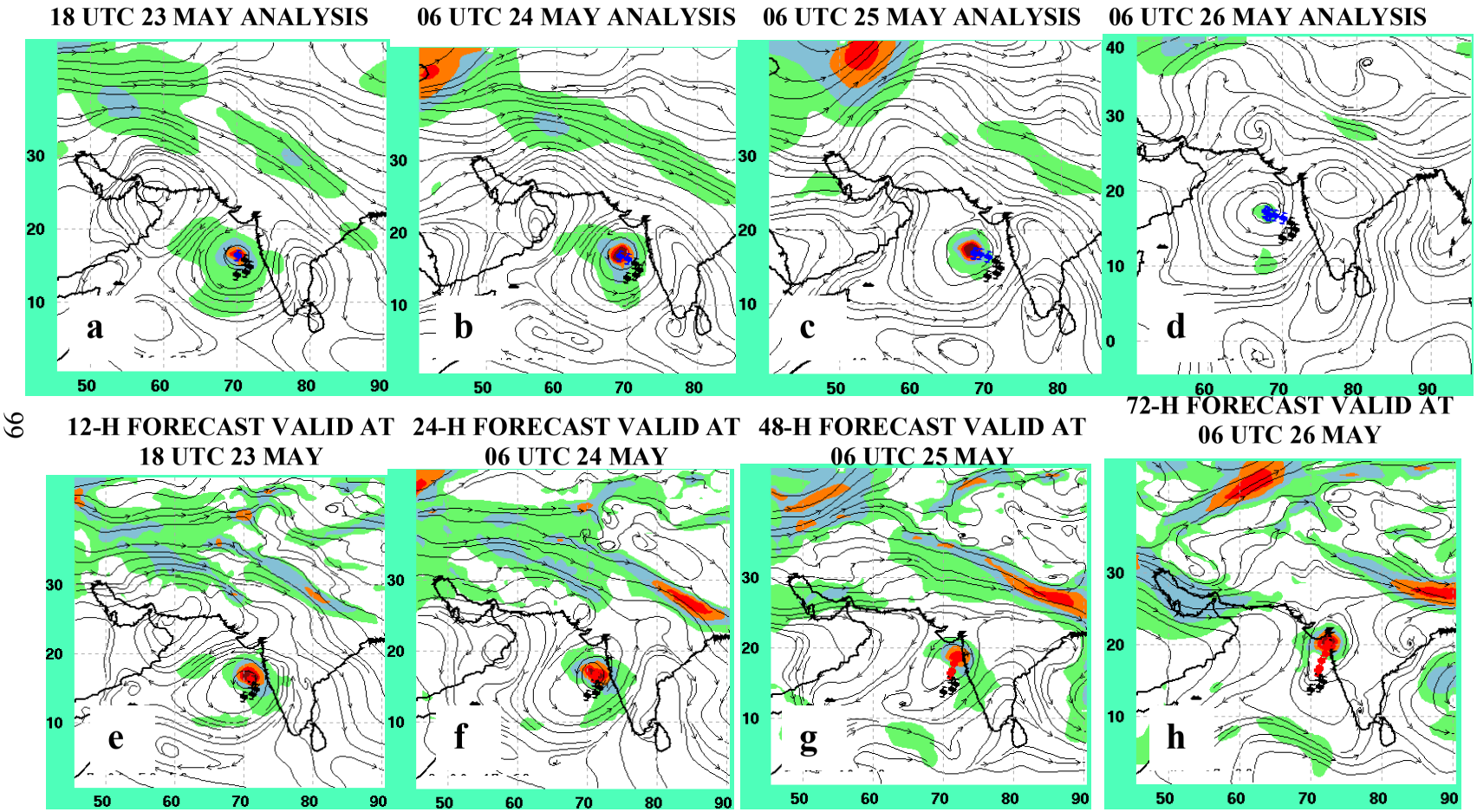

Figure 4.7. A comparison of the GFDN 500 mb verifying analyses and wind forecasts for TC 01A initiated at 06 UTC 23 May 2001. Panels (a)-(d) are the verifying GFDN 500 mb wind analyses, panels (e)-(h) are the 12-, 24-, 48-, and 72-h GFDN forecasts. Isotach shading begins at 20 kt with increments of 20 kt.

E-MCG. In the 48- and 72-h forecasts (Fig. 4.7g,h), the peripheral anticyclone weakens more than in reality (Fig. 4.7c,d), and TC 01A is forecast to have a slightly slower northward motion. However, the initial model error of E-MAL during the 12- and 24-h forecasts is what initially caused the GFDN model to track to the northeast, and resulted in an FTE of 322 n mi. This is not a case of Excessive Ridge Modification by a TC (E-RMT) because GFDN actually depicts the peripheral anticyclone quite accurately.

c. UKMO E-MAG Case Study

The UKMO global model accurately predicted the role of the subtropical anticyclone during the turn of TC 01A away from India (not shown), while the NOGAPS and GFDN models did not (Fig. 4.4). However, the UKMO model did have large errors later in the life of TC 01A. For example, the UKMO global model had a large 72-h FTE of 288 n mi during the 12 UTC 25 May model integration (Fig. 4.8).

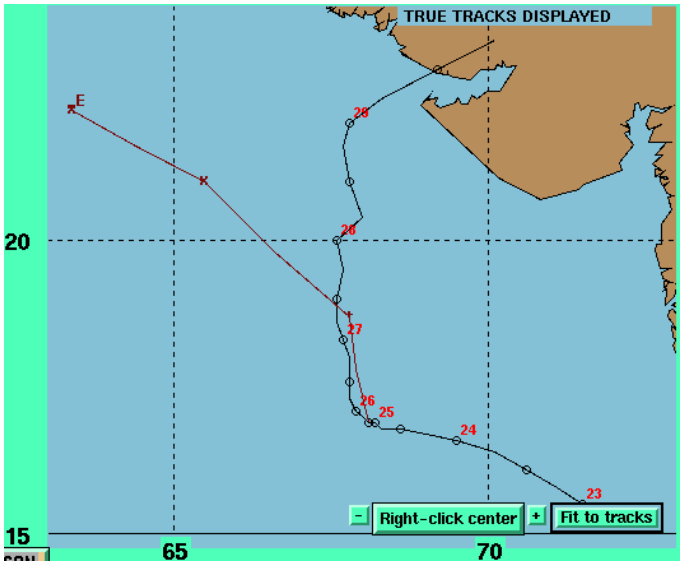

Figure 4.8. Verifying track of TC 01A 2001 with UKMO (E) 72-h forecast track initiated at 12 UTC 25 May 2001.

At 12 UTC 25 May (Fig. 4.9a), TC 01A is slowly moving toward the northwest while in a transition from a S/TE to a P/PF pattern/region. A midlatitude trough to the northwest of TC 01A is displacing the weak subtropical anticyclone centered at 65 deg E toward the east at 12 UTC 26 May (Fig. 4.9b), while the peripheral anticyclone to the southeast of TC 01A has amplified. By 12 UTC 27 May (Fig. 4.9c), TC 01A is moving toward the north in the P/PF pattern/region under the influence of the

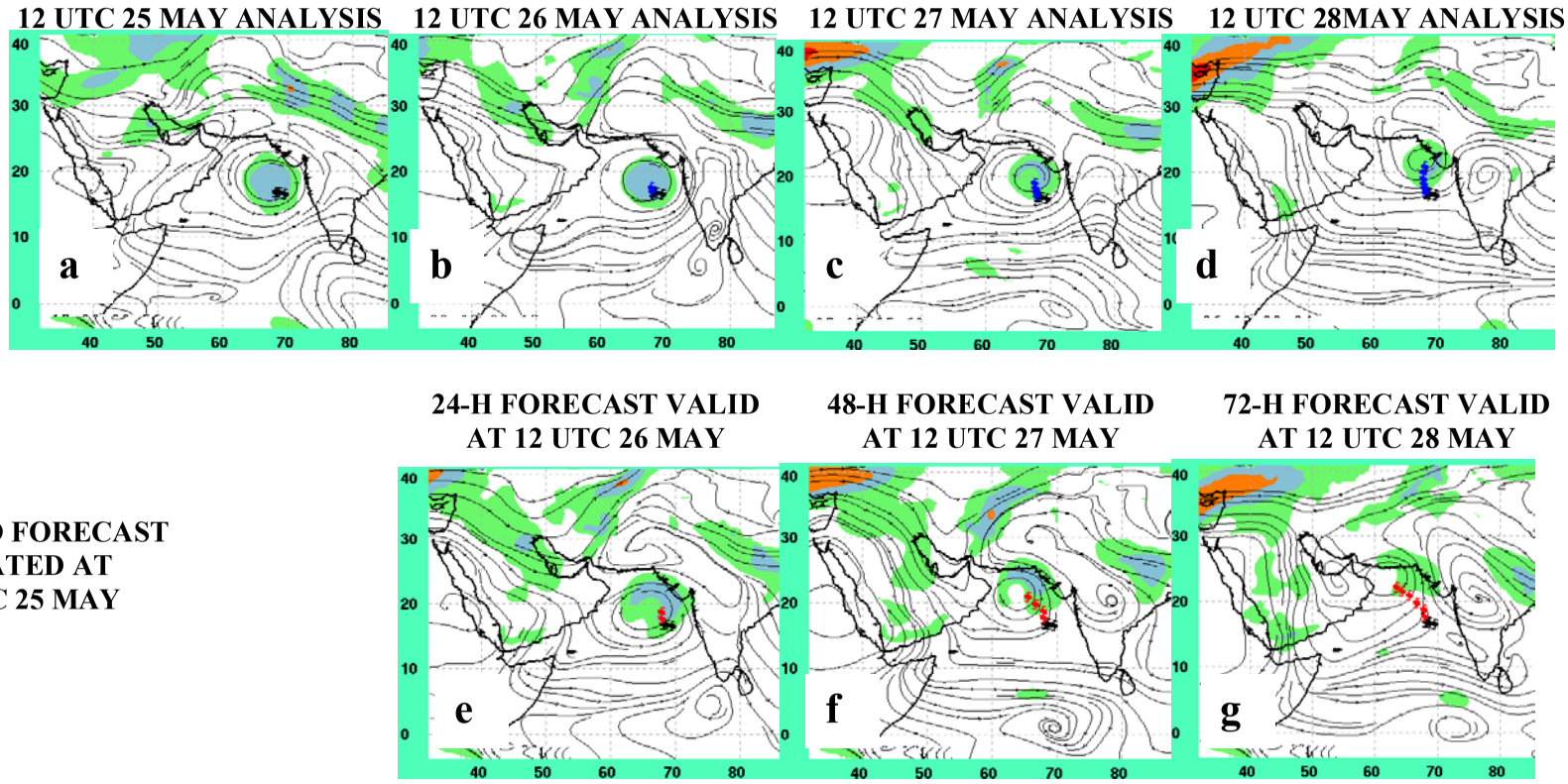

Figure 4.9. As in Fig. 4.5, except for the UKMO forecast from 12 UTC 25 May 2001.

peripheral anticyclone to the east. The subtropical anticyclone to the north of TC 01A continues to weaken through 12 UTC 28 May (Fig. 4.9d), at which time a low has formed over Oman (23 deg N, 55 deg E), while the midlatitude trough to the northwest of TC 01A has started to move out. Although the weak subtropical anticyclone is still to the north, it is the peripheral anticyclone that has steering control and the track is to the northeast (Fig.4.8).

The 24-h UKMO forecast valid at 12 UTC 26 May (Fig. 4.9e) has the midlatitude trough approaching from the northwest to be stronger than in the analysis, as supported by the more extensive isotach maximum on the western side of the trough. Presumably via Rossby wave energy dispersion to the east, the deepening trough has contributed a relatively strong subtropical anticyclone to the north of TC 01A, and the anticyclone extends around to the northeast of the TC circulation. The 48-h forecast (Fig. 4.9f) has predicted that the midlatitude trough and subtropical anticyclone would continue to be noticeably deeper than in the analysis (Fig. 4.9c). The large area of over 20 kt winds to the northeast of TC 01A, with a smaller isotach maximum to the west of the TC, is evidence that the stronger subtropical anticyclone north of TC 01A is steering it toward the northwest. The large UKMO track error is then attributed to an Excessive Midlatitude Anticyclogenesis (E-MAG) error mechanism. In the 72-h forecast (Fig. 4.9g), the deep midlatitude troughing has left a cutoff cyclonic circulation over the United Arab Emirates, while the subtropical anticyclone has weakened and is now centered over northern India, which is well east of the TC. With the 20 kt wind maximum now east of TC 01A, the UKMO model has belatedly predicted an imminent turn to the north (Fig. 4.8). However, the excessive growth of the subtropical anticyclone north of TC 01A via E-MAG already at 24 h has made this northward turn far too late.

2. Erroneous Equatorial Wind Burst

The TC-Environment Transformation called the Equatorial Westerly Wind Burst (EWB) has previously been described only in the Southern Hemisphere (Fig. 4.10) by Bannister et al. (1998). In this model, a TC initially is on the poleward side of an east-west oriented monsoon trough and thus is in the westward environmental steering flow of the S/TE pattern/region. The poleward shift or an intensification of the anomalously

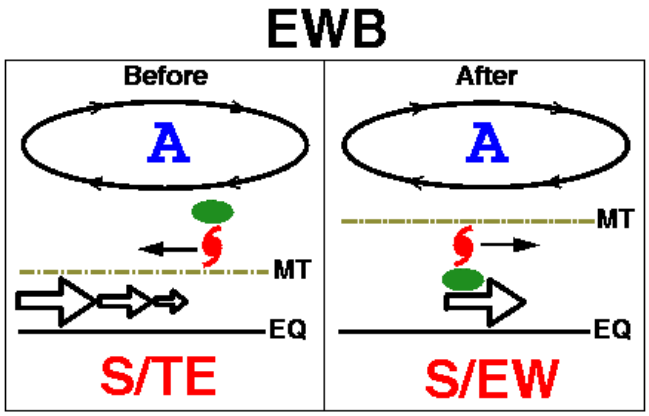

Figure 4.10. Conceptual model of an Equatorial Wind Burst from Bannister et al. (1998).

strong equatorial westerly winds on the equatorward side of the TC is occasionally sufficient to make it the dominant steering mechanism for a TC rather than the tropical easterlies, and in that case the steering for the TC would be toward the east.

Although an actual EWB event with a TC track change was never observed during 1991-2001, one case of E-EWB in NOGAPS was observed during the 2001 season. Tropical Cyclone 02A of 2001 only reached 35 kt and never made landfall (Fig. 4.11). In the 700 mb analysis valid at 12 UTC 24 September (Fig. 4.12a), TC 02A was under the steering influence of the zonally-oriented subtropical anticyclone axis centered at 22 deg N. By 12 UTC 25 September, TC 02A had a transition from the S/TE to the S/PF pattern/region as a result of MCG at the 500 mb level (not shown). The monsoon depression centered over the BOB has increased in intensity, with a corresponding increase in equatorial westerlies to the south of TC 02A (Fig. 4.12a). Tropical Cyclone 02A then continued on a track toward the northwest (Fig. 4.11) through 12 UTC 26 September under the steering influence of the subtropical anticyclone to the north (Fig. 4.12c). The subtropical anticyclone at 500 mb has strengthened due to MCL by 12 UTC 27 September (not shown), and TC 02A has a transition back to the S/TE pattern/region

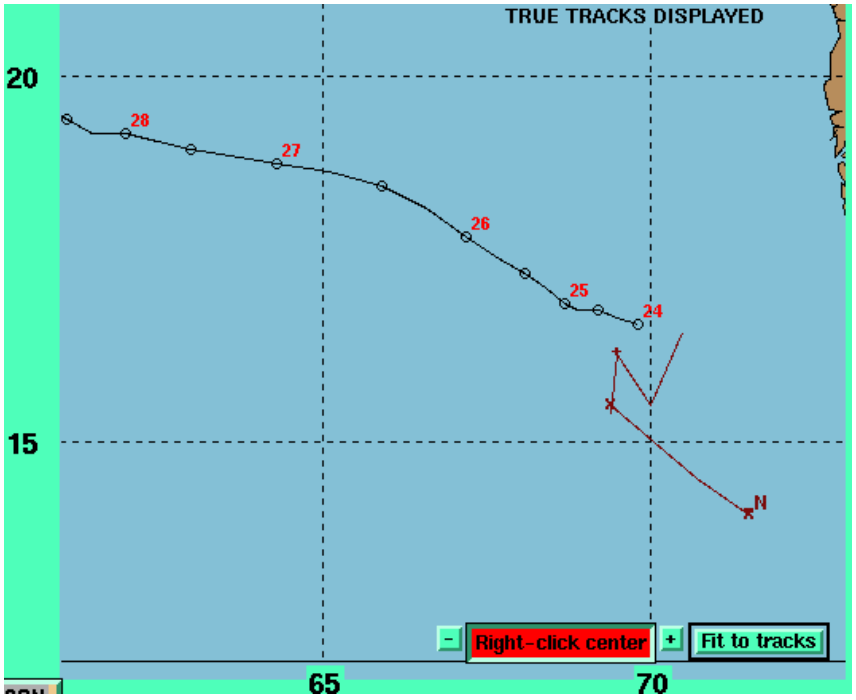

Figure 4.11. As in Fig. 4.4, except for TC 02A 2001 with NOGAPS (N) 72-h forecast track initiated at 12 UTC 24 September 2001.

The NOGAPS model forecast moves TC 02A to the south-southwest in the first 12 hours. By 24–h (Fig. 4.12e), NOGAPS is forecasting the TC to be moving northwestward much as TC 02A actually moved (Fig. 4.11). The 24-h NOGAPS 700 mb streamline forecast valid at 12 UTC 25 September 2001 (Fig. 4.12d) is quite similar to the verifying analysis (Fig. 4.12b) except for the lack of 20 kt northeasterly winds over Oman and Yemen on the southeast side of the northwestern subtropical anticyclone. In the 48-h forecast (Fig. 4.12f) and 72-h forecast (Fig. 4.12g), the excessive equatorial westerly flow south of TC 02A results in a predicted track toward the southeast. The forecast TC track is then in the opposite direction as the actual track. Because a significantly less intense equatorial westerly flow is present in the 48-h and 72-h analyses (Fig. 4.12c,d) than in the NOGAPS prediction, the error mechanism is assigned to be an Excessive Equatorial Wind Burst (E-EWB).

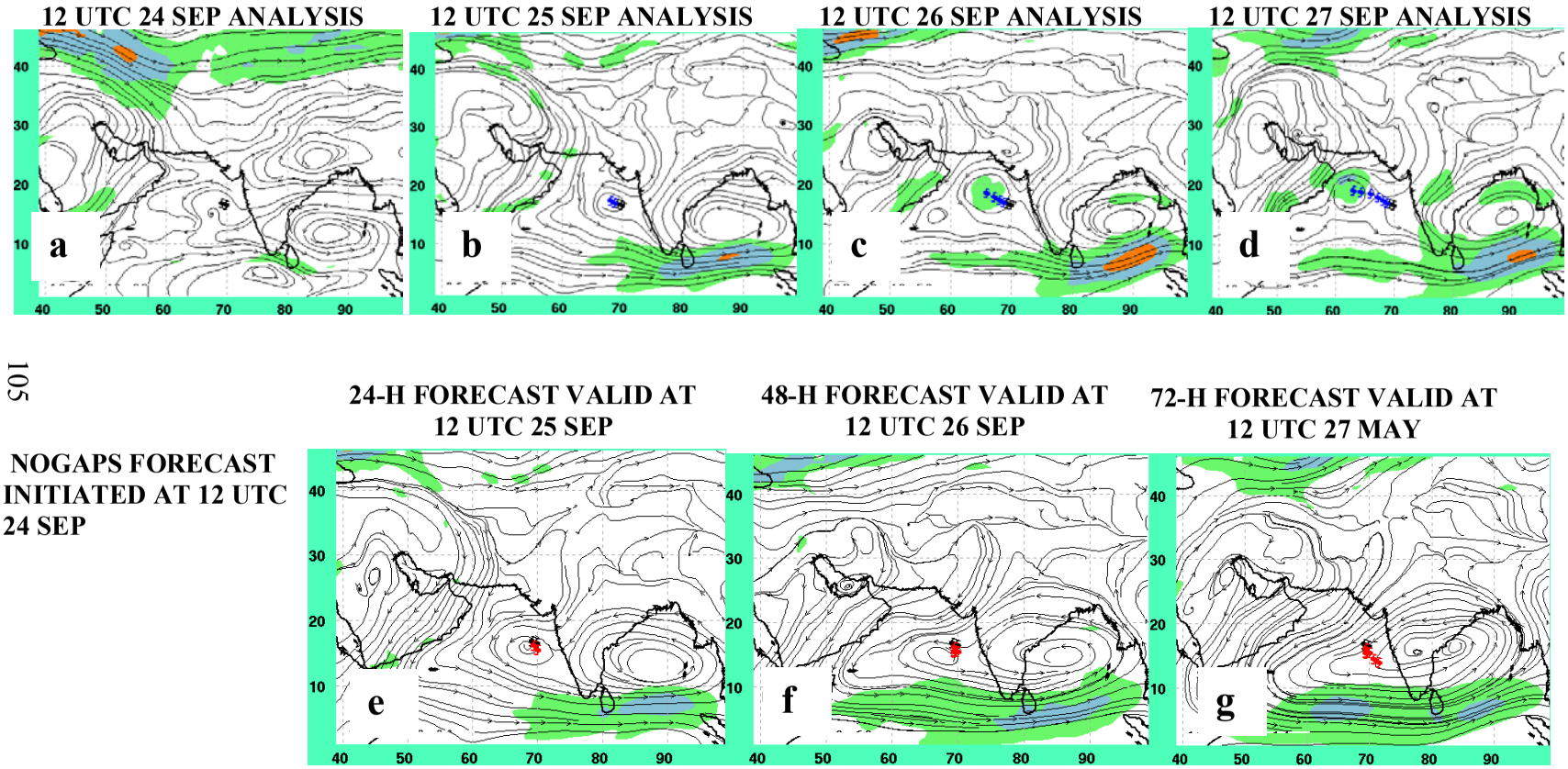

Figure 4.12. As in Fig. 4.5, except for NOGAPS 700 mb wind forecast initiated at 12 UTC 24 September 2001.

3. Erroneous Ridge Modification by a TC

The only beta effect-related TC-Environment Transformation error that occurred during the 2000-2001 NIO seasons was Excessive Ridge Modification by a TC (E-RMT). If a TC generates a peripheral anticyclone that is too large such that the transition from the S/TE to the P/PF pattern/region occurs too quickly (Fig. 4.13), a TC track error due to E-RMT results. Oftentimes, the TC and its peripheral anticyclone are downstream from another anticyclone and possibly a second cyclone in a Rossby wave train. Dynamical models have a tendency to excessively transport energy downstream in such an arrangement. After first weakening the western anticyclone too much, the model then strengthens the eastern anticyclone too much, which then erroneously steers the TC poleward. Although it did not occur in this sample, Insufficient-RMT would be assigned if the transition does not occur quickly enough.

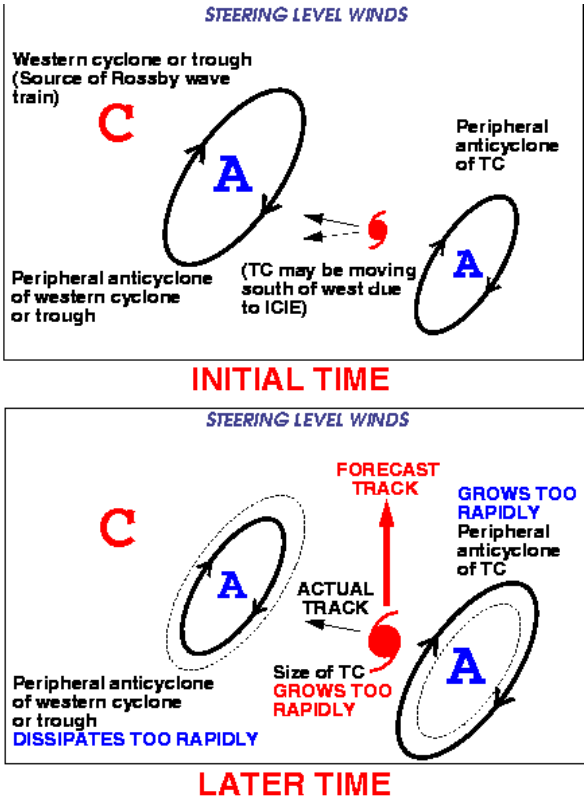

Figure 4.13. Conceptual model of Excessive Ridge Modification by a TC in which Rossby wave dispersion from a western cyclone-anticyclone couplet results in excessive amplification of the peripheral anticyclone to the east of the TC, which then turns poleward.

Tropical Cyclone 01A was moving toward the northwest (Fig. 4.14a) under the primary steering influence of the subtropical anticyclone to the northwest, although a peripheral anticyclone was present to the southeast in the analysis valid at 12 UTC 23 May 2001(Fig. 4.14b). At 00 UTC 24 May 2001 (Fig. 4.15a), TC 01A was under the steering influence of the western subtropical anticyclone cell that was centered over Oman, but extended eastward to the Indian coast. A peripheral anticyclone to the southeast of TC 01A evidently had little, if any, steering influence on TC 01A. The presence of a 20 kt isotach to the north and northwest of TC 01A, with no isotach maximum to the southeast, is evidence that the northwestern subtropical anticyclone (not the peripheral anticyclone) was the dominant steering flow. While the northwestern subtropical anticyclone has started to weaken by 12 UTC 24 May (Fig. 4.15b), the peripheral anticyclone has strengthened. The isotach maximum has now shifted slightly northeast, and an isotach maximum has started to form to the southeast, which is indicative of supporting stronger northeastward flow. Tropical Cyclone 01A slowed to 1 kt (Fig. 4.14), and was in a transition between the S/TE and P/PF pattern/regions by 12 UTC 25 May (Fig. 4.15c) as the peripheral anticyclone continued to grow and extend northward to the east of TC 01A. A small isotach maximum to the southeast of the storm is again indicative of the slow transition toward a northward track. The subtropical anticyclone to the northwest has continued to weaken, and has now built meridionally

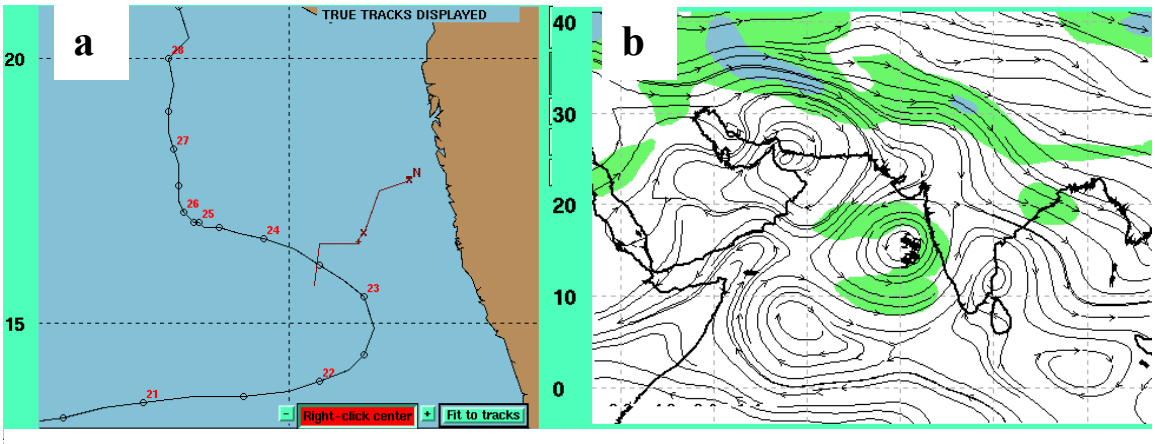

Figure 4.14. As in Fig. 4.4, except for TC 01A 2001 with NOGAPS (N) 72-h forecast track initiated at 12 UTC 23 May 2001; (b) 500 mb wind analysis valid at 12 UTC 23 May 2001.

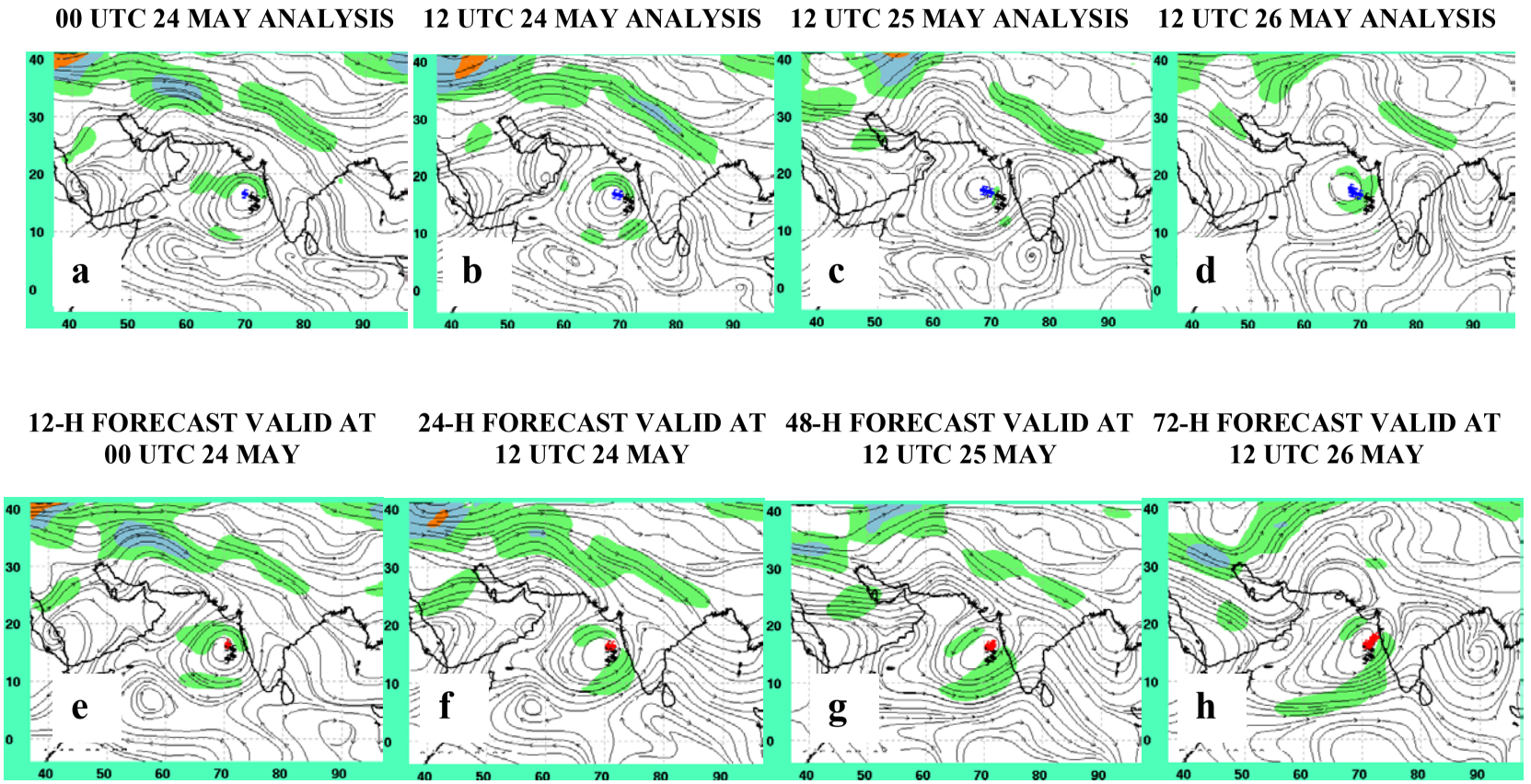

Figure 4.15. As in Fig. 4.5, except for the NOGAPS forecast initiated at 12 UTC 23 May 2001.

along 60 deg E in response to a midlatitude trough approaching from the northwest. By 12 UTC 26 May (Fig. 4.15d), a significant Poleward pattern has been established with a peripheral anticyclone that extends from a buffer cell south of TC 01A and connects the peripheral anticyclone east of the storm to the subtropical anticyclone. A strong isotach maximum southeast of TC 01A is consistent with the northward track (Fig. 4.14). The subtropical anticyclone has weakened and been displaced to the east by the approaching midlatitude trough and is now well north of TC 01A.

The NOGAPS 12 UTC 23 May 72-h FTE was 263 n mi (Fig. 4.14) while TC 01A was at an intensity of 100 kt. The TC structure and peripheral anticyclone in the 12-h 500 mb forecast field (Fig. 4.15e) are very similar to the verifying analysis (Fig. 4.15a). However, notice that two isotach maxima to the north and south of the TC in the 12-h forecast fields would imply opposing steering flows, which would be consistent with a slow forecast track. By contrast, the clearly stronger isotach maximum to the north of the TC in the analysis (Fig. 4.15a) would imply the dominant steering flow is toward the west. In the 24-h forecast (Fig. 4.15f), the NOGAPS model predicts a slightly weaker subtropical anticyclone to the northwest of TC 01A. The stronger predicted isotach maximum to the southeast of the TC associated with the peripheral anticyclone is consistent with the erroneous TC track toward the northeast (Fig. 4.14). Although the predicted peripheral anticyclone appears to be comparable in size to the analysis, the isotach to the southeast is significantly stronger in the forecast than in the analysis. This is consistent with the E-RMT conceptual model in Fig. 4.13 in that the NOGAPS model has predicted a weaker subtropical anticyclone to the northwest and a stronger peripheral anticyclone to the southeast.

In the 48-h forecast (Fig. 4.15g), the peripheral anticyclone maintains steering control over TC 01A as indicated by the isotach maximum to the southeast. By the 72-h forecast (Fig. 4.15h), NOGAPS has slightly underpredicted the weakening of the subtropical anticyclone by the approaching midlatitude trough. However, it is the excessively strong peripheral anticyclone that remains the primary steering mechanism and continues to drive the TC toward the northeast, which is consistent with the large area of southwesterly winds in excess of 20 kt to the south and southeast of TC 01A. The

cause of the large FTE thus originated early in the NOGAPS forecast in that the strengthening of the peripheral anticyclone was forecast to be too strong and too soon. The actual RMT transitional mechanism did not occur until about 48 h after the initial time. Consequently, the assigned track error mechanism is Excessive Ridge Modification by a TC (E-RMT).

Slight differences in the strength of the subtropical and peripheral anticyclones between the forecast and analysis fields, and the sensitivity of the dominant steering flow to the position of TC 01A, create a difficult forecast situation. The consistency of the isotach maximum position with the predicted track indicates the dominant circulation and reveals the cause of the error in the retrospective studies. In a real-time forecast situation, the forecaster would know that a significant track change is being predicted by NOGAPS and may be able to determine the error based on the knowledge that E-RMT is a common error mechanism in this model.

4. Initial Position Error

During the first few forecasts of a developing TC, initial position errors are more likely to occur due to inaccurate fixes of the center within a highly disorganized circulation. A poor position of the synthetic TC observations supplied to the model can result in the initial placement of the TC circulation center well away from the actual position. Thus, the model may incur a large FTE from the start of the forecast. This initial position error occurred once in each of the UKMO and NOGAPS models.

a. UKMO IPE case study

Tropical Cyclone 04B was in the S/TE pattern/region at 00 UTC 25 December 2000 with an intensity of 40 kt. The 72-h FTE for the UKMO global model was 284 n mi, as the forecast track was south of the best track (Fig. 4.16). The initial track orientation toward the south is a major contributor to the large FTE. Were it not for the initial jump to the south, the 72-h forecast error would presumably be small. At 12 UTC 25 December (not shown), the primary steering influence is due to the zonal subtropical anticyclone centered along 15 deg N. Since the position and strength of the subtropical anticyclone are very similar in the 12-h forecast and analysis fields, one would expect a 12-h forecast track toward the west as actually occurred (Fig. 4.16).

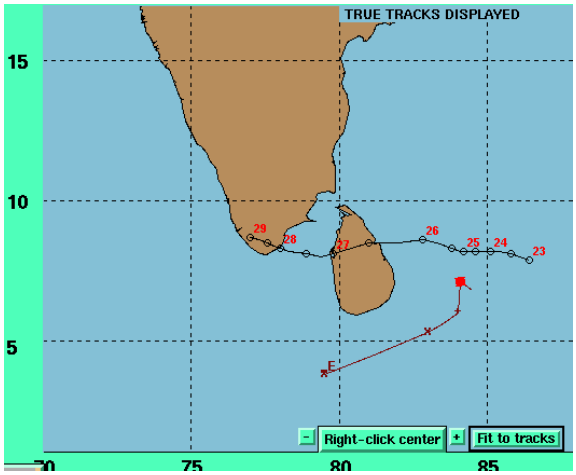

Figure 4.16 As in Fig. 4.4, except for TC 04 B during 2000 with a non-translated UKMO (E) 72-h forecast track initiated at 00 UTC 25 May 2000 showing initial position error.

However, the TC is forecast to immediately move south because the UKMO model initial position is in error. In addition to starting the model forecast from the wrong location, an incorrect initial position in the UKMO model will also affect the past-motion vector calculation that is a part of the synthetic TC observation routine. With the erroneous initial position to the south as in Fig. 4.16, the past 12-h motion vector will be southward. Since the average of the synthetic TC observations is required to agree with this erroneous past-motion vector, the correction added to the synthetic TC observations forces an erroneous southward initial motion. Since the synthetic TC observations are added as rawinsondes over a relatively large domain, this southward error will continue for a large portion of the forecast track (as in Fig. 4.16).

b. NOGAPS IPE case study

At the beginning of the 00 UTC 9 November 2001 forecast, TC 04B had an intensity of only 25 kt. However, the NOGAPS forecast track began with an initial position error of approximately 2 deg. longitude to the west (Fig. 4.17). Consequently, a 72-h FTE of 379 n mi that occurred in NOGAPS was substantially a result of misplacement of the forecast initial position (Fig. 4.17). Had it not been for this initial displacement toward the west, the initial NOGAPS track during the early forecast period would better represent the verifying best track. However, the additional westward

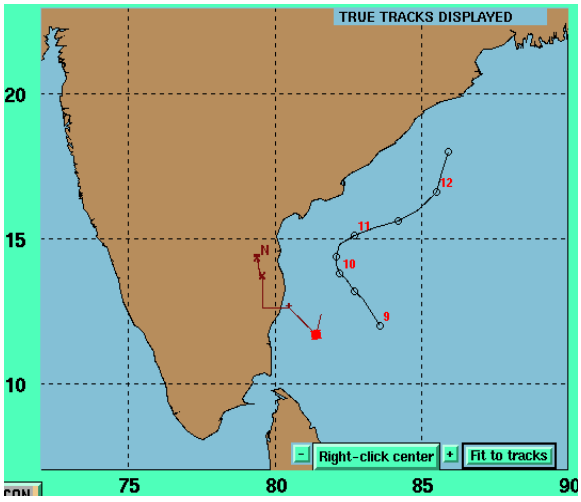

Figure 4.17. As in Fig. 4.4, except for TC 04 B 2001 with non-translated NOGAPS (N) 72-h forecast track initiated at 00 UTC 9 November 2001 showing the initial position error.

component in the synthetic TC observations also brought the track over land, which contributed to errors later in the forecast.

E. CONCLUSIONS

This study examined 12 cases of large FTEs that occurred during the 2000-2001 NIO seasons to establish a preliminary Dynamical Model Forecast Traits Knowledge Base for the NIO. Although this NIO study must be regarded as tentative, it completes a global Dynamical Model Forecast Traits Knowledge Base for the Systematic Approach initiated by Carr and Elsberry (1999).

Of the 12 large FTEs that occurred in the NIO during this period, 7 (58%) were midlatitude related errors, 2 (17%) were beta effect-related errors, 1 (8%) was a tropical-related error and 2 (17%) were related to initial position errors. In contrast to previous model error studies for the western North Pacific, Southern Hemisphere, and Atlantic basins, no large FTEs due to E-DCI were identified. Due to the small sample size though, errors due to model cyclonic interaction cannot be ruled out. An alternate explanation is that adjacent circulations are not as common in the NIO as in the other basins. At least for NOGAPS, the implementation of the Emanuel cumulus parameterization technique prior to the beginning of the sample period may have reduced the occurrences of excessive growth of the cyclonic circulations that lead to E-DCI.

It is important to note that no new model errors were identified in the NIO, which thus supports a global application of the Dynamical Model Forecast Traits Knowledge Base.

THIS PAGE INTENTIONALLY LEFT BLANK

V. CONCLUSIONS

A. SUMMARY

The purpose of this study was to create the TC Motion Meteorology and Dynamical Model Forecast Traits Knowledge Bases for the North Indian Ocean, and thus complete the global database for the Systematic and Integrated Approach to Tropical Cyclone Track Forecasting initiated by Carr and Elsberry (1994). The Joint Typhoon Warning Center (JTWC), Pearl Harbor, HI has a goal of 50, 100, and 150 n mi FTEs for the 24-, 48-, and 72-h forecast periods to ensure Naval Commands are provided with the most accurate track predictions. These improved warnings will allow vessels at sea to be routed for optimum safety, and assets ashore will be sortied only when necessary. The TC Motion Meteorology and Dynamical Model Forecast Traits Knowledge Bases of the Systematic Approach provide for this requirement by assisting the forecaster in generating a track forecast with improved accuracy.

The database for the North Indian Ocean TC Motion Meteorology Knowledge Base covers eleven years (1991-2001) and 656 cases. The synoptic pattern/region was determined through examination of NOGAPS analysis fields at four primary levels: 200, 500, 700, and 850 mb. Although the Environment Structure has some significant differences from other global regions so far examined, the three common synoptic patterns found in the western North Pacific, eastern/central North Pacific, Atlantic, and Southern Hemisphere basins are also found in the NIO. However, two of the pattern/regions were not observed during 1991-2001. The Poleward/Equatorward Flow pattern/region was not observed in part due to the infrequency of two tropical cyclones existing simultaneously in the NIO. The Midlatitude/Midlatitude Easterlies pattern/region was not observed because the topography associated with the Himalayan Mountains precludes the advancement of tropical cyclones to high latitudes. In contrast to the four previously studied basins, no unique NIO synoptic patterns were observed. The most common pattern/region was the Standard/Tropical Easterlies as the dominant environmental steering mechanism in the NIO was the subtropical anticyclone centered near 20 deg. N at 500 mb.

Not all Transitional Mechanisms (Fig. 2.5) identified in the four tropical cyclone basins previously studied were found to exist in the NIO. Additionally, no unique transitional mechanisms were identified. A total of 86 recurring transitions (meaning the transition occurred more than once) were identified during 1991-2001. The most common transition in the NIO (29%) was from the S/TE to the S/PF pattern/region, which may occur by the ADV, BEP, MCG, or MAL mechanisms. Transitions from the S/PF pattern/region into the P/PF pattern/region occurred 9 of 26 (35%) cases, while only 6 of 26 (23%) of the S/PF transitions were directly into the midlatitudes (M/PF pattern/region). Similar to other tropical cyclone basins, a total of 11 of 26 (42%) of the transitions from the S/PF pattern/region are back into the tropics: 6 of 26 (23%) of the S/PF transitions are to the S/EF pattern/region, and 5 of 26 (19%) of the transitions are to the S/TE pattern/region. The P/PF to M/PF pattern/region transition is the second-most common due to the frequent occurrence of the RMT transitional mechanism, which occurred 32 times in the 64 TCs examined between 1991-2001. The smaller number of TCs in the NIO compared to previous studies in other tropical cyclone basins obviously limits the number of Environment Structure transitions. Thus, fewer options exist for transitions among pattern/regions. This information assists the forecaster in narrowing down the possible track changes a TC will make during its lifetime.

The Dynamical Model Forecast Traits Knowledge Base study examined the forecasts of eight tropical cyclones over a two-year period (2000-2001) made by the Navy Operational Global Atmospheric Prediction System (NOGAPS), the Geophysical Fluid Dynamics Lab (Navy version – GFDN), and the UK Meteorological Office (UKMO) global model. Because of the infrequency of larger model errors, and lower average model errors of tropical cyclones in the NIO, a large Forecast Track Error (FTE) was defined as 225 n mi, as opposed to 300 n mi established in the western North Pacific. Only six of eight TCs that formed in the NIO during the 2000-2001 seasons provided the 12 large error cases for this study. Of those 12 cases, six occurred in TC 01A of 2001. Midlatitude System Evolutions (MSEs) account for 7 (58%) of the large FTEs, while errors associated with beta-effect and tropical-related TC-Environment transformations resulted in 2 (17%) and 1 (8%) of large FTEs. Initial position errors resulted in 2 (17%)

of the large FTEs. Although no large FTEs due to Cyclonic Interactions were identified in this small sample, this does not preclude the possibility of their existence in the NIO. Finally, no new model error sources were identified in the NIO, which thus supports a global application of the Dynamical Model Forecast Traits Knowledge Base.

B. FUTURE RESEARCH

During examination of the TC Motion Meteorology Knowledge Base, tropical cyclone frequency in the North Indian Ocean appeared to increase (up to 8 TCs) during El Nino years and decrease (approximately 4 TCs) during La Nina years. A study of TC frequency and warm sea-surface temperature anomalies in the North Indian Ocean may provide a better understanding of the possible connection between the two meteorological phenomenon.

This Dynamical Model Forecast Traits Knowledge Base study focused on the performance of the NOGAPS, GFDN, and UKMO models only, even though the SAFA system used by JTWC incorporates up to five models. The two remaining models not included in this study are the National Center for Environmental Prediction Aviation Model (AVN) and the Japanese Global Spectral Model (JGSM), as they were not available for the entire two-year period that was studied. An expanded observation of the errors associated with these five models over a longer period of time would provide a more substantial database for inclusion in the SAFA program. Development of a North Indian Ocean training module is required to complete the SAFA training program, and this should be followed by an application of the TC Motion Meteorology and Dynamical Model Forecast Traits Knowledge Bases in a real-time forecasting test.

THIS PAGE INTENTIONALLY LEFT BLANK

LIST OF REFERENCES

Bannister, A.J., M.A. Boothe, L.E. Carr, III, and R.L. Elsberry, 1997: Southern Hemisphere Application of the Systematic Approach to Tropical Cyclone Track Forecasting. Part I. Environmental Structure Characteristics. Tech. Rep. NPS-MR-98-001, Naval Postgraduate School, Monterey, CA 93943-5114, 96 pp.

Bannister, A.J., M.A. Boothe, L.E. Carr, III, and R.L. Elsberry, 1998: Southern Hemisphere Application of the Systematic Approach to Tropical Cyclone Track Forecasting. Part II. Climatology and Refinement of Meteorological Knowledge Base. Tech. Rep. NPS-MR-98-004, Naval Postgraduate School, Monterey, CA 93943-5114, 69 pp.

Boothe, M.A., 1997: Extension of the Systematic Approach to Tropical Cyclone Track Forecasting in the Eastern and Central North Pacific. M.S. Thesis, Naval Postgraduate School, Monterey, CA 93943, 134 pp.

Boothe, M.A., R.L. Elsberry, and L.E. Carr, III, 2000: Atlantic Application of the Systematic Approach to Tropical Cyclone Track Forecasting. Part I. Environmental Structure Characteristics. Tech. Rep. NPS-MR-00-003, Naval Postgraduate School, Monterey, CA 93943-5114, 77 pp.

Brown, D.S., 2000: Evaluation of Dynamic Track Predictions for Tropical Cyclones in the Atlantic During 1997-1998. M.S. Thesis, Naval Postgraduate School, Monterey, CA 93943, 92 pp.

Cantrell, C.E., and R.A. Jeffries, 2002: Analysis of the First Operational Test of the Systematic Approach to Tropical Cyclone Forecasting Aid at the Joint Typhoon Warning Center During the 2000 Tropical Cyclone Season. Preprints, 25th Conf. Hurr, Trop. Meteor, San Diego, CA, Amer. Meteor. Soc., 305-306.

Carr, L.E., III, and R.L. Elsberry, 1994: Systematic and Integrated Approach to Tropical Cyclone Track Forecasting. Part I. Approach Overview and Description of Meteorological Basis. NPS Tech. Rep. NPS-MR-94-002, Naval Postgraduate School, Monterey, CA 93943-5114, 273 pp.

Carr, L.E., III, and R.L. Elsberry, 1997: Models of Tropical Cyclone Wind Distribution and Beta-Effect Propagation for Application to Tropical Cyclone Track Forecasting. *Mon. Wea. Rev*, **125**, 3190-3209.

Carr, L.E., III, and R.L. Elsberry, 1999: Systematic and Integrated Approach to Tropical Cyclone Track Forecasting. Part III: Traits Knowledge Base for JTWC Track Forecast Models in the Western North Pacific. Tech. Rep. NPS-MR-99-002, Naval Postgraduate School, Monterey, CA 93943-5114, 227 pp.

Carr, L.E., III, and R.L. Elsberry, 2000a: Dynamical Tropical Cyclone Track Forecast Errors. Part I: Tropical Region Error Sources. *Wea. Forecasting*, **15**, 641-661.

Carr, L.E., III, and R.L. Elsberry, 2000b: Dynamical Tropical Cyclone Track Forecast Errors. Part II: Midlatitude Circulation Influences. *Wea. Forecasting*, **15**, 662-681.

Carr, L.E., III, R.L. Elsberry, and M.A. Boothe, 1997: Condensed and Updated Version of the Systematic Approach Meteorological Knowledge Base Western North Pacific. NPS Tech. Rep. NPS-MR-98-002, Naval Postgraduate School, Monterey, CA 93943-5114,169 pp.

Carr, L.E., III, R.L. Elsberry, and M.A. Boothe, 1999: Condensed and Updated Version of the Systematic Approach Meteorological Knowledge Base for the Southern Hemisphere. Tech. Rep. NPS-MR-00-001, Naval Postgraduate School, Monterey, CA 93943-5114, 141 pp.

Elsberry, R.L., 1995: Tropical Cyclone Motion. *Global Perspectives on Tropical Cyclones*, R.L.Elsberry, Ed., WMO/TD-No. 693, Rep. TCP-38, World Meteorological Organization, 106-197.

Reader, G., M.A. Boothe, R.L. Elsberry, and L.E. Carr, III, 1999: Southern Hemisphere Application of the Systematic Approach to Tropical Cyclone Track Forecasting. Part III. Updated Environmental Structure Characteristics. Tech. Rep. NPS-MR-99-004, Naval Postgraduate School, Monterey, CA 93943-5114, 73 pp.

Reader, G., M.A. Boothe, R.L. Elsberry and L.E. Carr, III, 2000: Southern Hemisphere Application of the Systematic Approach to Tropical Cyclone Track Forecasting. Part IV. Sources of Large Track Errors by Dynamical Models. Tech. Rep. NPS-MR-00-004, Naval Postgraduate School, Monterey, CA 93943-5114, 51 pp.

INITIAL DISTRIBUTION LIST

1. Defense Technical Information Center

2. Dudley Knox Library
   Naval Postgraduate School

3. Commanding Officer
   Naval Pacific Meteorology and Oceanography Center/
   Joint Typhoon Warning Center

4. Commanding Officer
   Naval Pacific Meteorology and Oceanography Center Yokusuka

5. Professor R. L. Elsberry
   Department of Meteorology
   Naval Postgraduate School

6. Professor Carlyle H. Wash
   Department of Meteorology
   Naval Postgraduate School

7. Professor Patrick A. Harr
   Department of Meteorology
   Naval Postgraduate School

8. Mark A. Boothe
   Department of Meteorology
   Naval Postgraduate School

9. CAPT R. Clark
   SPAWAR (PMW 155)

10. Superintendent
    Naval Research Laboratory